Distribution Agreement

In presenting this thesis or dissertation as a partial fulfillment of the requirements for an advanced degree from Emory University, I hereby grant to Emory University and its agents the non-exclusive license to archive, make accessible, and display my thesis or dissertation in whole or in part in all forms of media, now or hereafter known, including display on the world wide web. I understand that I may select some access restrictions as part of the online submission of this thesis or dissertation. I retain all ownership rights to the copyright of the thesis or dissertation. I also retain the right to use in future works (such as articles or books) all or part of this thesis or dissertation.

Signature:

_____ _____

Tara D. Wabbersen **Date**

Generation of Zebrafish (*Danio rerio*) Animal Models for Congenital Short Bowel Syndrome and Hirschsprung's Disease

By
Tara D. Wabbersen
Doctor of Philosophy

Graduate Division of Biological and Biomedical Sciences
Biochemistry, Cell and Developmental Biology

_____
Advisor: Iain T. Shepherd, Ph.D.

_____
Committee Member: Ping H. Chen, Ph.D.

_____
Committee Member: Andreas Fritz, Ph.D.

_____
Committee Member: Michael H. Koval, Ph.D.

_____
Committee Member: Kenneth H. Moberg, Ph.D.

Accepted:

_____
Lisa A. Tedesco, Ph.D.
Dean of the James T. Laney School of Graduate Studies

_____
Date

Generation of Zebrafish (*Danio rerio*) Animal Models for Congenital Short Bowel Syndrome and Hirschsprung's Disease

By

Tara D. Wabbersen

B.A., Rollins College, 2007

Advisor: Iain T. Shepherd, Ph.D.

An abstract of a dissertation submitted to the Faculty of the James T. Laney School of Graduate Studies of Emory University in a partial fulfillment of the requirements for the degree of Doctor of Philosophy in the Graduate Division of Biological and Biomedical Sciences, Biochemistry, Cell and Developmental Biology, 2016

Abstract

Generation of Zebrafish (*Danio rerio*) Animal Models for Congenital Short Bowel Syndrome and Hirschsprung's Disease

Tara D. Wabbersen

Pediatric intestinal disorders range from minor to severe, and have the potential of causing life-long problems. Congenital short bowel syndrome (CSBS) occurs when only the first fifth of the small intestine is formed, leading to malnutrition and high mortality rates. Hirschsprung's disease is the lack of neurons in the distal region of the large intestine, which results in obstruction of the colon requiring surgery, leading to long-term complications and sometimes death. The genetic components of each of these diseases are highly sought after. In conjunction with our collaborators, who genetically screened five patients with CSBS, I confirmed CAR-like membrane protein (CLMP) as the causative gene of CSBS and established a zebrafish animal model to further understand the role of CLMP in intestinal development. By making this zebrafish model, I helped confirm CLMP as the causative gene of CSBS, as well as providing a tool to further our understanding of the role of CLMP in intestinal development. Additionally, I used zebrafish to model Hirschsprung's disease and identified the fibroblast growth factor and Hedgehog signaling pathways as required for the development of the enteric nervous system. These signaling pathways are required for neural crest migration to the developing gut tube, and when perturbed, lead to a Hirschsprung's-like phenotype. These discoveries will improve genetic screens to aide in diagnosis and treatment of patients with developmental disorders of the gut.

Generation of Zebrafish (*Danio rerio*) Animal Models for Congenital Short Bowel Syndrome and Hirschsprung's Disease

By

Tara D. Wabbersen

B.A., Rollins College, 2007

Advisor: Iain T. Shepherd, Ph.D.

A dissertation submitted to the Faculty of the James T. Laney School of Graduate Studies of Emory University in a partial fulfillment of the requirements for the degree of Doctor of Philosophy in the Graduate Division of Biological and Biomedical Sciences, Biochemistry, Cell and Developmental Biology, 2016

Acknowledgements

First, I would like to thank Dr. Iain Shepherd, as well as my committee members: Dr. Andreas Fritz, Dr. Kenneth Moberg, Dr. Ping Chen, Dr. Shanthi Srinivasan, and Dr. Michael Koval.

I would like to thank our collaborators Dr. Robert Hofstra and Christine Van Der Werf. It was a pleasure to work with both of you.

A big thanks to lab members who have contributed to my time in graduate school, you have become like family. Special thanks to Colin, Becky, Alex, Jackie, Lu, Jimmy, and Greg, lab would not have been the same without you!

I would like to thank Dr. Dawn Mielke and Dr. Sol Jacobs for their medical knowledge and intuition that saved my life, I am forever grateful.

I would like to thank Dr. Pat Marsteller for taking me under her wing, believing in me, and showing me what higher education can be.

To the many members of BCDB and the Biology Department, you have made my time at Emory fun and meaningful, which I will always hold dear.

To all the friends I have made in graduate school, you have made a tough time so much easier. To John, Megan, Molly, Katie, and Sara, I could not have asked for better friends to go through graduate school with!

To all the friends I have made in Atlanta, you guys are awesome. Thanks for always making things fun and adventurous!

To my First Descents family, especially to Lauren (Chewie), Asha (Spud), Caryn (Kemp), and Jenny (Gin), thank you and here's to being "here."

To my extended family, thank you for supporting me and understanding all my hard work, I love you!

To the Wahbe family, thank you for supporting me and always being cheerleaders for my time in graduate school, it means so much to me. Love you!

To my Mom and Trystan, thank you for always being there for me, and always being so excited for all of my accomplishments, big or small. I love you!

To my Dad and Lauren, thank you for always being there when I needed it most and being my safety net. And thank you for encouraging my love of science. I love you!

And last, but not certainly not least, to Paul, thank you for enduring this with me. I couldn't have done this without you. I love you!

Table of Contents

List of Tables and Figures:

Chapter 1: Introduction to Gut and Intestinal Development in Zebrafish

Chapter 2: CLMP Is Required for Intestinal Development, and Loss-of-Function Mutations Cause Congenital Short-Bowel Syndrome

Chapter 3: Fibroblast Growth Factor and Hedgehog Signaling are Required for Enteric Nervous System Development in Zebrafish

Appendix A: Figures in support of "CLMP Is Required for Intestinal Development, and Loss-of-Function Mutations Cause Congenital Short-Bowel Syndrome"

Appendix B: In Vivo Visualization of the Development of the Enteric Nervous System Using a Tg(28.3bphox2b:Kaede) Transgenic Zebrafish

List of Abbreviations in this document:

AKT/PKB.....Protein Kinase B

BMP.....Bone Morphogenic Protein

Ca^{2+}.....Calcium

casp3.....Caspase3

CAR.....Coxsackie and Adenovirus Receptor

CHO.....Chinese Hampster Ovary

CLMP.....CAR-like Membrane Protein

COT.....Cardiac Outflow Tract

CSBS.....Congenital Short Bowel Syndrome

CTX.....Cortical thymocyte Marker

DAG.....diacylglycerol

dhh.....desert hedgehog

DMSO.....Dimethyl sulfoxide

dn.....dominant negative

Ece1.....Endothelian Converting Enzyme 1

Edn3.....Endothelian 3

Ednrb.....Endothelian Receptor B

EGFP.....Green Fluorescent Protein

Elv.....early neuronal marker

ENCCs.....enteric neural crest cells

ENS.....enteric nervous system

Erks.....extracellular signal-regulated kinases

ESAM.....endothelial cell-selective adhesion molecule

Etv5b.....ets variant 5b

FGF.....fibroblast growth factor

FGFR.....fibroblast growth factor receptor

Frs2.....fibroblast growth factor receptor substrate 2

Gab1.....Grb2 associated binding protein

gdnf.....glial derived neurotrophic factor

GI.....gastrointestinal

Gli.....glioblastoma transcription factor

Grb2.....growth factor recptor-bound substrate 2

hpf.....hours post fertilization

HSCR.....Hirschsprung's disease

hsp.....heat shock protein

ihh.....indian hedgehog

IP3.....inositol triphosphate

JAM.....junctional adhesion molecule

JNKs.....Jun amino-terminal kinases

MAPk.....mitogen activated protein kinases

MO.....mopholino

OV.....otic vesicle

PA.....pharyngeal arches

PCR.....polymerase chain reaction

PDGF.....platelet derived growth factor

PDK.....phosphoinositide dependent protein kinase

PH3.....phosphohistone H3

phox2b.....paired-like homeobox 2

PI3K.....phosphoinositide 3-kinase

PKC.....protein kinase C

Ptch.....Patched

qRT-PCR.....quantitative Real-Time PCR

RET.....rearranged in trasnfection

RT-PCR.....reverse transcription PCR

SBMO.....splice blocking morpholino

shh.....shh

Shp2.....protein tyrosine phosphatase

Sip1.....SMAD interacting protein

Smo.....Smoothened

SNP.....single nucleotide polymorphism

Sos1.....son of sevenless

spry.....sprouty

STATs.....signal transducer and activator of transcription

T.....thymus

TBMO.....translation blocking morpholino

TF.....transcription factor

Tg.....transgenic

TGF-β.....transforming growth factor beta

TTF1.....thyroid transcription factor 1

WT.....wild-type

ZO.....zonula occludens

CHAPTER 1:

Introduction to Gut and Intestinal Development in Zebrafish

1.1 PURPOSE AND CENTRAL HYPOTHESIS

The goal of this work is to identify and characterize genetic factors in pediatric developmental disorders of the gut. Congenital short bowel syndrome (CSBS) and Hirschsprung's disease are both pediatric developmental disorders affecting the intestines. CSBS is characterized by an abnormally short small intestine. Our collaborators identified car-like membrane protein (CLMP) as a potential causative gene in CSBS. I set out to confirm CLMP as the causative gene through the generation of a zebrafish animal model. This included confirming expression of CLMP in the developing gut, knocking down expression of CLMP, and visualizing the gut of the CLMP knockdown animals at the cellular level. I also worked to identify potential signaling pathways and genes involved in Hirschsprung's disease. Hirschsprung's disease is characterized by the lack of enteric neurons in the distal colon. I determined that fibroblast growth factor signaling and hedgehog signaling are required for enteric nervous system development.

1.2 GASTROINTESTINAL TRACT ARCHITECTURE

1.2.1 Gastrointestinal Tract Introduction

The gastrointestinal (GI) tract is made up of the mouth, esophagus, stomach, small intestine, large intestine (including the rectum), and anus (Fig. 1). The salivary glands, liver, pancreas, and gall bladder are also part of the digestive system and help the GI tract digest food (Fig. 1). The goal of the GI tract is to digest the food and liquids we ingest, absorb nutrients and excrete the waste. (Your Digestive System and How it Works, 2013). The esophagus is a muscular tube responsible for transporting food from the mouth to the stomach. Once in the stomach, the stomach mixes the food and liquids with the gastric juices it produces to digest it before it passes into the small intestine. The small intestine absorbs nutrients from our food, while the large intestine prepares the leftover waste to be passed in a bowel movement (Gastrointestinal Tract, n.d.).

1.2.2 Small Intestine

The small intestine is made up of three regions, the duodenum, the jejunum, and the ileum (Fig. 1). The duodenum is the first part of the small intestine and absorbs iron and other minerals (Short Bowel Syndrome, 2015). The duodenum extends from the pyloric sphincter at the transfer point between the stomach and small intestine to the ligament of Treitz, a fibrous, muscular band (Rao and Wang 2010). The jejunum and ileum follow, lying between the ligament of Treitz and the ileocecal sphincter, the transfer point between the small and large intestine. The first third of this segment is the jejunum and the remainder is the ileum (Rao and Wang 2010). Carbohydrates, proteins, fats and most vitamins are absorbed

in the jejunum. The ileum absorbs bile acids and vitamin B12 (Short Bowel Syndrome, 2015). In adults, the small intestine is approximately three to five meters long (Small Intestine, n.d.).

The small intestine is made up of four main layers: the mucosa (epithelium, lamina propria, and muscular mucosae), the submucosa, the muscularis propria (inner circular muscle layer, intermuscular space, and outer longitudinal muscle layer), and the serosa (Fig 2) (Rao and Wang, 2010). The mucosa is the innermost layer and is where nutrient absorption occurs. The extensive infolding of the small intestine allows for a large surface area of the mucosal layer to allow for maximum absorption. The mucosa consists of three layers. The first is a single epithelial layer facing the lumen of the intestines, which is attached to the basement membrane of the second layer, the lamina propria. The lamina propria is made up of connective tissue and lymph nodes and it lies on a sheet of smooth muscle called the muscular mucosae (Rao and Wang, 2010). The mucosa rests on the submucosa, which contains a variety of inflammatory cells, lymphatics, autonomic nerve fibers, and ganglion cells. Beneath the submucosa is the muscularis propria, which contains smooth muscle arranged into an inner circular layer and an outer longitudinal layer. Between the outer and inner layers are prominent autonomic neural fibers and ganglionic clusters that for the myenteric plexus. The main function of the muscularis propria is to control peristalsis, which is the wavelike contractions of the intestines that propel food forward. The outermost layer of the intestines is the serosa, which is made up of

the mesothelium, a continuous sheet of squamous epithelial cells (Fig. 2) (Rao and Wang, 2010).

The defining feature of small intestine is the columnar cells of the innermost epithelial layer. These columnar epithelial cells exhibit invaginations known as the crypts of Lieberkuhn. The crypts are predominately comprised of proliferating cells and finger-like projections called villi that contain the majority of differentiated absorptive cells (Rao and Wang, 2010). These cells are responsible for the terminal digestion and transport of nutrient, ions, and water. The villi contain enterocytes (intestinal absorbative cells), enteroendocrine (gastrointestinal hormone producing cells), and goblet cells. (mucus producing cells). At the base of the crypts are Paneth cells, which secret antimicrobial agents. The remaining part of the crypts are made up of stem cells and proliferating progenitors (Rao and Wang 2010).

1.2.3 Large Intestine

The large intestine is made up of multiple regions: the cecum, ascending colon, hepatic flexure, transverse colon, splenic flexure, descending colon, sigmoid colon, rectum, and anus (Fig. 1) (Rao and Wang, 2010). The cecum is a pouch at the transfer point between the small and large intestine (Cecum, n.d.). The ascending colon is the first main part of the colon and is typically on the right side of the abdomen (Ascending colon, n.d.). The hepatic flexure is the turn in the colon from ascending to transverse colon and is in the region of the liver. The transverse colon is the second main part of the colon and crosses the abdomen

from right to left (Transverse colon, n.d.). The splenic flexure is the turn of the colon from transverse to descending colon and is in the region of the spleen. The descending colon is on the left side of the abdomen and typically stores stool (Descending colon, n.d.). The sigmoid colon is s-shaped and connects the descending colon to the rectum (Sigmoid colon, n.d.). The rectum is the last few inches of the colon before the anus, which is the opening at the end of the gastrointestinal tract where the contents of the bowel leave the body (Fig. 1) (Rectum, n.d., Anus, n.d.). In adults, the large intestine is approximately 1.5 meters in length (Rao and Wang, 2010).

The structure of the large intestine is very similar to the small intestine (Fig 2). It contains the same four main layers: the mucosa, the submucosa, the muscularis propria, and the serosa. The major difference between the architecture of the small and large intestine is in the innermost epithelial layer. The mucosa layer of the large intestine does not have villous projections, but instead has deep tubular pits that increase in depth toward the rectum (Fig. 2) (Rao and Wang, 2010). The mucosal epithelial cells of the large intestine include absorptive cells, goblet mucus cells, undifferentiated columnar crypt cells, caveolated cells, Paneth cells, and M-cells (immune cells), similar to the small intestine. The main role of the large intestine is to reclaim luminal electrolytes and water, as well as packaging waste for excretion (Rao and Wang, 2010).

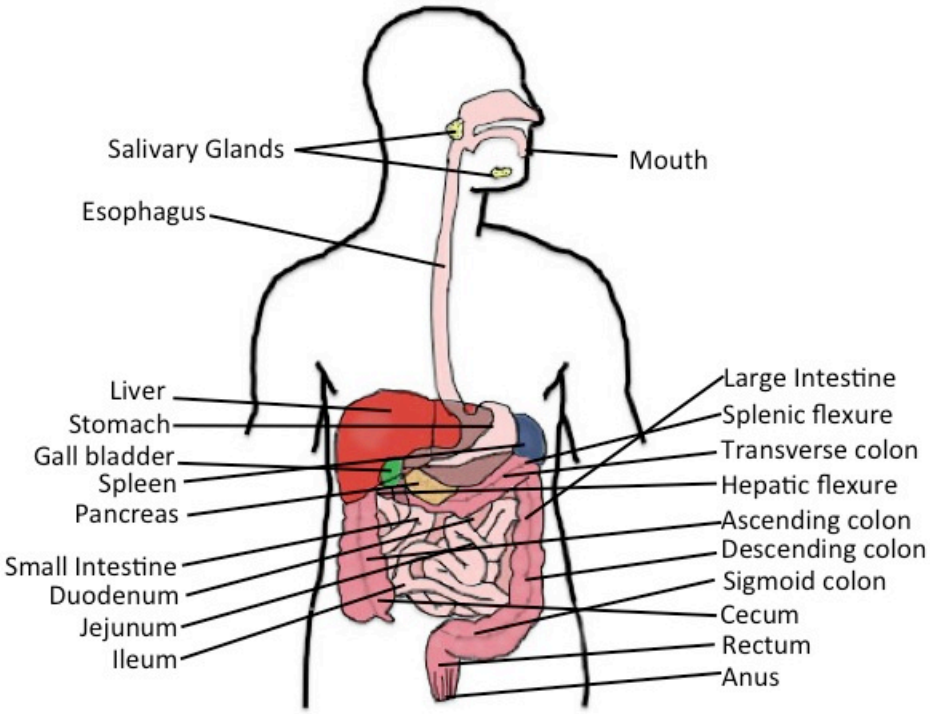

Figure 1: The Digestive Tract

The gastrointestinal tract is made up of the mouth, esophagus, stomach, small intestine, large intestine, rectum, and anus. Supporting organs include the salivary glands, liver, pancreas, spleen and gall bladder. The small intestine is made up of three parts: the duodenum, jejunum, and the ileum. The large intestine is made up of: the cecum, ascending colon, hepatic flexure, transverse colon, splenic flexure, descending colon, sigmoid colon, rectum, and anus.

1.2.4 Enteric Nervous System

The enteric nervous system (ENS) is the nervous system that lies in the gut wall. It is an extensive network of neurons and glia, and there are approximately 400-600 million enteric neurons in adult humans (Furness, 2012). Eighteen different functional classes of neurons have been identified in the ENS (Brookes, 2001). The ENS is organized in two concentric rings of interconnected ganglia. The innermost ring is the submucosal, or Meissner's, plexus, which lies between the submucosal layer and the longitudinal muscle layer. The submucosal plexus is absent in the esophagus. The outermost ring is the myenteric, or Auerbach's, plexus, and lies between the longitudinal and circular muscle layers (Goldstein, Hofstra, and Burns, 2012). The ENS coordinates gut function through muscle contraction (leading to peristalsis), blood flow, and water and electrolyte secretion (Furness, 2006).

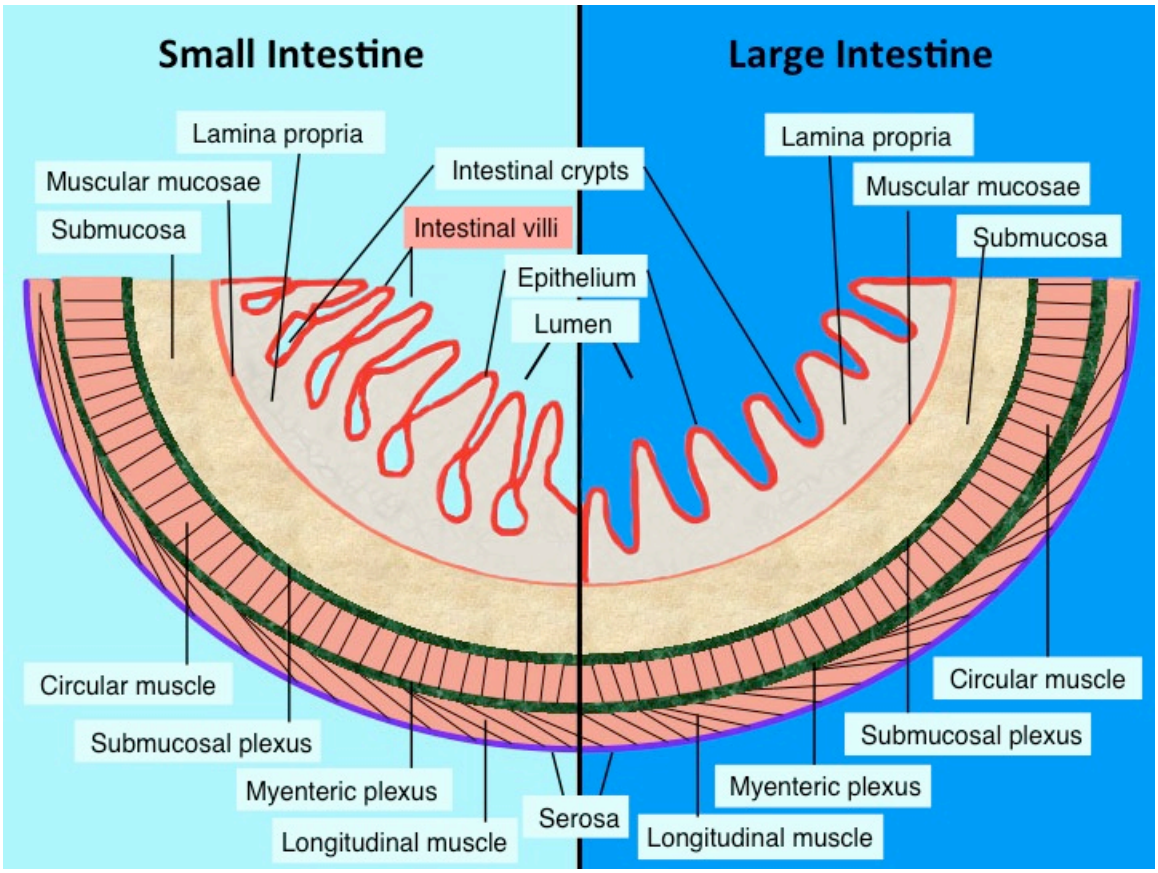

Figure 2: Structure of the small and large intestine

The small intestine and large intestine are made up of four main layers: the mucosa, the submucosa, the muscularis propria, and the serosa. The mucosa membrane is made of the epithelium, lamina propria, and muscular mucosae. The muscularis propria is made up of inner circular muscle layer, intermuscular space, and outer longitudinal muscle layer. The enteric nervous system lies in two plexuses. The submucosal plexus lies between the submucosa and the circular muscle layers. The myenteric plexus lies between the circular and longitudinal muscle layers. The defining difference between the small and large intestine is that the small intestine contains villi while the large intestine does not.

1.3 GUT AND ENTERIC NERVOUS SYSTEM DEVELOPMENT

1.3.1 Intestinal development

Following gastrulation, the embryonic endoderm forms the lining of the primitive gut tube, which extends the length of the body (Gilbert, 2000). Following gut tube expansion, the epithelial layer transitions into stratified epithelial cells with apical basal polarity. The epithelial cells then reorganize into columnar form, which coincides with villi formation (Noah, Donahue, and Shroyer, 2011). The endoderm interacts with mesodermal mesenchyme to allow for differentiation along the gut tube into the specific cell types that make up the esophagus, stomach, small and large intestines (Gilbert, 2000). The crosstalk between the endoderm and mesoderm derived cells has been previously shown to involve signaling pathways, such as BMP, Hedgehog, PDGF, TGF-β, and Wnt pathways. This crosstalk involves multiple additional pathways that must work together in parallel to coordinate development of multiple cell types within the developing gut tube simultaneously. Differentiation into the distinct cell types that make up the GI tract leads to completion of intestinal organogenesis (Noah, Donahue, and Shroyer, 2011).

1.3.2 Enteric Nervous System development

In all vertebrate species, the enteric nervous system is derived entirely from neural crest cells (Le Douarin and Kalcheim 1999, Burns 2005, Heanue and Pachnis 2007, Newgreen and Young 2002b). Neural crest cells are a population of embryonic stem cells that delaminate from the closing neural tube and migrate throughout the body to form various cell types and structures. Neural crest cells

are derived from neural ectoderm, unlike the structures within the gut, which are derived from endoderm and mesoderm (Gilbert, 2000). In mammalian and avian model systems, the vagal neural crest provides the majority of enteric neurons, while the sacral neural crest has a small contribution. Enteric neural crest cells (ENCCs) migrate from the vagal region to the anterior end of the gut then migrate rostro-caudally along the developing gut. ENCCs proliferate as they migrate and differentiate into various neuronal subtypes (Furness 2006). The migration, proliferation, and differentiation of ENCCs are regulated by cell-cell and cell-environmental interactions (Heanue and Pachnis 2007, Newgreen and Young 2002a,b).

1.4 CONGENITAL DISEASE OF THE SMALL AND LARGE INTESTINE

1.4.1 Congenital intestinal diseases

When developmental processes in gut and ENS development fail, it can lead to congenital gastrointestinal disease. Congenital GI disorders range from malrotation to atresia (when part of the GI tract is malformed or absent), to motility disorders. However, there are many different types of congenital anomalies in infants (Cochran, 2013). The focus of this dissertation is on two congenital intestinal diseases: Congenital short bowel syndrome and Hirschsprung's disease.

1.4.2 Congenital Short Bowel Syndrome

Congenital short bowel syndrome (CSBS) was first described 1969 (Hamilton et al., 1969). Patients with CSBS are born with a shortened small intestine. CSBS patients' mean length of small intestine is approximately 50cm, as compared to 190-280cm in normal babies, and typically includes the duodenum and a small part of the jejunum (Fitzsimmons et al. 1998, Reiquam et al. 1965, Siebert, 1998). Due to the hugely reduced absorptive surface of the small intestine, patients with CSBS may develop severe malnutrition. Diagnosis typically occurs following a barium-contrast radiograph and exploratory laparotomy. Patients typically present within a few days after birth with vomiting and diarrhea or failure to thrive (Van Der Werf et al. 2015). Infants with either congenital or acquired short bowel syndrome need parenteral nutrition to survive. Parenteral nutrition, also known as intravenous feeding, can itself have life-threatening complications, such as liver failure and sepsis. Due to these potential complications, patients

with congenital short bowel syndrome have a high rate of mortality early in life (Huysman et al. 1991, Ordonez et al. 2006, Hasosah et al. 2008, Schalamon et al. 1999).

1.4.3 Hirschsprung's disease, an enteric nervous system disorders

When enteric neural crest precursors fail to properly populate the gut, it can lead to Hirschsprung's disease or other enteric nervous system disorders (Brooks et al. 2005, Gershon and Ratcliffe 2004). Hirschsprung's disease is a pediatric developmental disorder characterized by colonic aganglionosis, which is the lack of neurons in the distal colon. It occurs in 1:5000 live births and is typically diagnosed after a newborn does not pass meconium, or the first stool, and then followed by a barium-contrast radiograph and intestinal biopsy. The current treatment is surgical removal of the affected region or pull-through surgery (Amiel et al. 2008). Hirschsprung's disease can be either sporadic or inherited and can affect a long or short segment of the colon. Sporadic short-segment is the most common type seen in clinical settings. Patients with Hirschsprung's disease and other enteric nervous system disorders have life-long gastrointestinal disorders and complications (Prato et al. 2011).

1.5 GUT AND ENTERIC NERVOUS SYSTEM DEVELOPMENT IN ZEBRAFISH

1.5.1 Zebrafish as a model system

Zebrafish, or *Danio rerio*, has become an excellent model system for vertebrate biology. Zebrafish embryos are transparent and result from external fertilization of the egg, making them a great model to study early vertebrate developmental processes. Additionally, zebrafish have high fecundity and short generation times, which allows for ease of genetic analyses (Dooley and Zon, 2000). These strengths provide zebrafish significant advantages over other vertebrate models. We, along with others, have developed zebrafish as a model CSBS and Hirschsprung's (Goldstein, Hofstra and Burns 2013).

1.5.2 Zebrafish gut development

Early zebrafish gut development is closely related to that of mammals. Like other cyprinids, zebrafish lack a stomach. However, the intestinal bulb performs a similar function to the mammalian stomach. The intestine forms early in zebrafish development, and they can begin actively feeding by 5 days post fertilization (Wallace et al. 2005, Veldman and Lin, 2008). At approximately 26-30 hours post fertilization (hpf), the primitive gut tube forms in zebrafish. The primitive gut is made up of a continuous thin layer of endoderm, and this tissue extends from a site close to wear the mouth will form to the position of the future anus (Ng et al. 2005). During intestinal organogenesis, the pancreas, liver, and swim bladder bud off of the developing gut tube. By 52hpf, rapid intestinal morphogenesis occurs. Endoderm adjacent to the hepatic duct forms the

primitive gut. Due to the absence of a stomach, the esophagus connects directly to the intestine in zebrafish. Zebrafish also lack a cecum, the transfer point between the small and large intestine (Ng et al. 2005). The intestinal bulb, the anterior most region of the gut tube, with its large luminal space, acts as a reservoir, and can be comparable to the function of the stomach (Wallace et al. 2005). Lumen formation is initiated in the intestinal bulb primordium and advances rostra-caudally along the primitive intestine. As the lumen is formed, the lining endodermal cells are arranged into a monolayer. By 76hpf, the mouth opens, forming a continuous lumen from mouth to anus, although the anus remains closed (Ng et al. 2005). With this opening of the lumen, the polarization of the epithelial cells occurs, and mesenchymal tissue is first visible around the epithelium. At 98hpf, the intestine undergoes extensive remodeling and compartmentalization (Ng et al. 2005).

Compartmentalization of the zebrafish intestine results in three main segments: the intestinal bulb, the mid-intestine, and the posterior intestine. By this time, the intestinal bulb achieves its expanded luminal space and begins to develop invaginations. The mid-intestine is characterized by the appearance of mucus secreting goblet cells, which are absent in the intestinal bulb and posterior intestine. At 120hpf, the developing gut is functional, and the mesenchymal tissue surrounding the epithelial layer thickens. As the developing embryo continues to progress through the juvenile stage, the intestine continues to develop, fold, and differentiate into specific intestinal cell types that make up the adult zebrafish intestine (Ng et al. 2005).

1.5.3 Enteric Nervous System Development in zebrafish

Like other vertebrates, the zebrafish ENS is derived from neural crest cells. In zebrafish, the ENS is only derived from the vagal neural crest and does not have a sacral contribution. In addition to the ENS, the vagal neural crest gives rise to cells supporting the thymus, the cardiac outflow tract, and the pharyngeal arches in zebrafish (Fig. 3) (Shepherd and Eisen, 2011). These enteric neural crest cells (ENCCs) migrate to the anterior region of the gut tube and then migrate in two parallel chains along the gut (Shepherd et al. 2004). These precursors proliferate as they migrate, followed by differentiation into the appropriate neuronal subtypes. Zebrafish lack a submucosal plexus, and the myenteric neurons do not lie in a plexus (Wallace et al. 2005). Despite these morphological differences, factors involved in ENS development in humans and other model systems have been showed to have orthologous function in zebrafish (Heanue and Pachnis, 2008).

As with other model systems, the temporal patterning of the ENS in zebrafish has been established. As seen in Figure 4, cells migrate from the vagal neural crest region to the anterior end of the gut tube from 30-36 hours post fertilization (hpf). From 36-60hpf, cells migrate in two chains down the length of the gut tube. These cells undergo extensive proliferation during this period, with the first wave of neuronal differentiation occuring at 72hpf. ENCC precursor cells undergo further waves of differentiation at 96 and 120hpf. At 120hpf the gut is functional. The undifferentitated enteric precursors continue to proliferate and

differentiate so that overall neuronal number grows as juvenile zebrafish develop into adults.

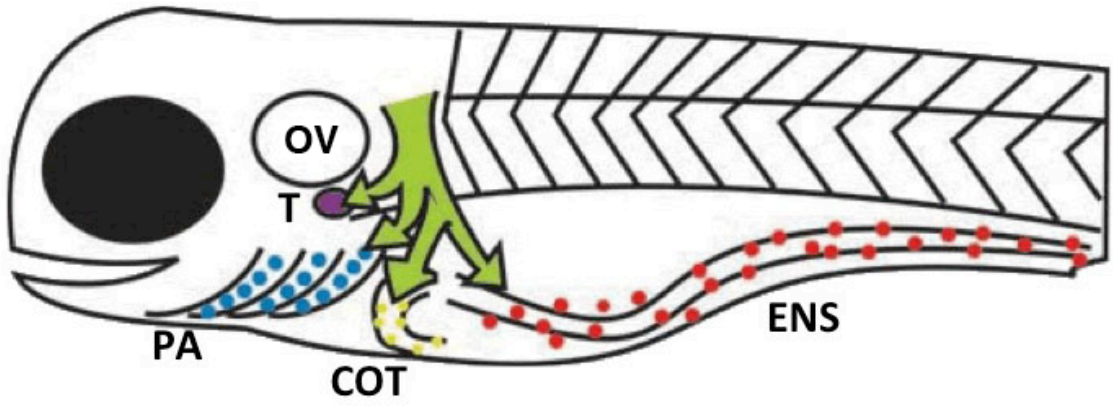

Figure 3: Vagal neural crest migration in the zebrafish

In zebrafish, the vagal neural crest lies between the otic vesicle and the first and second somites. These neural crest cells migrate to give rise to cells supporting the thymus, the pharyngeal arches, the cardiac outflow tract, and the enteric nervous system. T, thymus; PA, pharyngeal arches; COT, cardiac out flow tract; ENS, enteric nervous system.

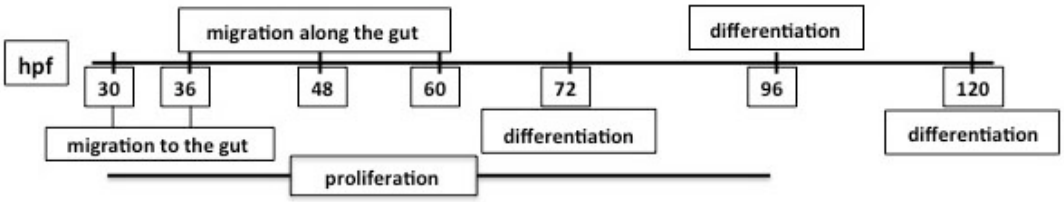

Figure 4: Timeline of enteric nervous system development in zebrafish

From 30-36 hours post fertilization (hpf), enteric neural crest cells (ENCCs) migrate from the vagal region to the anterior region of the gut tube. From 36-60hpf ENCCs migrate along the length of the gut. These cells proliferate as they migrate, from 30-96hpf. Starting at 72hpf and continuing at 96 and 120hpf, waves of differentiation of the ENCCs into the various neuronal subtypes that make up the ENS occurs. At 120hpf the gut is functional and embryos can begin feeding.

1.6 CONGENITAL SHORT BOWEL SYNDROME IN HUMANS AND ZEBRAFISH

1.6.1 Congenital short bowel syndrome (CSBS) in the literature

CSBS has been previously discussed in the medical literature in terms of patient case studies. A review in 2008 identified 37 published cases in the literature (Hasosah et al. 2008). While mortality is high in CSBS, some long-term survivors have been reported (Huysman et al. 1991, Schalamon et al. 1999, Ordonez et al. 2006, Hasosah et al. 2008). In Chapter 2 we report the largest case study of CSBS with five patients, identify the causative gene, and create an animal model of CSBS in zebrafish.

1.6.2 Coxsackievirus and adenovirus receptor-like membrane protein (CLMP)

CAR-like membrane protein (CLMP) is a member of the cortical thymocyte marker (CTX) superfamily of the immunoglobulin superfamily. As a transmembrane protein, it colocalizes with critical tight junction proteins. CLMP is specifically colocalized with the tight junction protein ZO-1 and occludin (Sze et al. 2008). CLMP is detected primarily in epithelial cells, and is expressed in the developing human gut along with other embryonic tissues. Our collaborators identified mutations in CLMP in five patients from four families. Each of these mutations was confirmed to be sufficient to cause no protein formation or mislocalization of the protein *in vitro* (Van Der Werf et al. 2012). Because CLMP is expressed in other tissues during development, but a defect is only detected in the small intestine, it implies a functional redundancy for CLMP with a specific function in the intestine (Van Der Werf et al. 2012).

CLMP colocalizes with critical tight junction proteins, such as ZO-1 and occludin. Tight junctions are the most apical of cell-to-cell contact in epithelial cells (Krause et al. 2007). Tight junctions are required to form the continuous intercellular barrier between epithelial cells. This intercellular barrier is critical to separate tissue spaces and regulate the movement of solutes across the epithelium (Anderson and Itallie, 2009). Under electron microscopy, tight junctions appear as the plasma membranes of each cell being fused together and that this is occurring through intramembranous network of strands. These strands are made up of transmembrane proteins such as claudins, occludin, and tricellulin (Krause et al. 2007). Additionally, immunoglobulin superfamily membrane proteins are associated with tight junctions, such as JAMs, CAR, and ESAM. On the cytoplasmic side of the tight junction the ZO family of proteins bind claudins. Claudins and the ZO family of proteins are directly involved in tight junction strand formation, while occludin and tricellulin associate with claudins to modulate tight junction strand formation (Furuse, 2010). Due to the association of CLMP with these important tight junction proteins in the intestinal epithelium, we believe CLMP is critical for proper formation and regulation of intestinal epithelial tight junctions. We show that mutations in CLMP lead to loss of CLMP protein or a mislocalization of the protein, and that it is required for proper intestinal development in zebrafish.

1.6.3 Car-like membrane protein in zebrafish

Prior to our experiments, expression patterns of CLMP were unknown in zebrafish. Critical tight junction proteins, however, have been well defined in zebrafish. Claudins, occludins, and the ZO family of proteins have all been established as having function in zebrafish (Zhang et al. 2012, Hunziker et al. 2009, McKee et al. 2014). In Chapter 2, we demonstrate expression and role of CLMP in intestinal development in zebrafish. We analyzed the zebrafish genome and identified two potential orthologs of CLMP (Fig. 7). Using wholemount *in situ* hybridization we determined that *CLMPa* had strong expression in the developing zebrafish intestine, while *CLMPb* had much less pronounced intestinal expression (Fig. 13A). We determined the phenotype of loss of *CLMPa* in zebrafish during intestinal development. When *CLMPa* was knocked down using a morpholino, morphant embryos exhibited a smaller gut as well as a small body phenotype, implying a potential role for CLMP in convergent extension in early development (Fig 13B). Sections of *CLMPa* morphants revealed a loss of goblet cells in morphant intestines (Fig 13C). We establish zebrafish as a model for CSBS.

1.7 FIBROBLAST GROWTH FACTOR AND HEDGEHOG SIGNALING IN ENTERIC NERVOUS SYSTEM DEVELOPMENT IN ZEBRAFISH

1.7.1 Signaling Pathways in ENS development in zebrafish

In addition to studying the intestinal disorder CSBS using the zebrafish we have also used the zebrafish to study the pediatric gastrointestinal disorder Hirschsprung's disease (HSCR). Hirschsprung's disease is a complex, multifactorial disorder, and mutations in signaling pathways have been associated with ENS defects. Through extensive work in humans and animal models, multiple signaling molecules and their associated receptors have been implicated in ENS development. The most well characterized pathway in ENS development is the GDNF pathway (Goldstein, Hofstra and Burns 2013). The ligand GDNF binds to a receptor tyrosine kinase RET, and mutations in these factors have been shown to result in colonic aganglionosis in model systems and human Hirschsprung's disease patients (Cacalano et al 1998, Enomoto et al 1998, Goldstein, Hofstra and Burns 2013, Moore, et al, 1996, Pichel et al 1996, Schuchardt et al 1994). In addition to RET and GDNF, mutations have been found in ten other genes: EDNRB (Puffenberger et al. 1994), EDN3 (Edery et al. 1996, Hofstra et al. 1996), ECE1 (Hofstra et al. 1999), Neurturin (Doray et al. 1998), SOX10 (Pingault et al. 1998), PHOX2B (Amiel et al. 2003), KIAA1279 (Brooks et al. 2005), SIP1 (Cacheux et al. 2001, Wakamatsu et al. 2001), TTF1 (Garcia-Barcelo et al. 2005), Neuroregulin1 (Garcia-Barcelo et al. 2009). These mutations account for approximately 20% of HSCR disease patients (Goldstein, Hofstra and Burns 2013). We are interested in identifying other potential signaling pathways that may be involved in HSCR patients whose mutations are

unaccounted for. With temporal and spatial patterning of the ENS established in zebrafish, we set out to identify additional factors involved in ENS development. We have focused on the fibroblast growth factor signaling pathway as a candidate for a potential role in ENS development in zebrafish.

1.7.2 Fibroblast growth factor signaling pathway

The fibroblast growth factor (FGF) signaling pathway is involved in a wide array of functions in both the developing embryo and the adult human. The identified roles of FGF signaling range from mesoderm patterning in the early embryo, organogenesis, angiogenesis, and cancer pathogenesis (Kimelman and Kirschner 1987, De Moerlooze et al. 2000, Turner and Grose 2010). FGF factors are expressed in many cell types and regulate different functions, such as proliferation, differentiation and survival. In humans, the FGF pathway has four highly conserved transmembrane receptors (*fgfr1, fgfr2, fgfr3*, and *fgfr4*), and 22 ligands (Turner and Grose 2010). The ligands are *fgf1-23*, however humans lack *fgf15*. Human *fgf19* is an ortholog to mouse *fgf15* (Itoh and Konishi, 2007). As seen in Figure 5, FGF ligands bind FGF receptors, which heterodimerize and cross-phosphorylate to lead to a downstream cascade that regulates downstream target genes. There are four main pathways that FGF signaling employs: RAS/MAPK pathway, PI3K-AKT pathway, phospholipase Cγ (PLCγ), and the signal transducer and activator of transcription (STAT) pathway. Additionally, internal inhibitors allow for negative regulation of the FGF pathway, including the sprouty family of proteins. Depending on the cellular context, other potential pathways can be activated, such as p38, JUNK, and MAPK pathways. The

RAS/MAPK pathway is the predominate signaling pathway of FGF, followed by the PI3K-AKT pathway (Turner and Grose 2010). The downstream targets help FGF regulate its context dependent processes. The variation in activation of downstream targets allows for FGF to play differing roles during development.

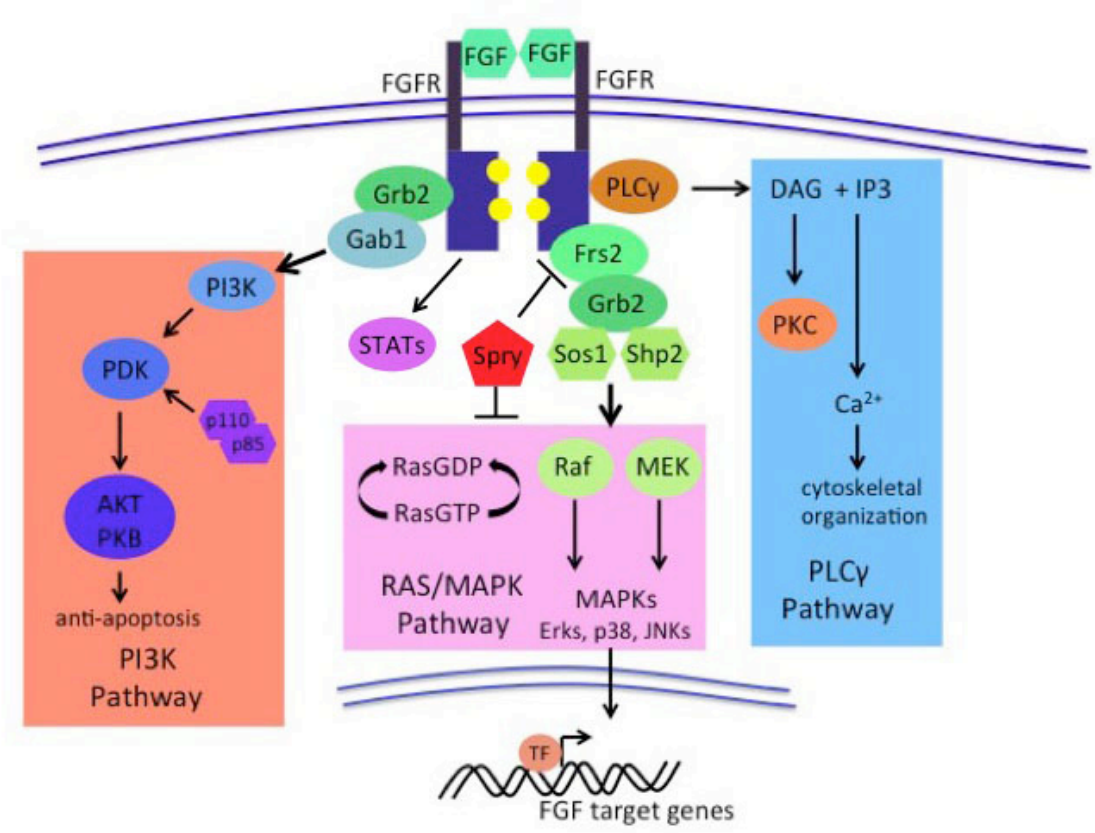

Figure 5: Fibroblast growth factor signaling pathway

FGF ligands bind to FGF receptors (FGFR), which heterodimerize and cross-phosphorylate, leading to a downstream signaling cascade. There are four main pathways that FGF signaling follows: the PI3K pathway, the RAS/MAPK pathway, the PLCγ pathway, and STATs signaling. The PI3K pathway acts through Grb2 interacting with Gab1, leading to activation of PI3K. PI3K activation, along with the action of p110 and p85, leads to PDK mediated activation of AKT/PKB. This results in regulation of apoptosis. The RAS/MAPK pathway acts through the interaction of Frs2, Grb2, Shp2 and Sos1. This activates Ras, Raf, and MEK, which in turn activates MAPKs such as Erks, p38, and JNKs. These MAPKs then regulate downstream target genes. Sprouty (spry)

is an internal regulator of FGF signaling and mainly acts through inhibiting the RAS/MAPK pathway. The PLCγ pathway begins with activation of PLCγ, leading to activation of DAG and IP3. This leads to PKC activation and upregulation of Ca^{2+}, which regulates cytyoskeletal reorganization. FGF signaling also acts through STATs. These various downstream pathways allow for differences in regulation depending on context.

AKT/PKB, protein kinase B; Ca^{2+}, calcium; DAG, diacylglycerol; Erks, extracellular signal-regulated kinases; FGF, fibroblast growth factor; FGFR, fibroblast growth factor receptor; Frs2, fibroblast growth factor receptor substrate 2; Gab1, grb2 associated binding protein; Grb2, growth factor receptor-bound 2; IP3, inositol triphosphate; JNKs, Jun amino-terminal kinases; MAPK, mitogen activated protein kinases; PDK, phosphoinositide dependent protein; PI3K, phosphoinositide 3-kinase; PKC, protein kinase C; PLCY, phospholipase C; Shp2, protein tyrosine phosphatase; Sos1, son of sevenless; Spry, sprouty; STATs, signal transducer and activator of transcription; TF, transcription factor.

1.7.3 Fibroblast growth factor signaling in zebrafish

In zebrafish, there are 27 FGF ligands. The additional number of ligands arose due to a genome duplication even that occurred in teleost fish (Postlethwait et al. 2000). As a restul, some zebrafish FGF ligands have two copies, such as *fgf10a* and *fgf10b*. However, some of these duplicated ligands have been lost over time so that some ligands only have a single copy. All human orthologs have been identified in zebrafish, except for fgf9. With respect to the receptors, zebrafsih have single orthologs for the four known human receptors (Itoh and Konishi, 2007). The specific role of some of these fgf ligands in zebrafish development have been previously identified: *fgf3* and *fgf8* are required for otic placode and vesicle formation (Maroon et al. 2002), *fgf10a* is required for esophageal and swim bladder development (Korzh et al. 2011), *fgf10a, fgf16* and *fgf24* are required for fin bud development (Noruma et al. 2006, Norton et al. 2005, and Fischer et al. 2003), *fgf20a* is required for fin regeneration (Whitehead et al. 2005), and *fgf21* is required for hematopoiesis (Yamauchi et al. 2006). In this dissertation, I show that FGF signaling is required for normal ENS development in zebrafish.

1.7.4 Previous implications of fibroblast growth factor signaling in enteric nervous system development

Previously, studies have suggested a role for FGF in ENS development. A knockout mouse for FGF receptor antagonist sprout2 yielded a hyperganglionic gut (Taketomi et al. 2005). Additionally, a microarray screen for genes expressed in the ENS showed that *fgf13* has significantly higher expression in non-mutant

mouse intestines (Heanue and Pachnis 2006). Finally, in vitro studies of *fgf2* knockout mouse neurons showed decreased neurite outgrowth as compared to their wild-type counterparts (Hagl et al. 2012), and *fgf2* is expressed in human bowel biopsy tissue (Yoneda et al. 2001).

1.7.5 Hedgehog signaling pathway

In mammals, the Hedgehog (Hh) signaling pathway has three secreted ligands: sonic hedgehog (shh), indian hedgehog (ihh), and desert hedgehog (dhh) (Ingham et al. 2001, Briscoe and Therond, 2013). The gene shh has been shown to have a critical role in the organizing centers in early embryonic development, such as in the limb bud, the floorplate of the neural tube, and the notochord (Cohn and Tickle, 1996, Jessell 2000). Bone and cartilage development is regulated by ihh. Peripheral nerve sheath formation and germ cell development in the testes are both regulated by dhh (Briscoe and Therond, 2013). As seen in Figure 6, the Hh transmembrane receptor Patched (Ptch) constitutively inhibits Hh signaling through the repression of the G-coupled protein receptor Smoothened (Smo). When a Hh ligand binds to Ptch, it stops the repression of Smo and allows for downstream signaling to occur. Once Smo is no longer repressed, a zinc finger family of proteins, Gli, is activated. Gli act as transcription factors that can both repress or activate downstream transcription of target genes. Throughout embryonic development, Hh signaling plays critical and varying roles, such as pattern formation and controlling cell proliferation (Briscoe and Therond, 2013).

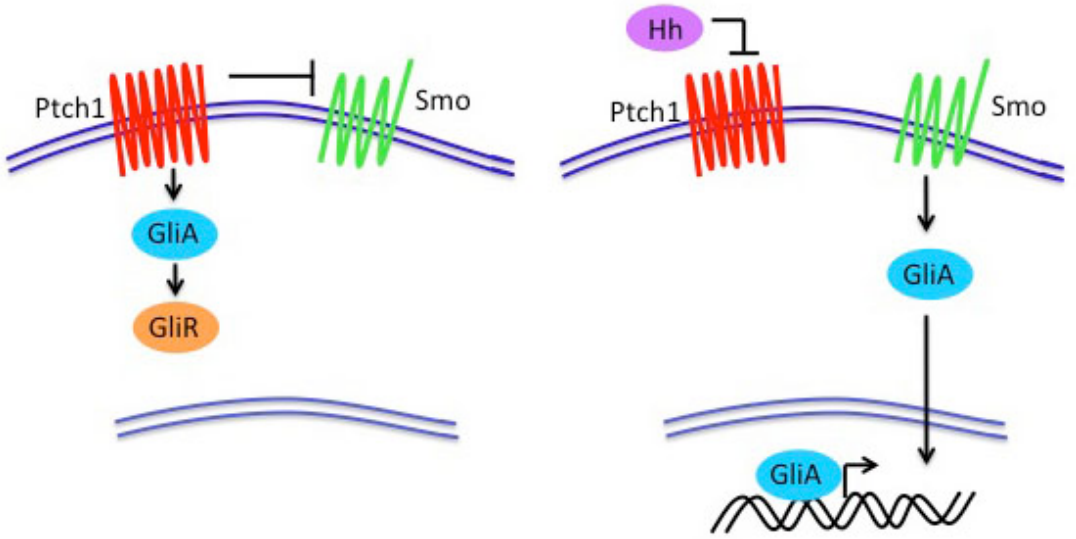

Figure 6: Hedgehog signaling pathway

Patched receptor 1 (Ptch1) represses Smoothened (Smo). This leads to downstream Gli in its repressor state. When a Hedgehog (Hh) ligand binds Ptch1, Smo is no longer repressed, which leads to Gli being in its activator form. Once Gli is an activator it regulates downstream Hedgehog target genes. GliA, gliobastoma transcription factor activator; GliR, gliobastoma transcription factor repressor; Hh, Hedgehog; Ptch1, patched receptor 1; Smo, smoothened.

1.7.6 Hedgehog signaling pathway in zebrafish

Most vertebrate species posses one member from each Hedgehog signaling class: shh, ihh, or dhh (Avaron et al. 2013). However, zebrafish have at least 5 hedgehog genes. There are two from the sonic hedgehog class of genes: shh (Krauss et al. 1993) and tiggywinkle (Ekker et al. 1995); two from the indian hedgehog class of genes: echidna (Currie et al. 1996) and ihh (Avaron et al. 2006); and one from the desert hedgehog class of genes: dhh (Avaron et al. 2006). Ptch, Smo, and Gli proteins are all conserved in zebrafish

1.7.7 Previous implications of Hedgehog signaling in enteric nervous system development

Our lab has previously defined the role of shh in ENS development in zebrafish. shh is secreted in the intestinal endoderm in developing zebrafish and is sufficient to enable enteric neural crest cells to migrate from the vagal region to the foregut (Reichenbach et al. 2008). During this migration, shh is acting as a mitogen and required for these neural crest precursors to migrate to and along the gut tube. shh is also required for the normal proliferation of the enteric neural crest precursors. Additionally, shh is required for normal expression of gdnf, and this perturbation of gdnf when shh is lost leads to the Hirschsprung's like phenotype of the shh knockdown zebrafish. Overall, shh is necessary for ENS development in zebrafish (Reichenbach et al. 2008).

Ihh knockout mice have a Hirschsprung's like phenotype, but the cellular and molecular mechanisms of ihh in ENS development have not been elucidated

(Ramalho-Santos et al. 2000, Garcia-Barcelo et al. 2003). Ihh has been shown to interact with fgf10 in esophageal and swim bladder development. The swim bladder buds off of the developing gut tube, implying a potential role for ihh in gut tube and ENS development (Korzh et al. 2011). In this study, we demonstrate that ihh in required for ENS development in zebrafish, as discussed in Chapter 3.

1.8 INTRODUCTION OVERVIEW

The goal of the digestive system is to digest the food and liquids we eat, absorb the nutrients, and excrete the waste products. The gastrointestinal tract must function properly for us to live. Our small and large intestine have similar anatomy, with the major difference being the presence of villi in the small intestine only. Both intestines contain enteric neurons, which drive muscle contractions, blood flow, and water and electrolyte secretion. When the intestines are malformed in development, it can lead to congenital intestinal diseases. Congenital short bowel syndrome (CSBS), is the loss of the majority of the small intestine, and results in malnutrition and high mortality rates. Hirschsprung's disease is the lack of enteric neurons at the distal region of the large intestine, and requires surgical intervention. Both of these diseases have genetic components that we are attempting to elucidate.

In this work, I show that patients with CSBS were genetically screened and CLMP was identified as a candidate gene. I created an animal model for CSBS and confirmed the causative gene CLMP is sufficient to result in loss of small intestinal development. Additionally we show that fibroblast growth factor and Hedgehog signaling are required for ENS development. The following studies demonstrate the use of zebrafish as a model for CSBS and Hirschsprung's disease.

Chapter 2:

CLMP Is Required for Intestinal Development, and Loss-of-Function Mutations Cause Congenital Short-Bowel Syndrome

Van Der Werf, Christine S. et al, *CLMP Is Required for Intestinal Development, and Loss-of-Function Mutations Cause Congenital Short-Bowel Syndrome*. Gastroenterology, 2012

References provided at the end of the dissertation

CLMP Is Required for Intestinal Development, and Loss-of-Function Mutations Cause Congenital Short-Bowel Syndrome

Christine S. Van Der Werf,* Tara D. Wabbersen,‡ Nai-Hua Hsiao,§ Joana Paredes, Heather C. Etchevers,¶ Peter M. Kroisel,# Dick Tibboel,** Candice Babarit,¶ Richard A. Schreiber,‡‡ Edward J. Hoffenberg,§§ Michel Vekemans,¶ Sirkka L. Zeder, Isabella Ceccherini,¶¶ Stanislas Lyonnet,¶ Ana S. Ribeiro, Raquel Seruca, Gerard J te Meerman,* Sven C. C. Van Ijzendoorn,§ Iain T. Shepherd,‡ Joke B. G. M. Verheij,* and Robert M. W. Hofstra*

*Department of Genetics, § Membrane Cell Biology Section, Department of Cell Biology, University Medical Center Groningen, University of Groningen, Groningen, The Netherlands; ‡ Department of Biology, Emory University, Atlanta, Georgia; The Cancer Genetics Group, Institute of Molecular Pathology and Immunology of the University of Porto, Porto, Portugal; ¶ Département de Génétique, INSERM U781, Hôpital Necker-Enfants Malades, Université Paris Descartes, Paris, France; # Institute of Human Genetics; Department of Pediatric Surgery, Medical University of Graz, Graz, Austria; **Department of Pediatric Surgery, Erasmus MC-Sophia Children's Hospital, Rotterdam, The Netherlands; ‡‡Division of Gastroenterology, BC Children's Hospital, Vancouver, British Columbia, Canada; §§Department of Pediatrics, Section of Pediatric Gastroenterology, Hepatology, and Nutrition, University of Colorado, Denver, Colorado; ¶¶Laboratorio di Genetica Molecolare, Istituto Giannina Gaslini, Genoa, Italy

2.1- ABSTRACT

BACKGROUND & AIMS: Short-bowel syndrome usually results from surgical resection of the small intestine for diseases such as intestinal atresias, volvulus, and necrotizing enterocolitis. Patients with congenital shortbowel syndrome (CSBS) are born with a substantial shortening of the small intestine, to a mean length of 50 cm, compared with a normal length at birth of 190 –280 cm. They also are born with intestinal malrotation. Because CSBS occurs in many consanguineous families, it is considered to be an autosomal-recessive disorder. We aimed to identify and characterize the genetic factor causing CSBS.

METHODS: We performed homozygosity mapping using 610,000 K single-nucleotide polymorphism arrays to analyze the genomes of 5 patients with CSBS. After identifying a gene causing the disease, we determined its expression pattern in human embryos. We also overexpressed forms of the gene product that were and were not associated with CSBS in Chinese Hamster Ovary and T84 cells and generated a zebrafish model of the disease.

RESULTS: We identified loss-of-function mutations in Coxsackie- and adenovirus receptor-like membrane protein (CLMP) in CSBS patients. CLMP is a tight-junction–associated protein that is expressed in the intestine of human embryos throughout development. Mutations in CLMP prevented its normal localization to the cell membrane. Knock-down experiments in zebrafish resulted in general developmental defects, including shortening of the intestine and the absence of goblet cells. Because goblet cells are characteristic for the midintestine in zebrafish, which resembles the small intestine in human beings, the zebrafish model mimics CSBS.

CONCLUSIONS: Loss-of-function mutations in CLMP cause CSBS in human beings, likely by interfering with tight-junction formation, which disrupts intestinal development. Furthermore, we developed a zebrafish model of CSBS.

Keywords: ASAM; Animal Model; Genetic Analysis; Embryology.

Abbreviations used in this paper:

CHO, Chinese hamster ovary; CLMP, Coxackie and adenovirus receptor-like membrane protein; CSBS, congenital short-bowel syndrome; hpf, hours post fertilization; PCR, polymerase chain reaction; RT, reverse transcription; SBMO, splice-blocking morpholino; SBS, short-bowel syndrome; SNP, single-nucleotide polymorphism; TBMO, translation-blocking morpholino; WT, wild type; ZO-1, zonula occludens 1.

Acknowledgments

The authors would like to thank the patients and their families for participating in this study; Jackie Senior for editing the manuscript; and Dr Arrigo Barabino (Paediatric Gastroenterology Unit, G. Gaslini Institute) for providing details about Italian patients, whose samples were obtained from the Cell Line and DNA Biobank from Patients affected by Genetic Diseases at G. Gaslini Institute–Telethon Genetic Biobank Network (project GTB07001).

Conflicts of interest

The authors disclose no conflicts.

2.2- INTRODUCTION

Patients with congenital short-bowel syndrome (CSBS) are born with a shortened small intestine. The mean length of the small intestine in CSBS patients is approximately 50 cm, compared with a normal length at birth of 190 –280 cm. (Fitzsimmons *et al.* 1998, Reiquam *et al.* 1965, Siebert *et al.* 1980). Patients with CSBS may develop severe malnutrition as a result of the hugely reduced absorptive surface of the small intestine. This is similar to acquired short-bowel syndrome (SBS), which results from surgical resection of the small intestine for diseases such as intestinal atresias, volvulus, and necrotizing enterocolitis. CSBS usually is diagnosed by barium-contrast radiographs and confirmed by exploratory laparotomy. Infants with SBS, whether congenital or acquired, need parenteral nutrition to survive, although parenteral nutrition itself causes life-threatening complications such as sepsis and liver failure, and a high rate of mortality early in life. However, some long-term survivors of CSBS have been reported (Huysman *et al.* 1991, Ordonez *et al.* 1996, Hasosah *et al.* 2008, Schalamon *et al* 1999). Because consanguinity frequently is seen in families in whom CSBS occurs, an autosomal-recessive pattern of inheritance is suspected. Until now, nothing was known about the genetic cause of this disease.

Here, we report the identification and characterization of the Coxsackie- and adenovirus receptor-like membrane protein (CLMP) as a gene underlying CSBS.

2.3- PATIENTS AND METHODS

Research Subjects

The CSBS patients included in this study, aged 0 –26 years, were either described previously in the literature or were known to physicians in the field (Huysman *et al.* 1991, Ordonez *et al.* 1996, Hasosah *et al.* 2008, Schalamon *et al* 1999). Patients were born with a shortened small intestine with a length of 30 to 54 cm (Table 1). Patients, of whom some were seen by an experienced clinical geneticist, did not show any other clinical features besides CSBS. All parents were reported as normal. Patients 2-1, 3-1, and 3-2 were from consanguineous families. All patients were Caucasians, except for patients 3-1 and 3-2, who were of Turkish ancestry. The study protocol was approved by the institutional and national ethics review committees at the University Medical Centre Groningen (NL31708.042.10), and written informed consent was obtained.

Homozygosity Mapping

Genomic DNA of all participants was extracted from peripheral lymphocytes by standard methods. A genome-wide scan was performed on 5 patients of families 1– 4 using the Illumina 610,000 single-nucleotide polymorphism (SNP) array (Illumina, San Diego, CA) according to the manufacturer's instructions. Homozygosity mapping was performed by an automatic search for a minimum of 400 markers in a row (~2–3 MB) that were homozygous in at least 3 of the 4 families, and identical for patients 3-1 and 3-2 (because they were from the same consanguineous family).

Mutation Screening

Analysis of the 7 exons of CLMP (NM_024769.2) and the flanking intronic regions was performed in all patients and their parents as well as in 77 Caucasian control individuals (154 control chromosomes). For primer sequences see Table 2. Sequencing was performed (forward and reverse) with dye-labeled primers (Big Dye Terminator v3.1 Sequencing Kit; Applied Biosystems, Foster City, CA) on an ABI 3730 automated sequencer (Applied Biosystems).

In Silico Analysis of the Missense Mutation

After analysis of the CLMP protein sequence (NP_079045.1) with the blastp algorithm (available: http://blast. ncbi.nlm.nih.gov/Blast.cgi), homologous sequences were obtained. The program M-Coffee was used to align them (available: http://www.tcoffee.org) (Moretti *et al.* 2007).

The effect of the missense mutation was evaluated by the Russell method at European Molecular Biology Laboratory (available: http://www.russell.embl-heidelberg.de/aas/)(Betts *et al.* 2003), the polymorphism phenotyping algorithm (http://genetics.bwh.harvard.edu/pph/), and the Sort Intolerant From Tolerant algorithm (http://sift. jcvi.org/).

Functional Analysis of the Splice Site Mutation

To determine the effect of the splice site mutation found in patient 1-1, we performed an exon trapping assay. We first generated polymerase chain reaction (PCR) 2.1-TOPO plasmids (Invitrogen, Carlsbad, CA), containing the sequences

of the exon of interest (wild type or mutant) and the flanking intronic sequences. The sequence of interest was PCR-amplified using either a control or the patient's genomic DNA as the DNA template. We used the primers GGCG-Ecor1, 5′-AAACCTGCAAATACTCATTC-3′, and GACG-BamH1, 5′-AAGTGTTTGTTGAGGATAAG-3′. The amplification was performed using Pushion High-fidelity DNA polymerase (Finnzymes, Helsinki, Finland). The PCR products were inserted into the PCR 2.1 Topo constructs and thereafter digested with BamH1 and EcoR. The inserts from control and mutant subsequently were cloned into the exon trapping vector pSPL3 (Invitrogen). The inserts were checked by direct sequencing.

Human embryonic kidney 293 cells were grown in Dulbecco's modified Eagle medium supplemented with 10% fetal calf serum and 1% antibiotic solution (penicillin/streptomycin; Invitrogen) at 37°C in 5% CO2. Human embryonic kidney 293 cells were plated in 6-well plates containing 6 x 105 cells/well. After 24 hours the cells were transfected with 1 μg of the corresponding plasmid using polyethylenimine (Polyscience, Inc, Warrington, PA) according to the manufacturer's instructions. Transfections of the vector containing the wild-type sequences or the empty pSPL3 vector were used as controls. After 48 hours cells were lysed and RNA was isolated according to the manufacturer's instructions (Qiagen, Venlo, The Netherlands). A total of 5 μg of total RNA was used as a template to synthesize complementary DNA (cDNA) using the cDNA primer pd(N)6 (GE Healthcare, Hoevelaken, The Netherlands). PCR was performed

using the primers (SD6) 5′-CTGAGTCACCTGGACAACC- 3′ and (SA2) 5′-ATCTCAGTGGTATTTGTGAGC-3′, and the following amplification program: 5 minutes at 94°C, 35 cycles for 1 minute at 94°C, 1 minute at 60°C and 5 minutes at 72°C, and a final elongation time of 10 minutes at 72°C. Five microliters of cDNA was used for the PCR in a total volume of 50 μL. PCR products were checked by gel electrophoresis and the exon trapping results were confirmed by direct sequencing.

Expression of Wild-Type and Mutant CLMP in Chinese Hamster Ovary Cells and T84 Cells

A pCMV6-CLMP-green fluorescent protein (GFP) vector was obtained from Origene (Rockville, MD). The missense mutation was introduced in this vector by site-directed mutagenesis (Stratagene, Amstelveen, Santa Clara, CA) (for primer sequences see Table 3). The wild-type (WT) and mutant cDNA were amplified using the primers CCGCC-NheI, 5′- ATGTCCCTCCTCCTTCTCC-3′, and GGGCGC-XhoI, 5′- TCAGACCGTTTGGAAGGCTCTG-3′. The amplification was performed using Pushion High-fidelity DNA polymerase (Finnzymes). The PCR products were inserted into PCR 2.1- TOPO plasmid (Invitrogen). The PCR 2.1 Topo constructs were digested by NheI and XhoI restriction enzymes and the fragments were cloned into the vector pCMV-internal ribosomal re-entry site (IRES) coupled to eGFP (GFP like protein). The clones were checked by direct sequencing.

Chinese hamster ovary (CHO-K1) and human intestinal epithelial T84 cells were grown in commercially available alpha modification of eagle's medium (AMEM) medium and Dulbecco's modified Eagle medium/F-12, respectively, supplemented with 4.5 mg/L L-glutamine, 10% heat-inactivated fetal bovine serum, and 1% antibiotic solution (penicillin–streptomycin; all Invitrogen). The cells were maintained at 37°C in a humidified atmosphere with 5% CO2.

WT or mutant pCMV-CLMP-IRES-EGFP was transfected in CHO-K1 cells and T84 cells (1.5×10^5) with Lipofectamine 2000 Transfection Reagent (Invitrogen) in a 1:3 dilution, and transfection efficiencies were evaluated by measuring EGFP expression by flow cytometry.

To observe the cell localization of CLMP, transfected CHO-K1 cells were stained by immunofluorescence. Cells were cultured on glass coverslips (Becton Dickinson Labware, Franklin Lakes, NJ), and fixed with 4% paraformaldehyde (20 minutes). After fixation, cells were treated with 50 mmol/L NH4Cl for 10 minutes, washed with PBS, and permeabilized with 0.1% Triton X-100 (Sigma Aldrich, Zwijndrecht, The Netherlands) in PBS for 5 minutes at room temperature. Nonspecific binding was blocked by cell treatment with PBS containing 5% bovine serum albumin, for 30 minutes at room temperature. Cells then were stained with a rabbit anti-human CLMP antibody (antiAP000926.6, Sigma HPA002385, Sigma Aldrich), for 1 hour at a 1:100 dilution. An Alexa 594 – conjugated goat anti-rabbit antibody (Invitrogen) then was used as the secondary antibody. After a wash with PBS, each sample was mounted with Vectashield

(Vector labs, Peterborough, United Kingdom) and 4′,6-diamidino-2-phenylindole–stained. The cell staining was observed using a Zeiss microscope (Imager Z1, Zeiss, Sliedrecht, The Netherlands) with apotome, and images were taken using Axiovision software (Zeiss).

Transfected T84 cells were fixed with 4% paraformaldehyde at 37°C for 30 minutes. Cells then were treated with 0.1 mol/L glycine for 10 minutes, washed with PBS, and permeabilized with 0.1% Triton X-100 in PBS at room temperature for 2 minutes. Nonspecific binding was blocked by incubating the cells with PBS containing 1% bovine serum albumin and 0.05% Tween 20 (Sigma Aldrich) at room temperature for 1 minute. Cells were immunolabeled with the rabbit polyclonal antibody for CLMP (anti-AP000926.6, Sigma HPA002385), in 1:100 dilution at 37°C for 1 hour. Cells subsequently were washed 5 times with PBS and incubated with mouse monoclonal anti–zonula occludens 1 (ZO-1) antibodies (Zymed, San Francisco, CA) at 1:100 dilution. An Alexa-546 – conjugated goat anti-rabbit antibody (Invitrogen) and a Cy5-conjugated goat anti-mouse antibody were used as secondary antibodies both at a 1:500 dilution. 4′,6-Diamidino-2-phenylindole (at a 1:1000 dilution) and/or DRAQ5 (Cell Signaling Technology, Leiden, The Netherlands) (at a 1:500 dilution) were used for nuclear staining. After a wash with PBS, samples were mounted and analyzed with a Leica SP2 AOBS confocal laser scanning microscope (Wetzlar, Germany).

CLMP Expression During Human Development

CLMP expression was examined by immunohistochemistry in human embryos and fetal tissue obtained from terminated pregnancies using the mifepristone protocol in concordance with French legislation (94-654 and 08-400) and approved by the Necker Hospital Ethics Committee. Embryonic and fetal tissues were fixed in 4% paraformaldehyde, pH 7.4, or in 11% formaldehyde, 60% ethanol, and 10% acetic acid, embedded in paraffin blocks, and sectioned at 5 μm. Sections were deparaf- finized, rinsed in PBS, and incubated for 30 minutes in 0.5 mol/L ammonium chloride, rinsed again, and nonspecific binding was blocked by 10% fetal calf serum in PBS for 30 minutes. Classic antigen unmasking in citrate buffer was performed for 20 minutes. Slides were incubated overnight at 4°C in a humid chamber with the rabbit primary anti-human CLMP antibody (anti-AP000926.6, Sigma HPA002385) at a 1:50 dilution in PBS with 2% fetal calf serum and then rinsed. A goat anti-rabbit– alkaline phosphatase–conjugated secondary antibody was applied at 1:200 dilution in PBS/2% fetal calf serum, and alkaline phosphatase activity was revealed by the standard nitro-blue tetrazolium chloride (NBT)-5-bromo-4-chloro-3′-indolyphosphate p-toluidine salt (BCIP) chromogenic reaction to reveal the immunolocalization of CLMP. Adjacent sections stained without the primary antibody anti-human CLMP were used as negative controls.

Expression Pattern of Orthologs in Zebrafish and Knock-Down Experiments

Zebrafish were kept and bred under standard conditions at 28.5°C (Westerfield, 1993). Embryos were staged and fixed at specific hours after fertilization (hpf).

Embryos were grown in media supplemented with 0.2 mmol/L 1-phenyl-2-thiourea (Sigma) to inhibit pigment formation (Westerfield, 1993).

A search for the predicted zebrafish orthologs of CLMP was performed in the Ensembl database (available: www.ensembl. org). To clone the complete open reading frames of the zebrafish orthologs, multiple reverse-transcription (RT)-PCR primers were designed to amplify 5′ and 3′ overlapping segments of the open reading frame based on the predicted sequences. The cDNA segments were subcloned and sequenced. Sequencher DNA sequence analysis software (Applied Biosystems) was used to assemble the resulting sequences. Rapid amplification of cDNA ends was used to amplify the 5′ and 3′ ends of the open reading frame. Rapid amplification of cDNA ends was isolated from 72-hpf embryos using a Smart rapid amplification of cDNA ends Amplification Kit (Clonetech, Mountain View, CA). The resulting PCR products were subcloned and sequenced to complete the open reading frame sequence for the orthologs. The continuity of the full-length sequence was confirmed by RT-PCR on single-stranded cDNA isolated from 48-hpf embryos. The orthologs were cloned and the sequences were determined by direct sequencing.

Homology studies were completed using publicly accessible programs from SDSC Biology Workbench (San Diego, CA). ClustalW (SDSC) was used to align the amino acid sequences of both zebrafish orthologs (called CLMPa and CLMPb), rat, and human CLMP (called h.CLMP) (Figure 7).

To determine the temporal expression of CLMPa and CLMPb, RT-PCR was performed at various time points during embryonic and larval development. The primers used amplified a segment of the open reading frame spanning nucleotides 38 – 881 of CLMPa and nucleotides -3 to 851 of CLMPb. The following primers were used: CLMPa forward, 5′-GTGATGTCTGCCAGCGCTCG-3′, CLMPa reverse, 5′- GGGACGACGACAGAGAGTTC-3′, CLMPb forward, 5′-CTGCAGCTGACTGACTCTGG-3′, CLMPb reverse, 5′-GTCTGAAAGGCCTTGCTTTG-3′. The predicted fragment sizes were as follows: for CLMPa, 843 base pairs, and for CLMPb, 854 base pairs. To determine the spatial expression patterns of CLMPa and CLMPb, antisense digoxigenin-labeled probes for both genes were generated and whole mount in situ hybridization was performed as described by Thisse et al (1993).

Two different, nonoverlapping, translation-blocking morpholinos (TBMO), a splice-blocking morpholino (SBMO), and a 5-mispair morpholino were designed to target CLMPa and were generated by gene tools (available: www.gene-tools.com; for morpholino sequences see Table 4). Morpholinos were injected to determine the effects of knocking down CLMPa protein levels (Nasevicisu *et al.* 2000). The morpholinos were diluted in sterile filtered water over a range of concentrations from 1 to 10 μg/μL. Approximately 1 nL of diluted morpholino was injected at the 1- to 2-cell stage using a gas-driven microinjection apparatus. The morpholino dilutions that resulted in a consistent knockdown of CLMPa were as follows: CLMPa TBMO1 (Appendix A) and TBMO2: 2 μg/μL, and SBMO:

1 μg/μL. A p53 translation-blocking morpholino was co-injected at a concentration of 1.5 times the morpholino concentration to rule out the possibility that the morphant phenotype was caused by a cytotoxic side effect of the morpholinos. A negative control 5– base pair mismatch morpholino based on the sequence of TBMO1 was generated and injected at a concentration of 2 μg/μL (Table 4). To verify the effectiveness of the CLMP SBMO, RT-PCR was performed on messenger RNA (mRNA) isolated from SBMOinjected and control embryos. The primers used for RT-PCR were as follows: CLMPaRTPCR forward, 5′-CGCCCTGCTCTTAGTATTGC - 3′; and CLMP-aRTPCR reverse, 5′-GGGGTTTTGATGGCTTCAAG - 3′.

H&E staining was performed on 3-μm paraffin sections from 96 hpf control and SBMO-injected embryos using standard procedures. The sections were heated for 20 minutes at 60°C, deparaffinized, and hydrated to water. The sections were stained in Hematoxylin 7211 (Richard Allan Scientific, Kalamazoo, MI) for 4 minutes, rinsed in water, immersed in Clarifier (Richard Allan) for 1 minute, and rinsed again in water. Subsequently, slides were immersed in Bluing (Richard Allan) for 1 minute, followed by a brief immersion in 95% ethanol, followed by a 45-second immersion in Eosin-Y 7111 (Richard Allan). Slides then were dehydrated in 95% ethanol, followed by absolute ethanol, cleared in xylene, and coverslipped.

For the rescue experiment CLMPa mRNA was made from a pCS2 expression vector containing the complete Open Reading Frame sequence of the CLMPa ortholog. Synthetic mRNA was synthesized using a mMessage mMachine kit (Life Technology, Bleiswijk, The Netherlands).

2.4- RESULTS

Loss-of-Function Mutations in CLMP Cause Congenital Short-Bowel Syndrome

To map the disease gene we performed Illumina 610,000-SNP arrays on 5 patients (1-1, 2-1, 3-1, 3-2, and 4-1; Figure 8A). We identified a homozygous region shared by 4 (patients 2-1, 3-1, 3-2, and 4-1) on 11q24.1, comprising approximately 2 MB and containing 20 genes. In addition, a homozygous deletion in patient 4-1 was identified that involved 5 SNPs (rs7113273, rs7109445, rs4936775, rs7121089, and rs11218981). This deletion leads to a loss of exonic and flanking intronic sequences of exon 2 of CLMP (also called adipocyte specific adhesion molecule [ASAM]). The deletion results in a frameshift and a premature stop codon. Through PCR and direct sequencing we confirmed that 12,483 base pairs were deleted. Direct sequencing of CLMP in the other patients revealed more mutations. Patient 1-1 was compound heterozygous, carrying a paternally derived heterozygous frameshift mutation (c.589delA) in exon 3, leading to a premature stop codon, and a maternally derived heterozygous potential splice donor site mutation (c.1180GA). With an in vitro exon trapping assay, we confirmed that c.1180GA impairs splicing and likely excludes exon 6 (Figure 9). For the WT sequences the exon was trapped, however, for the mutant it was not. Patient 2-1 carried a homozygous missense mutation (c.730TA, p.V124D) in exon 3. This missense mutation of a highly conserved amino acid was predicted to be pathogenic by the Russell, polymorphism phenotyping, and Sort Intolerant From Tolerant programs (Figure 9). In patients 3-1 and 3-2 we did not find any mutations in the coding sequences of CLMP. We did identify a homozygous deletion (on the array) in the first intron of CLMP encompassing SNP rs7115102.

We confirmed the presence of this deletion with PCR and we showed that this deletion co-segregates with the disease phenotype in this family (Figure 9). However, we were not able to fine-map the deletion using primers in the flanking region. PCR using primer sets flanking the deletion yielded the expected PCR product from controls (of around 5 kb), but no PCR product was detected in the patients (Figure 7), whereas a PCR product of around 4 kb was expected. As a result we hypothesized that an inversion might be present as a way to explain the fact that we were not able to amplify the flanking regions. However, using fluorescence in situ hybridization we were not able to identify a large inversion (data not shown), although a small inversion cannot be excluded. Finally, in patient 5-1, we found a homozygous nonsense mutation (c.1025CT, p.R222X) in exon 5. The mutations identified were not reported in any of the known SNP databases and all presumably are loss-of-function mutations (Table 1 and Figure 8), and all were inherited from nonaffected heterozygous parents (data not shown). None of the mutations were found in 154 control chromosomes of Caucasian origin.

CLMP Expression During Human Development

Because CSBS is a developmental anomaly of the intestine we determined the pattern of CLMP expression in the intestine during human embryonic development. Immunostainings on human embryos at 7 and 8 weeks of development (Figure 10A and B) showed that CLMP was highly abundant in the rapidly dividing cells of the central and peripheral nervous systems, the mesenchyme of the frontonasal and mandibular processes, and the

dermamyotome, and critically it was expressed in the endodermal derivatives of the foregut, midgut, and hindgut, and also in the liver, lung, esophagus, and trachea. It was expressed less strongly in the prevertebral condensations and extra-embryonic tissues, and the dorsal head mesenchyme. During midterm fetal stages, 18 and 23 weeks of development (Figure 10C and E), increased immunoreactivity for CLMP was observed in the intestinal crypts while expression continued to be present in all tissues, with the lowest expression in the muscular and interstitial layers. Midterm liver and kidney tissues strongly express CLMP in the parenchyma of the lobules and cortex, respectively (Figure 10D and F). CLMP also was observed in the collecting ducts and to a lesser extent in the bile ducts and ureter.

CLMP expression thus was seen in the intestine during different stages of human development. Because CLMP also was expressed in many other tissues, this argues for functional redundancy with a specific function of CLMP during intestinal development.

Mutation of CLMP Abrogated its Normal Localization at the Cell Membrane

CLMP encodes for a transmembrane protein belonging to the CTX (cortical thymocyte marker) subfamily of the immunoglobulin superfamily. It acts as an adhesion molecule and co-localizes with tight junction proteins (Raschperger *et al.* 2004) To determine whether the missense mutation (c.730TA, p.V124D) affected the normal cell membrane localization, we transfected CHO and T84 cells with pCMV-CLMP-IRES-EGFP constructs. We expressed both the wild-type

protein (CLMP-WT) and the mutant protein (c.730TA, p.V124D, CLMP-mutant). CLMP was localized at the cell membrane when 2 neighboring CHO cells expressed the WT protein (Figure 11A). In contrast, the mutant protein was localized in the cytoplasm (Figure 11B). Similar results were obtained in a human intestinal epithelial cell model (T84 cells) (Figure 11C and D). However, expression of the WT protein in a cell that did not have a transfected neighboring cell resulted in the retention of the protein in intracellular punctate structures (Figure 11E). Because CLMP has been shown to co-localize with tight junction markers, we determined co-localization of CLMP with the tight junction marker ZO-1. Importantly, WT protein showed co-localization with ZO-1, whereas the mutant protein did not (Figure 12B, C, F, and E, arrows). Again, CLMP was localized only to points of membrane apposition when 2 neighboring cells were both transfected. Overexpression of the WT protein did not alter the localization of ZO-1 (compare Figure 12D with E). Instead, expression of the mutant protein resulted in an increased cytoplasmic pool of ZO-1 (Figure 12F).

Together, these results indicate that CLMP plays a role in tight junctions and that the mislocalization of the mutant protein influences the localization of the tight junction protein ZO-1.

A Zebrafish Model for Congenital Short-Bowel Syndrome

To understand the in vivo function of CLMP in intestinal development and gut length determination we investigated the function of CLMP orthologs in the zebrafish model organism. Analysis of the zebrafish genome (Sanger Zv8)

revealed 2 potential zebrafish CLMP orthologs (ENSDARG00000003145 and ENSDARG000 00073678) (Figure 9). The temporal and spatial expression patterns of both orthologs were determined by in situ hybridization (Figure 13A). One ortholog (CLMPa) specifically was expressed in the intestine at 48 and 72 hours after fertilization, while the other ortholog (CLMPb) had a much less pronounced intestinal expression (Figure 13A, arrowheads). To determine whether lossof-function of CLMPa leads to a CSBS-like phenotype in zebrafish, we performed a series of morpholino antisense knock-down experiments. Injection of either a TBMO or an SBMO morpholino targeting CLMPa resulted in a similar phenotype. Both SBMO and TBMO morphants showed a significant developmental delay. Morphants were smaller in overall body length as compared with WT controls. Likewise, the length of the intestine was shorter in CLMPa knockdown embryos than that of control embryos (mean length, 2.5 mm and 1.9 mm for WT vs morphant, respectively; P 7.0637E-06, n 10 vs 9), however, this shortening was proportional to the overall shorter body length of the morphants (mean gut length, 15.36 and 15.5 somites for WT vs morphant, respectively; P .3211, n 11 vs 8). To confirm the specificity of the morpholino we generated an additional translation-blocking morpholino for CLMPa (TBMO2) (Table 4), which caused a similar phenotype to that observed for the original CLMPa TBMO1 and SBMO (data not shown). A 5-base mis-match control morpholino for TBMO1 also was generated and injected and this did not show any phenotype (data not shown). The potential nonspecific cytotoxic side effect of the morpholinos was excluded by co-injection of a p53 translation-blocking

morpholino (Table 4). Critically, the knock-down phenotype was rescued by co-injection of CLMPa mRNA with the SBMO (Figure 13B).

H&E staining of sections of both 96-hpf control embryos and SBMO-injected embryos showed a significant difference in the overall gut morphology (Figure 13C). Goblet cells, which are characteristic of the midintestine in zebrafish, were seen in the control embryos but these cells were absent in the SBMO-injected embryos (Figure 13C, arrowheads). The zebrafish midintestine resembles the small intestine in human beings (Ng *et al.* 2005). This result taken with the overall reduction in intestinal length observed in the morphants suggests that loss of function of CLMPa in zebrafish results in abnormal intestinal development that has some similarities to the CSBS clinical phenotype.

2.5- DISCUSSION

Congenital short-bowel syndrome is a gastrointestinal disorder of which the genetic basis is unknown. Here we report the identification a number of loss-of-function mutations in the CLMP gene in patients with CSBS. The mutations we found are thought to result in a loss of CLMP function owing to nonsense mutations (family 5), frameshift/splicing mutations (families 1 and 4), and in mislocalization of the CLMP protein caused by a missense mutation (family 2). In addition, this missense mutation has an influence on the localization of the tight junction protein ZO-1.

To understand how loss of function of CLMP leads to CSBS, we undertook a series of zebrafish experiments. We showed that a zebrafish ortholog (CLMPa) is expressed in the intestine at 48 and 72 hpf. Knock-down of CLMPa in zebrafish resulted in a very severe phenotype including an affected intestine. A significant reduction in intestinal length was observed in the CLMPa morphants. Furthermore, CLMPa morphants also lacked goblets cells in the midintestine, suggesting that the CLMP function is required for normal small intestine development both in fish and human beings, and suggesting a potential evolutionary conservation in this gene's function.

Given the wide expression of CLMP during both human and zebrafish development (as shown in Figures 10 and 13A) and the severe phenotype observed in the zebrafish CLMPa morphants, it is intriguing that the phenotype in the human families we studied is so discrete. All of the patients we included in

our study did not have additional clinical features besides malrotation and intestinal neuronal dysplasia, which was reported only in patients 3-1 and 3-2. This all argues for functional redundancy of CLMP in human beings.

We have shown that loss-of-function mutations of CLMP underlie CSBS, and we can further speculate on the pathogenesis of this disease. We and others have shown that CLMP co-localizes with tight junction proteins. It is known that overexpression of CLMP in CHO cells induces cell aggregation, and overexpression of CLMP in MadinDarby canine kidney cells enhances transepithelial resistance.13 Thus, CLMP might play a crucial role in tight junction formation and functions. Because tight junction markers such as ZO-1 and its interacting protein zonula occludens 1 (ZO-1)-associated nucleic acid binding protein play an important role in cell proliferation (Balda *et al.* 2007, Matter *et al.* 2003), loss of function of CLMP also may play a crucial role in downregulation of proliferation of the small intestinal epithelial cells during human intestinal development, resulting in the CSBS phenotype. Because CLMP also is expressed in the small intestine in adults (Raschperger *et al.* 2004). CLMP might have an important function in adult life. Potentially, CLMP may play a role in the intestinal elongation process that occurs during a person's lifetime (the length of the intestine in adults is 600 cm on average, range, 260 – 800 cm2) and in the intestinal adaptation process after surgical resection. The effects on intestinal adaptation of growth factors such as growth hormone, keratinocyte growth factor, epidermal growth factor, and glucagon-like peptide-2 on intestinal adaptation have been studied (Wales *et al.* 2010, Yang *et al.* 2003, Kato *et al.*

1998, Martin *et al.* 2006) Further studies will elucidate the role of CLMP in intestinal adaptation in adults and its therapeutic potential.

2.6- FIGURES AND FIGURE LEGENDS

Table 1. Clinical and Molecular Data From All Congenital Short-Bowel Syndrome Patients

Family	Patient	Ethnicity	Consanguinity	Sex	Length of small bowel at birth, *cm*	Additional features	Mutations
1	1-1 (ref 5)	German-American	Unknown	Female	30		c.230delA (p.E77Gfsx24), exon 3 Heterozygous frameshift c.821G>A, exon 6 Heterozygous splice site mutation
2	2-1	Italian	+	Male	Unknown		c.371T>A (pV124D), exon 3 Homozygous missense mutation
3	3-1 (ref 7)	Turkish	+	Male	47	Intestinal neuronal dysplasia	Homozygous deletion (with presumed inversion) in intron 1
	3-2	Turkish	+	Female	Unknown	Intestinal neuronal dysplasia	Homozygous deletion (with presumed inversion) in intron 1
4	4-1 (ref 4)	Dutch	Unknown	Female	54		Homozygous deletion of 12483 bp (including exon 2)
5	5-1 (ref 6)	Canadian	Unknown	Male	50		c.666C>T (p.R222X), exon 5 Homozygous nonsense mutation
	5-2	Canadian	Unknown	Female	Unknown		c.666C>T (p.R222X), exon 5 Homozygous nonsense mutation

Table 1: Clinical and Molecular Data From All Congenital Short-Bowel Syndrome Patients

Supplementary Table 1

Primer Sequences for CLMP Mutation Analysis

Exon	Forward	Reverse	PCR product size, *bp*
1	AGGAGGCAACCATGTGGTTC	ACAATCTCGATGGCCGACTG	580
2	CACTTGCCCACGGGAACATC	GCCACCACACCCAGCAATAC	443
3	AAGGCAGGCTGAGAGTTACG	CGAGGTGACCTCTGAATGTG	383
4	AAACAGCACCACTGGAGTTG	AATGGCAGTTCAGGAGGTTC	512
5	GCATTACGGAATCTCAGCTCAG	GGCCAGTCAATTGTTGAGTG	402
6	AAACCTGCAAATACTCATTC	AAGTGTTTGTTGAGGATAAG	455
7	TACGAGGAAGCACCTATGAC	GTGACTTGAGCTCCAATGAC	525

NOTE. Primer sequences are 5′→ 3′. PCR conditions were as follows: 35 cycles of denaturation at 95°C for 1 minute, annealing at 60°C for 1 minute, and polymerization at 72°C for 1 minute.

Table 2: Primer Sequences for CLMP Mutation Analysis

Supplementary Table 2

Primer Sequences for Side-Directed Mutagenesis of pCMV6-CLMP-GFP Vector

Target	Primer sequence, 5′→ 3′	Base pair change	Amino acid change
Forward primer	CGCTACGTGTGGAGCCATGACATCTTAAAAGTCTTAG	T → A	Val125Asp
Reverse primer	CTAAGACTTTTAAGATGTCATGGCTCCACACGTAGCG	A → T	Val125Asp

Table 3: Primer Sequences for Site-Directed Mutagenesis of pCMV6-CLMP-GFP Vector

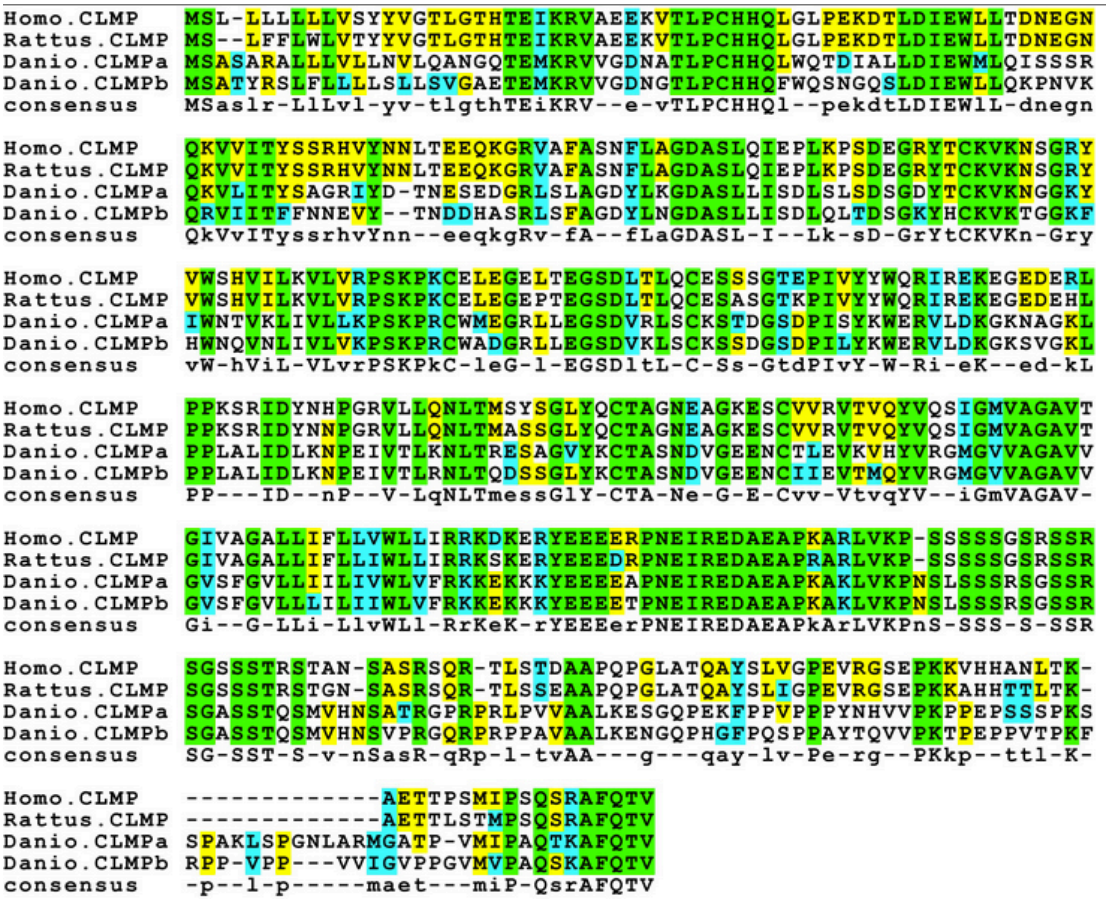

Figure 7: CLMP alignment for human, rat, and zebrafish

Supplementary Table 3

Morpholino Sequences

Morpholino sequences, 5′→ 3′	
First translation blocking morpholino	CGGACTGGGAATCCAACACAAATGT
Second translation blocking morpholino	CTGCTTTGCTCCTCAAACCGAACAC
5 mispair morpholino	CTcCTTTcCTgCTCAAAgCcAACAC
Splice blocking morpholino	GGCACACACCAGCACTCACCACTTT
p53 translation blocking morpholino	GCGCCATTGCTTTGCAAGAATTG

Table 4: Morpholino Sequences

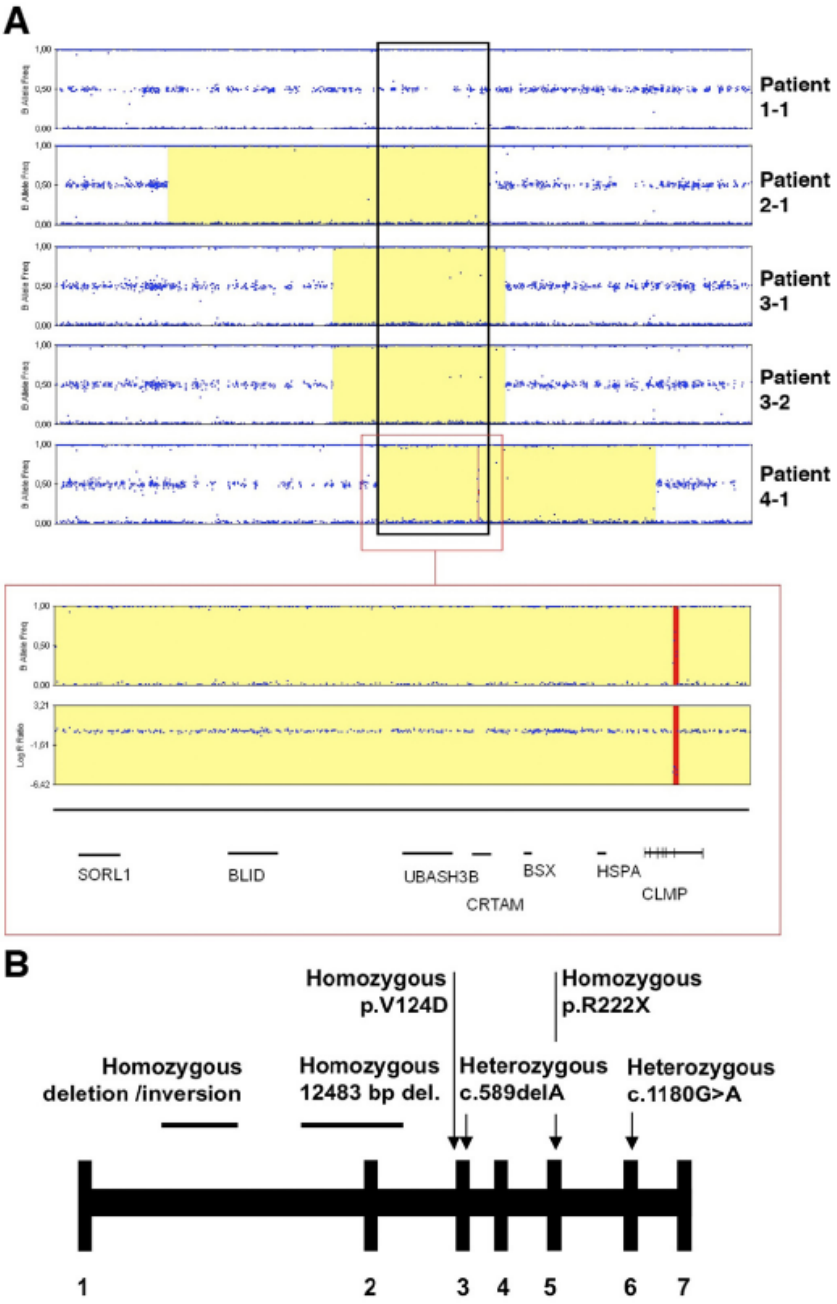

Figure 8: Identification of loss of-function mutations in CLMP in congenital short-bowel syndrome patients

(A), An overlapping homozygous region (yellow bars) was found in 4 of the 5 patients on the array. A homozygous deletion (red bars) concerning exon 2 of

CLMP was detected in patient 4-1. (B) An overview of CLMP with its 7 exons and all the identified mutations.

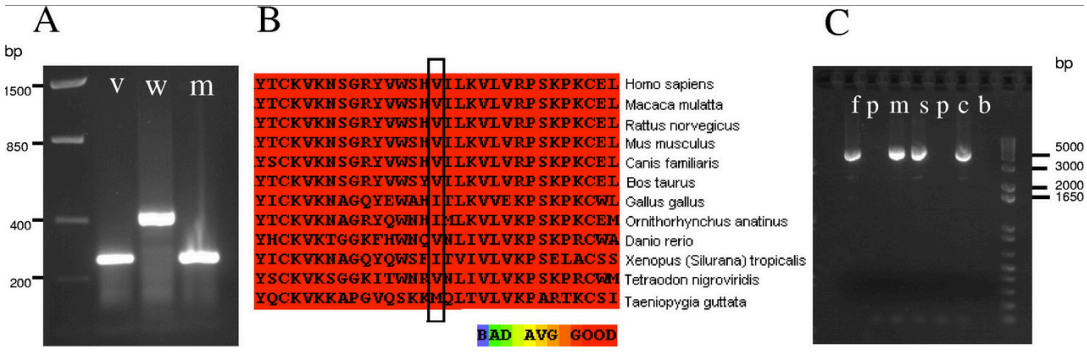

Figure 9: Conservation and intronic deletion in family 3

(*A*) Hek293 cells were transfected with the pSPL3 vector only (V), the pSPL3 vector with the wild-type sequence of exon 6 and its flanking sequences (W), and the pSPL3 vector containing the sequences of exon 6 and the presumed splice site mutation (M). The results of the amplification of the cDNA made of the mRNA of these transfected cells using the splice acceptor side and splice donor side primers are shown. The exon has been trapped in the wild-type situation (W), but has not been trapped in the mutated situation (M). This means that the splice site mutation affects the splice donor site so that it is not recognized by the splicing machinery. (*B*) The missense mutation found in patient 2-1 affects a codon that is evolutionary highly conserved. In the figure it can be observed that this amino acid and all the surrounding amino acids are colored red (labeled as good). Good indicates highly conserved, bad (blue) means not conserved. (*C*) A homozygous deletion surrounding SNP rs7115102 in intron 1 was detected in patients 3-1 and 3-2. PCR yielded results for the parents (f, father; m, mother) as well as for the unaffected sibling (s) and for the control (c), but no PCR product was detected in the patients (p). Lane b (b = blanco, negative control) is a PCR without adding DNA. By using primers flanking the deletion (forward, 5′-

ATTGGAGGATGTGACCTCTGAGTCTTATGG-3′ and reverse, 5′-GGCAGAGAAAGTGGGAAACCTATAGTAAGC-3′) the PCR product was expected to be approximately 5 kb for the normal situation. By using small sets of primer pairs surrounding SNP rs7115102, a region of around 1 kb could not be amplified in the patients. Therefore, the PCR product in the patients was expected to be around 4 kb. Because there is no PCR product from the patients' DNA at all, this is indicative of a more complex alteration than the simple deletion detected by the SNP array.

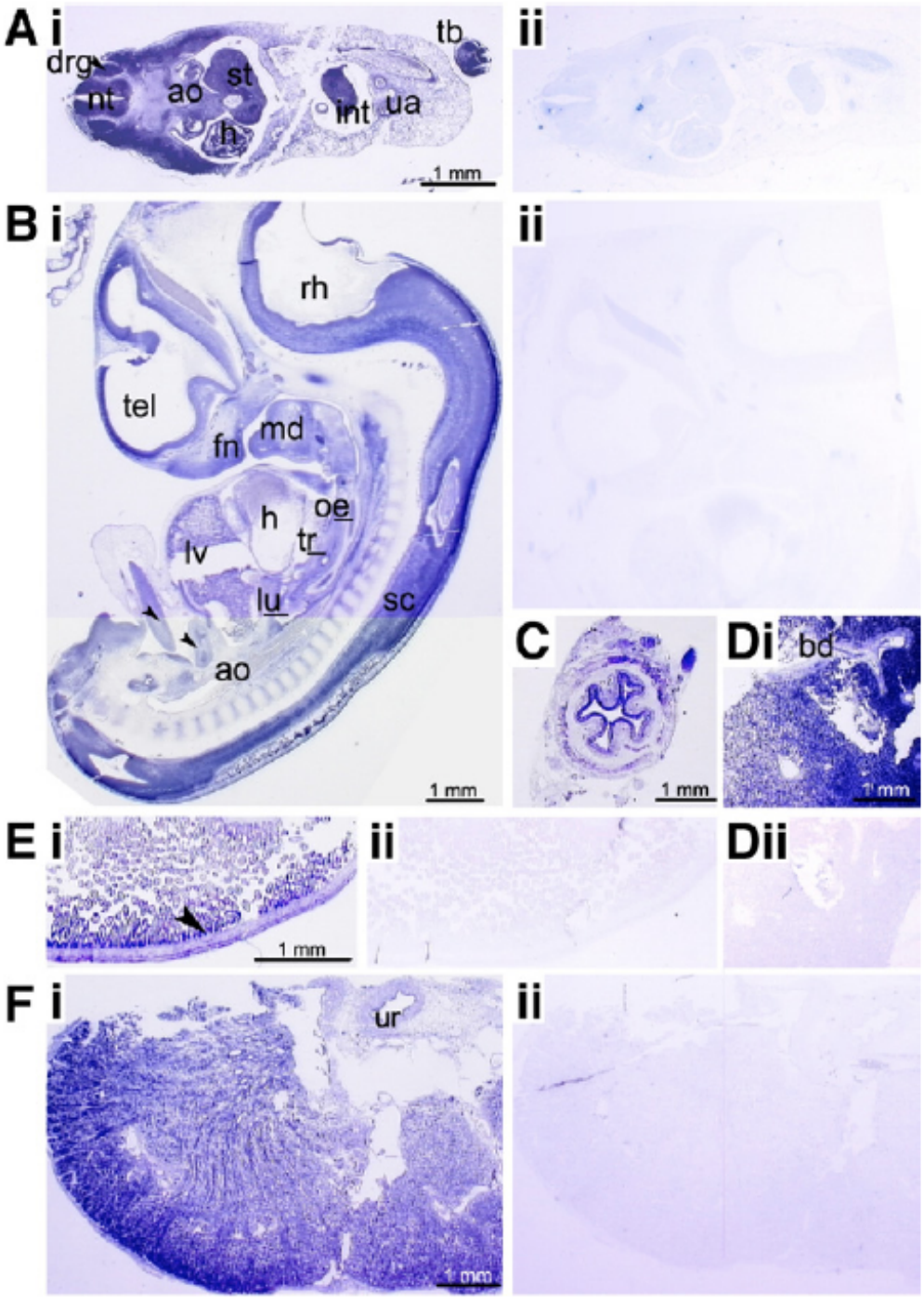

Figure 10: Immunohistochemistry of CLMP on human embryo and fetal tissues shows expression of CLMP in the intestine and in many other tissues

(A) Carnegie stage 15 (circa 33–36 days post-fertilization), cross-section, dorsal to left (and right, for tail bud). CLMP protein was expressed strongly by all embryonic tissues and the umbilical cord. Panels Aii-Fii: adjacent sections to panels A, B, and D–F, nonspecific immunoglobulin-negative controls. (B) Carnegie stage 18 (circa 44 days post-fertilization), parasagittal section, dorsal to right. CLMP protein was abundant throughout the central and peripheral nervous systems, through the endodermal layer derivatives of the foregut, midgut, and hindgut including the liver, lung, esophagus, and trachea, and in the mesenchyme of the frontonasal and mandibular processes. (C and E) Cross- and tangential sections, respectively, of the small intestine and a portion of the large intestine at 18 weeks of development, with increased immunoreactivity in the crypts. (D) Liver parenchyme at 21 weeks of development strongly expressed CLMP, which also was present but to a lesser degree in the bile ducts. (F) Cross-section of kidney at 23 weeks of development, showing medullocortical expression gradient with more CLMP in the glomeruli than the collecting ducts, and only light expression in the ureteral smooth muscle. ao, aorta; bd, bile duct; drg, dorsal root ganglion; fn, frontonasal process; h, heart; int, midgut intestinal herniation (arrowheads in panel B); lu, lung; lv, liver; md, mandible; nt, neural tube; oe, esophagus; rh, rhombencephalon; sc, spinal cord; st, stomach; tb, tailbud; tel, telencephalon; tr, trachea; ua, umbilical arteries; ur, ureter. Scale bar: 1 mm.

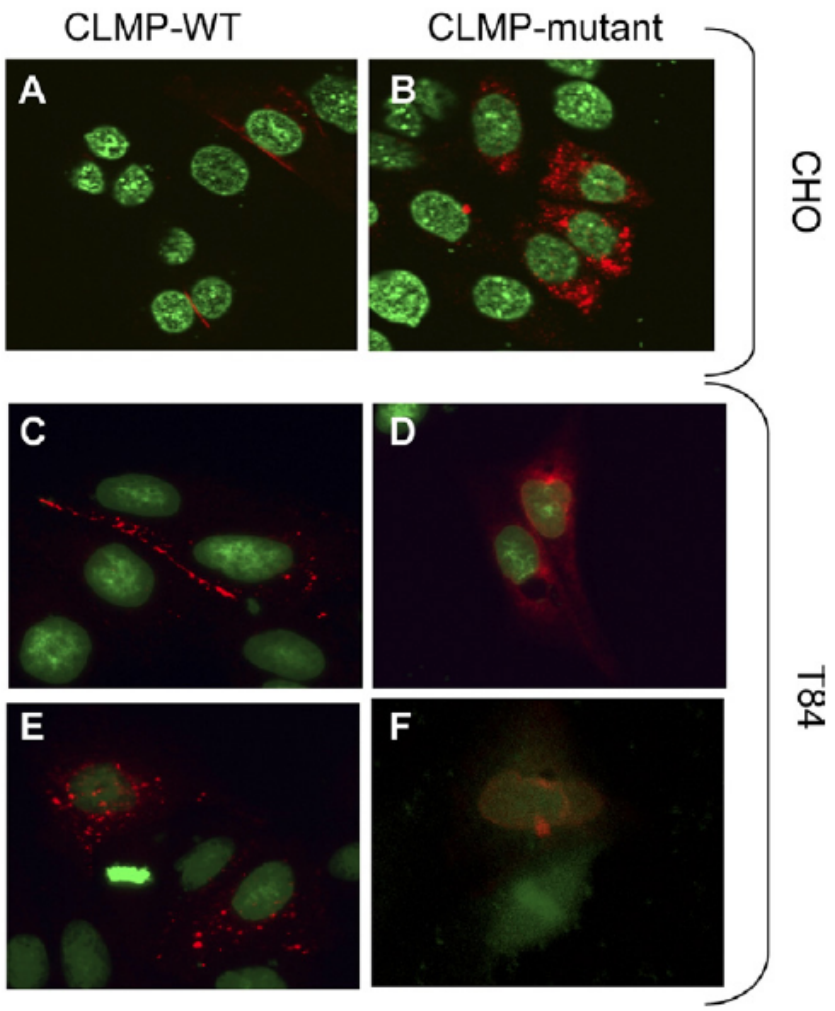

Figure 11: CLMP mutant (c.730TA, p.V124D) abrogated the normal cell membrane localization of CLMP when transiently expressed in CHO and human intestinal epithelial T84 cells

(A), CLMP-WT localized to the cell–cell contact area of CHO cells. (B) In contrast, CLMP mutant did not localize at the cell membrane but in the cytoplasm. (C) CLMP WT localized at the cell membrane of human intestinal epithelial T84 cells, (D) whereas CLMP mutant did not. (E) Expression of CLMP WT in a cell that did not have a CLMP-expressing neighbor cell caused an

intracellular retention of CLMP in punctate structures. (F) CLMP mutant did not show these structures.

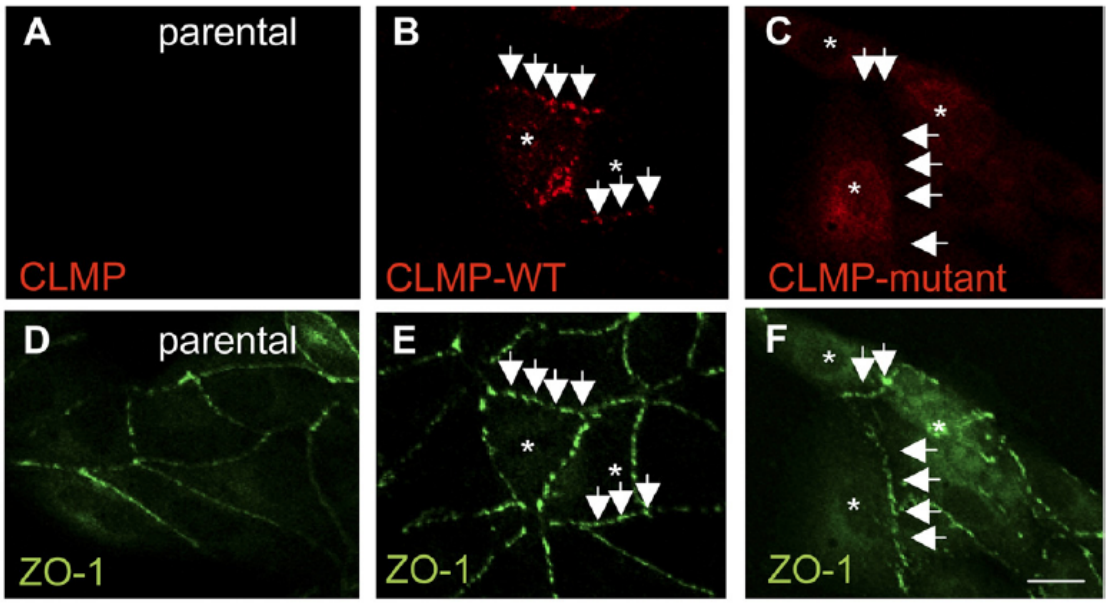

Figure 12: WT CLMP co-localizes with ZO-1 and CLMP mutant (c.730TA, p.V124D) resulted in an increase of cytoplasmic ZO-1 when transiently expressed in human intestinal epithelial T84 cells

(A) T84 cells do not express CLMP endogenously. (B) CLMP WT co-localized with the tight junction–associated protein ZO-1 (compare to E, arrows). (C) CLMP mutant failed to co-localize with the tight junction–associated protein ZO-1. (D) Endogenous expression of ZO-1 in T84 cells. (E) Expression of CLMP WT did not visibly alter the localization of ZO-1 (compare to D). (F) The intracellular expression of CLMP mutant resulted in an increased cytoplasmic pool of ZO-1 that overlapped with CLMP mutant, but did not inhibit the localization of ZO-1 at the cell membrane (arrows).

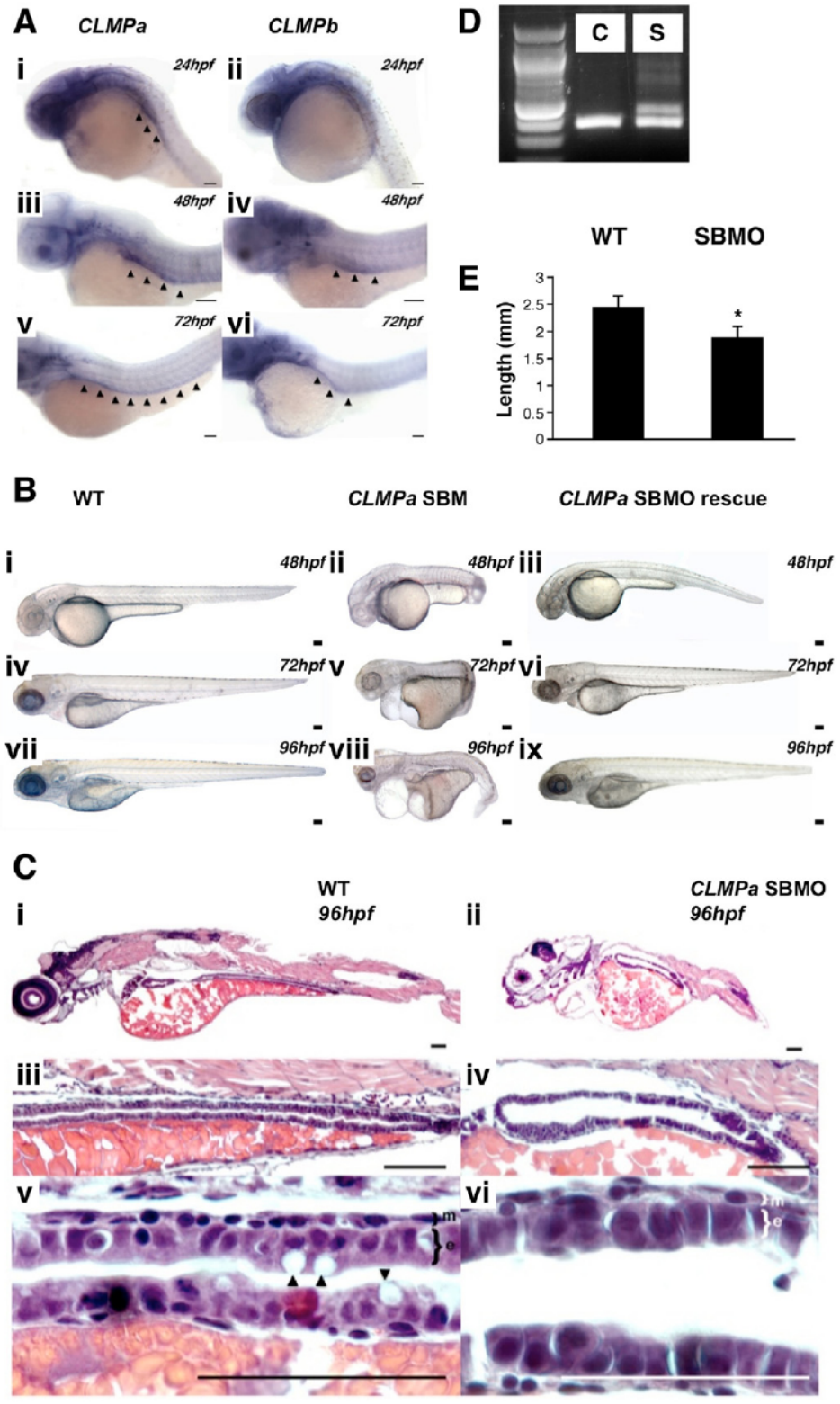
A
CLMPa
CLMPb
i
24hpf
ii
24hpf
iii
48hpf
iv
48hpf
v
72hpf
vi
72hpf
D
C
S
WT
SBMO
E
Length (mm)
3
2.5
2
1.5
1
0.5
0
*
B
WT
CLMPa SBM
CLMPa SBMO rescue
i
48hpf
ii
48hpf
iii
48hpf
iv
72hpf
v
72hpf
vi
72hpf
vii
96hpf
viii
96hpf
ix
96hpf
C
i
WT
96hpf
ii
CLMPa SBMO
96hpf
iii
iv
v
vi
m
e

Figure 13: CLMPa ortholog is expressed in the intestine of zebrafish embryos and knock-down of this ortholog results in a shortened and maldeveloped intestine

(A) 24 hpf (I, II), 48 hpf (III, IV), and 72 hpf (V, VI) whole mount in situ hybridized zebrafish embryos hybridized with either CLMPa (I, III, V) or CLMPb (II, IV, VI) antisense riboprobes. Arrowheads (I, III, IV, V, VI) indicate intestinal expression of CLMP orthologs. (B) Effect of CLMPa SBMO on morphologic development. Lateral views of control (I, IV, VII) CLMPa SBMO alone (II, V, VIII) and CLMPa SBMO plus CLMPa mRNA– (III, VI, IX) injected embryos at 48 hpf (I, II, III), 72 hpf (IV, V, VI) and 96 hpf (VII, VIII, IX). (C) H&E-stained parasagittal cross-sections of 96 hpf control (I, III, V) and CLMPa morphant (II, IV, VI) embryos. Arrowheads (V) indicate goblet cells. Intestinal muscle layer (m) and intestinal epithelia (e) are indicated (V, VI). (D) Knock-down of CLMPa verified by RT-PCR. Spliceblocking morpholino–injected embryos (S) show abnormal RT-PCR products as compared with the WT embryos (C). (E) The length of the intestine of the SBMO-injected embryos was significantly shorter. All scale bars: 50 μm.

Chapter 3:

Fibroblast growth factor and hedgehog signaling are required for enteric nervous system development in zebrafish

Fibroblast growth factor and hedgehog signaling are required for enteric nervous system development in zebrafish

Tara D. Wabbersen, Iain T. Shepherd

Department of Biology, Emory University, 1510 Clifton Rd. Atlanta GA, 30322

Keywords: fibroblast growth factor, indian hedgehog, sonic hedgehog, enteric nervous system, neural crest, cell migration, zebrafish

References provided at the end of the dissertation

3.1 ABSTRACT

The enteric nervous system (ENS) is formed from neural crest precursors. Fibroblast growth factor (FGF) signaling has been previously implicated in ENS development, however a definitive role for this signaling pathway has not been elucidated. Using the zebrafish model system we have determined the expression pattern of several FGF pathway components during gut development by in situ hybridization and RT-PCR. Subsequently, we have used the pharmacological inhibitor su5402 to perturb FGF signaling during ENS development. Zebrafish that were treated with su5402 from 24-120hpf had an 85.5% reduction in the number of enteric neurons at 120hpf, demonstrating a role for FGF signaling during ENS development. Shorter periods of drug treatments revealed that FGF signaling is required for proper vagal neural crest migration in zebrafish ENS development. Whole-mount in situ hybridization showed that enteric neural crest precursors from drug-treated embryos failed to migrate from the vagal neural crest to the anterior gut. Consequently, many fewer enteric neurons are present in the gut, which directly implicates FGF in the aganonglionic phenotype. To determine if FGF is interacting with other pathways previously suggested to play a role in ENS development, we used quantitative real time PCR. This revealed a potential interaction between FGF signaling and hedgehog signaling. We show that hedgehog signaling, specifically the indian hedgehog ligand, is also required for enteric neural crest migration in ENS development in zebrafish. In summary, we demonstrate that FGF and Hh signaling are required for vagal neural crest migration to the anterior gut during enteric nervous system development in zebrafish.

3.2 INTRODUCTION

Development of an enteric nervous system (ENS) during embryogenesis is required for the formation of a functional gut (Furness 2006). In all vertebrate species the ENS is derived from neural crest cells, primarily from the vagal region (Le Douarin and Kalcheim 1999, Burns 2005, Heanue and Pachnis 2007, Newgreen and Young 2002b). Enteric neural crest cells (ENCCs) migrate from the vagal region to the anterior end of the gut then migrate rostro-caudally along the developing gut. ENCCs proliferate as they migrate and differentiate into various neuronal subtypes (Furness 2006). The migration, proliferation, and differentiation of ENCCs are regulated by cell-cell and cell-environmental interactions. When ENCCs fail to properly populate the gut it can result in colonic aganglionosis, or the lack of neurons in the distal colon (Heanue and Pachnis 2007, Newgreen and Young 2002a,b). The best known human condition in which a disturbance of the ENS is underlying the disease is Hirschsprung's disease (HSCR) (Brooks et al. 2005, Gershon and Ratcliffe 2004).

Mutations in multiple different signaling pathways have been implicated in ENS development in various model systems, including GDNF (Cacalano et al 1998, Enomoto et al 1998, Moore, et al, 1996, Pichel et al 1996, Schuchardt et al 1994), BMP2/4 (Chalazonitis et al, 2004, Goldstein et al 2005, Sukegawa et al 2000, Wu and Howard 2002), Endothelin-3 (Baynash et al 1994, Hosoda et al 1994, Yanagisawa et al 1998) Neurturin (Heuckeroth et al 1999, Heuckeroth et al. 1998, Rossie et al 1999), among others. Perturbation of the function of these signaling pathways lead to defects in ENS development. Furthermore mutations in genes

encoding components of these pathways have been identified in HSCR patients (Amiel and Lyonnet 2001, Brooks et al 2005, Puri et al 1998).

In addition to these signaling pathways, fibroblast growth factor (FGF) signaling pathway has also been implicated as having a role in ENS development. The FGF pathway is a large family of signaling molecules that plays many critical roles in early embryonic development of many species. FGF is known for its roles in induction as a mitogen and regulating the migration of various different cells types (Silverio et al. 2007, Dorey and Amaya, 2010, Doseenbach et al. 2001). However the precise role of FGF signaling in ENS development has not been determined.

Previous studies have shown that a null mutant mouse for the FGF receptor antagonist *sprouty2* has enteric hyperganglionosis (Taketomi et all 2005). Furthermore, biopsy tissue from humans showed FGF2 expression in enteric neurons in the bowel (Yoneda et al 2001) and in vitro studies of FGF2 knockout mice showed decreased neurite outgrowth as compared to wild-type controls (Hagl et al. 2012). In addition a microarray screen for genes expressed in the ENS found *fgf13* to have higher expression in non-mutant mouse intestines (Heanue and Pachnis 2006). Due to this potential involvement of FGF signaling in ENS development, we have used the zebrafish model system to investigate FGF function in vivo during ENS development.

In this work we have investigated the role of FGF signaling in zebrafish ENS development. We show that multiple genes in the FGF pathway are expressed in

the developing gut. Additionally, we show that blocking FGF signaling, using the FGF inhibitor su5402, causes a failure of ENCCS migration to and along the developing gut, resulting in aganglionosis. We also show that while there is an increase in apoptosis in the vagal neural crest region when FGF signaling is inhibited, this does not cause the ENS phenotype associated with interfering with FGF signaling. Instead perturbation of FGF signaling causes either decreased proliferation or misspecification of the pre-enteric ENCCs in the vagal neural crest. Finally, we present data that shows that FGF interacts with the hedgehog signaling pathway and that Indian Hedgehog (IHH) is also required for ENS development.

3.3 METHODS AND MATERIALS

Zebrafish Maintenance and Breeding

Zebrafish were raised and kept at standard laboratory conditions at 28.5°C (Westerfield, 1993). Embryos were staged and fixed at specific hours post fertilization (hpf) as previously described I (Kimmel *et al.* 1995). To inhibit pigment formation, embryos were incubated with 0.2mM 1-phenyl-2-thiourea (Sigma). The [*Tg(hsp70:dn-fgfr1*]^{pd1} (Lee *et al* 2005) strain was obtained from Kenneth Poss.

Reverse Transcription PCR

Embryos were allowed to develop to the appropriate stage then euthanized and stored in RNAlater (life technologies). RNA was then extracted from isolated guts and whole embryos using the RNeasy mini kit (Qiagen). Reverse-transcription PCR was completed using the One-Step RT-PCR Kit (Qiagen). PCR products were run on 1.2% agarose gels with ethidium bromide and visualized with a UV source.

Embryonic Gut Dissections

Embryos were collected and staged appropriately. MS-222 (Sigma) was used to anesthetize embryos. Gut tissue was preserved in RNAlater (life technologies).

Whole-mount *in situ* hybridizations

Embryos were collected and processed for whole-mount in situ hybridization as previously described (Thisse et al. 1993). To clone FGF signaling pathway

products for the production of riboprobes, primers were designed as follows: *fgfr1*: F5' GCTTTGCTCAGGGACTCAAC 3', R5'CACCTCCAGGTACGTCTGGT 3', *fgfr2*: F5' AGCCTCTCCAACGTTCTCAA 3', R5' CCGGAGGCAGTGTTATGTTT 3', *fgfr4*: F5' GAAAAGGGGCACATGAGTGT 3', R5' GCCTGACCAGCTGAGTTTTTC 3', *fgf3*: F5'GCTTCTTGGATCCGAGTTTG 3', R5' GGAAGAGGGAAGCTTTGTCC 3', *fgf8*: F5' AATCCGGACCTACCAGCTTT 3', R5' CACATCCTGTGCTTCGCTTA 3', *fgf10*: F5' TCAGAGCTCAGTCTGCTCCA 3', R5' CGAACACAGGAACAGAAGCA 3', *fgf13a*: F5' ATTTGCAGCTCCAAGCAGAT 3', R5' GAGGTTTTGGTGAAGGCGTA 3', *fgf13b*: F5' GCTGCTTTGGATGTCTGTGA 3', R5' AGCGGTGGTTATGTGGACTC 3', *sprouty2* F5'ACTTTTGGGAATTGCAGGTG 3', R5' CCAGTTTTTGCCAATCCACT 3', *ihh*, F5' GAATTTTACGCACGGACGAT 3', R5' CGTAATGCAGCGAATCTTCA 3'. *phox2b, gdnf, crestin, shh, pdx1, foxa1, hand2, insulin* and *etv5b* probes were previously made in our lab. PCR products were run on a 1.2% agarose gel, extracted using the QIAquick Gel Extraction Kit (Qiagen) and ligated into TOPO TA pCR 2.1-TOPO vector (life technologies) to create templates. Digoxigenin-labeled riboprobes used in this study were synthesized from templates linearized and transcribed as follows: *fgfr1:* NotI, SP6*, fgfr2:* SpeI, T7*, fgfr4:* NotI, SP6*, fgf3:* NotI, SP6*, fgf8:* SpeI, T7*, fgf10:* NotI, SP6*, fgf13a:* SpeI, T7*, fgf13b:* NotI, SP6*, sprouty2:* SpeI, T7*, ihh:* NotI, SP6. Digoxigenin-labeled probes were visualized with NBT/BCIP coloration reactions.

su5402 treatments

su5402 (Santa Cruz Biotech) was dissolved in DMSO to create a 3.3 mM stock. The stock solution was diluted to a working solution of 5 μM. Embryos were

soaked in DMSO or su5402 containing embryo medium at 28°C for corresponding times. Media containing su5402 was replaced with fresh embryo media for treatments shorter than the final time point. Embryos were incubated until the appropriate developmental stage then fixed and processed as appropriate for the specific experiment.

Immunohistochemsitry

Embryos were processed for immunohistochemistry as previously described (Raible and Kruse, 2000). Differentiated neurons were visualized using the anti-Elv antibody (Molecular Probes). Cells undergoing apoptosis were labeled with anti-caspase3 rabbit polyclonal antibody (BD Biosciences). Proliferating cells were revealed with an anti-phosphohistone H3 (PH3) rabbit polyclonal antibody (Sigma). The anti-Elv antibody was visualized with an Alexa Fluor 568 anti-mouse IgG (Molecular Probes), while the anti-caspase3 and anti-PH3 antibodies were visualized with an Alexa Fluor 568 anti-rabbit IgG (Molecular Probes).

Quantitative real time PCR

qRT-PCR analysis was carried out using the iScript One-Step RT-PCR Kit with SYBR Green (BioRad). All real time assays were carried out in triplicate using a CFX96 Real-Time System with C1000 Thermal Cycler (BioRad). Forty amplification cycles were performed with the following parameters: RT step, 10 minutes, 50°C; PCR activation step, 5 minutes, 95°C; 2 step cycling: Denaturation, 10 seconds, 95°C, and combined annealing and extension, 30 seconds, 60°C. Primers were designed as follows: *elf1a*: F5'

CTGGAGGCCAGCTCAAACAT 3', R5' ATCAAGAAGAGTAGTACCGCTAGCATTA 3', *gdnf*: F5' TAGCCACGTGTTTGTTGCTC 3', R5' TTTGGGTTTGAGGTTTCAGG 3', *shh*: F5' CCACTACGAGGGAAGAGCTG 3', R5' GAGCAATGAATGTGGGCTTT 3', *ihh*: F5' CGGCTCATCTGCTGTTTGTA 3', R5' TGGACACCACACACTGACCT 3', *etv5b*: F5' CCCTTATCAACGCCAGATGT 3', R5' GGATCCCACCATTTCCTTTT 3', *ptch1*: F5' TCTGACTGGTGGCTGCTATG 3', R5' TGCTCGTACATCTGCTTTGG 3', *ptch2*: F5' CCATCCATGGTCCTATCCAC 3', R5' CAGATTCCAGCGAAAGAAGG 3', *fgf10*: F5' TCAGAGCTCAGTCTGCTCCA 3', R5' TCTAATCCCTGCTGTGTCCA 3'. All analyses included a reverse transcriptase control and a template control.

Embryonic microinjections

ihh morpholino (Gene Tools) was designed to target the transcription start site as previously described (Korzh et al. 2011). The sequence of the *ihh* morpholino is as follows: 5' GGAGACGCATTCCACCGCAAGCG 3'. *p53* control morpholino (Gene Tools) designed to suppress apoptotic effects induced by morpholinos was used as previously described (Robu et al. 2007). The sequence of the *p53* morpholino is as follows: 5' GCGCCATTGCTTTGCAAGAATTG 3'.

The morpholinos were resuspended in sterile filtered water and diluted to working concentrations of 100μM. Approximately 1 nl of diluted morpholino was injected into 1-to 2-cell embryos using a gas-driven microinjection apparatus.

Heat shock treatments

Tg(*hsp70:dn-fgfr1-EGFP*)^{pd1} fish were obtained from the Poss laboratory (Lee et al. 2005). pd1 embryos were treated at 37°C for one hour per 24 hour period. For embryos undergoing a single heat shock, this hour treatment occurred at 30hpf. For embryos undergoing daily heat shocks, hour treatments occurred at 30hpf, 54hpf, 78hpf, and 102hpf. When not being heat treated, embryos were maintained at 28°C.

3.4 RESULTS

Expression of FGF signaling pathway components during ENS development

Previous studies have suggested a role for FGF signaling in ENS development (Taketomi et all 2005, Yoneda et al 2001, Hagl et al. 2012, Heanue and Pachnis 2006). Consequently, we performed RT-PCR and whole-mount in situ hybridization to determine the temporal and spatial expression pattern of FGF pathway genes during ENS development. We examined three FGF receptors (*fgfr1, fgfr2, and fgfr4*), five FGF ligands (*fgf3, fgf8a, fgf10a, fgf13a, fgf13b*) and one gene whose expression plays an inhibitory role (*spry2*). Ligands were chosen because prior work had shown that *fgf3* and *fgf8* are involved in zebrafish epibranchial placode development (Nechiporuk et al. 2007), *fgf10a* is critical in zebrafish esophageal and swim bladder development (Korzh, et al. 2011), and *fgf13a* and *fgf13b* had altered expression in mice with mutant intestinal development as shown through microarray (Heanue and Pachnis 2006). Expression data from RT-PCR and in situ hybridization experiments are summarized in Table 1. FGF factors are expressed throughout ENS development, with the notable exception of *fgfr1* (Supplemental Figs. 1-3). Receptors, ligands and inhibitors are expressed temporally and spatially in patterns consistent with having a role in ENS development.

FGF is required early in ENS development in zebrafish embryos

We investigated whether enteric neuron number was affected treating embryos with the FGF inhibitor su5402 (Poss et al. 2000). Initially, embryos were treated with su5402 from 25-120hpf and then stained with anti-Elv, an antibody marker

for differentiated neurons (Fig. 1A-D). su5402 treated embryos had no swim bladder, decreased eye size, cardiac edema, and an 88.6% decrease in enteric neurons (Fig. 1Q). Treatment with su5402 also resulted in perturbation of cranio-facial cartilage, as determined by alcian blue staining (Sup. Fig. 4). Subsequently embryos were treated with su5402 during early stages of zebrafish ENS development, from 25-72hpf and then fixed and stained with anti-Elv at 120hpf. 25-72hpf su5402 treated embryos showed a similar defects as those treated 25-120hpf with an 87.1% decrease in enteric neurons (Fig. 1G-J, R). Treatment with su5402 from 55hpf-120hpf resulted in a loss of the swim bladder and decreased eye size, but did not result in any additional phenotypes (Fig. 1I-L). Significantly su5402 treated embryos from 55hpf-120hpf did not exhibit a significant decrease in enteric neuron number (Fig. 1S). This implied that there is an early requirement for FGF signaling during enteric nervous system development, so we treated embryos with su5402 from 25-36hpf (the pre-enetric phase of ENS development) and fixed and stained at 120hpf. 25-36hpf treated embryos exhibited a similar phenotype to both 25-120hpf and 25-72hpf su5402 treatments, with a 94.9% decrease in enteric neurons (Fig 1M-P, T). As su5402 treatment from 25-36hpf was sufficient to cause a significant decrease in enteric neurons at 120hpf, this shows that FGF signaling is required during the pre-enteric phase of zebrafish ENS development.

Enteric neural crest cells do not migrate to and along the developing gut upon FGF inhibition

To identify if enteric neural crest cells are present in the developing gut, but not differentiating into neurons, we performed in situ hybridization with a phox2b probe to label migrating ENS precursors (Fig. 2A-D). su5402 treated embryos lack phox2b positive cells in the gut, indicating that the ENS precursors are not migrating to and along the intestine. To determine if these precursors are migrating from the vagal neural crest to the anterior gut tube, we performed in situ hybridization using a *crestin* probe to label vagal neural crest cells (Fig. 2E, F). Compared to the DMSO control, su5402 treated embryos lack a chain of vagal neural crest cells migrating toward the anterior gut. The absence of enteric precursors in the gut, as well as the lack of migration of enteric neural crest cells from the vagal neural crest to the gut, demonstrates an early functional role for FGF signaling in ENS development.

FGF signaling in the vagal neural crest is crucial for normal ENS formation

FGF signaling has multiple downstream targets that regulate gene expression. To determine if there is a change in expression of a downstream target of FGF signaling, we performed in situ hybridization utilizing an *etv5b* probe. In DMSO control embryos at 36hpf*, etv5b* is expressed in the rhombomeres as well as the vagal neural crest (Supplemental Fig. 5A,C). Embryos treated with su5402 from 25-36hpf fail to express *etv5b* in the rhombomeres and vagal neural crest. The absence of *etv5b* expression in su5402 treated embryos demonstrates that FGF signaling is blocked in the vagal neural crest and not in the rhombomeres during

this critical period of the initial migration of enteric neuronal precursors from the vagal crest to the anterior end of the gut.

FGF signaling is not required for normal gut development.

As enteric neural crest precursors migrate from the vagal region to the anterior gut tube, if the anterior gut tube is malformed, it is possible that gut derived signals that are required for the normal migration of enteric vagal neural crest cells will be perturbed. To determine if initial gut development is disrupted in su5402 treated embryos we examined the expression of markers for the gut endoderm and mesoderm. Additionally, we assessed development of the pancreatic bulb that buds off of the gut tube during this developmental period to identify if there were any potential malformations of the gut tube. Embryos treated with su5402 from 25-36hpf and fixed at 52hpf did not exhibit any changes in expression of the endodermal gut marker *foxa1*, mesodermal gut marker *hand2*, or pancreatic markers *pdx1* or *ins* (Figure 3A-H). This suggests that perturbation of FGF signaling during this time period does not affect development of either mesodermal or endodermal components of the anterior gut.

Loss of neurons caused by su5402 is not due to apoptosis

To determine if vagal neural crest cells are not migrating to the anterior gut due to apoptosis, we stained su5402 and control embryos at 36hpf with an anti-caspase3 antibody. Embryos were also treated with the caspase3 inhibitor ZVAD, to determine if elevated apoptosis explained the su5402 induced enteric neuron

phenotype. Experimental embryos were treated from 25-36hpf, fixed, and stained with the anti-caspase3 antibody (Fig. 4A-D). su5402 treated embryos exhibited a significant increase in caspase3 positive cells (81%) (Fig. 4M) However embryos treated with both su5402 and ZVAD did not have an increase in caspase3 positive cells, indicating that ZVAD treatment is rescuing the apoptosis phenotype seen in the su5402 treatment. Embryos were then treated from 25-36hpf and fixed at 120hpf and stained with anti-Elv (Fig. 4E-L). su5402 treated embryos had an 81.1% decrease in enteric neurons compared to DMSO treated embryos, comparable to earlier su5402 treatment experiments. Embryos treated with both su5402 and ZVAD exhibited a 82.2% decrease in enteric neurons compared to embryos treated with DMSO and ZVAD, indicating that the capsase3 inhibitor did not rescue the su5402 induced ENS phenotype (Fig. 4N). Therefore while apoptosis is increased in the vagal neural crest region of su5402 embryos, this increase is not responsible for the enteric neuronal phenotype.

FGF inhibition results in a decreased proliferation in the vagal region but this change is not significant

To determine if vagal neural crest cells are not proliferating, we stained embryos at 36hpf with an anti-phosphohistone H3 (PH3) antibody, which is a mitotic marker. Experimental embryos were treated from 25-36hpf, fixed, and stained with the anti-PH3 antibody (Supplemental Fig. 6A,B). su5402 treated embryos exhibited a decrease in PH3 positive cells (41.6%), but this change was not statistically significant (Supplemental Fig. 6C). Therefore while proliferation is decreased in the vagal neural crest region of su5402 embryos, further studies are

needed to determine if this change could be responsible for the enteric neuronal phenotype.

ENS development is perturbed in embryos expressing a heat shock inducible dominant-negative fgfr1

To further support our results that suggested FGF signaling is involved in ENS development, we utilized Tg(hsp70I:dnfgfr1-EGFP)pd1 embryos. A dominant-negative FGFR1 is predicted to heterodimerize with all FGFR subtypes, thus blocking downstream FGF signaling for all FGFRs (Lee et al. 2005). First we heat shocked embryos for one hour at 30hpf, 54hpf, 78hpf and 102hpf, fixed at 120hpf, and stained with anti-Elv (Fig. 5A-D). Embryos undergoing 4 heat shocks and positively expressing EGFP lack a swim bladder and have a 48.8% decrease in enteric neurons compared to control embryos undergoing 4 heat shocks that did not express EGFP. Next, we heat shocked embryos for one hour at 30hpf, fixed at 120hpf and stained with anti-Elv (Fig. 5E-F). EGFP positive embryos undergoing a single heat shock have a 53.5% decrease in enteric neurons as compared to control embryos. Together with the su5402 treatment this further demonstrates FGF signaling is necessary for normal ENS development and this is an early requirement

hedgehog signaling is decreased in the vagal neural crest region in su5402 treated zebrafish embryos

Previous studies have shown that several other signaling pathways are involved in ENS development (Amiel and Lyonnet 2001, Brooks et al 2005, Puri et al

1998, Reichenbach et al. 2008). To determine if the FGF signaling pathway is interacting with any of these other known ENS signaling pathways we performed in situ hybridization on su5402 treated embryos using probes corresponding to previously identified critical ligands. The expression pattern of *gdnf, ihh* and *shh* were determined in 36hpf embryos treated with either DMSO or su5402 from 25-36hpf (Fig. 6 A-F). There appeared to be slight differences in the expression of all three ligands, however as in situ hybridization is not a quantitative method we dissected the vagal region of 36hpf embryos and used qRT-PCR to determine the relative expression of these three genes in experimental and control embryos. The dissected region consisted of tissue from the otic vesicles to the third and fourth somite. Tissue from both DMSO and su5402 treated embryos served as the template for qRT-PCR analysis to determine changes in *gdnf, ihh,* and *shh* expression. *gdn*f had a 0.93 fold decrease in su5402 treated embryos, while *ihh* and *shh* exhibited a 3.63 fold and 5.08 fold decrease, respectively (Fig. 6G). Given that Hedgehog signaling is significantly perturbed in su5402 treated embryos, this indicates a potential interaction between FGF signaling and hedgehog signaling that is required during ENS development in zebrafish. These data indicate that FGF signaling is interacting with hedgehog signaling during critical points of ENS development.

ihh morphant embryos have disrupted ENS development

We have previously shown that there is a role for *shh* in zebrafish ENS development, however the role of *ihh* in ENS development in zebrafish has not been elucidated (Reichenbach et al. 2008). We injected Tg(-8.3phox2b:Kaede)

transgenic embryos with an *ihh* morpholino, and imaged at 120hpf to determine if these embryos have an enteric neuronal phenotype (Fig. 7A-D). As an additional control *ihh* morphant embryos were co-injected with a *p53* morpholino (Fig 7E-H). *ihh* morphants have a curved body, small eyes, no swim bladder as well as a 87.0% decrease in enteric neurons as compared to uninjected controls (Fig. 7B,D,I). *p53* morphants have no discernible phenotype and do not exhibit a decrease in enteric neurons (Fig. 7E,G). *ihh/p53* double morphants no longer have a curved body phenotype, but maintain the small eye and lack of swim bladder phenotype (Fig. 7F). Furthermore there is an 82.3% decrease in enteric neurons in *ihh/p53* morphants as compared to *p53* morpholino controls (Fig. 7H,I). Thus, *ihh* is required for ENS development in zebrafish.

hedgehog signaling is required for the migration of vagal neural crest cells to the anterior gut tube

To determine if knockdown of the hedgehog signaling and specifically *ihh* morphants display a similar vagal neural crest phenotype to that seen in the su5402 treated embryos, we performed crestin in situ hybridization on *ihh* morphants and cycolpamine treated embryos (Fig 8A-D). *ihh* morphants lack vagal neural crest cells migrating in and toward the anterior gut tube. Embryos treated with cyclopamine from 25-36hpf also lack appropriate vagal neural crest cell migration. Significantly knockdowns of *ihh* and *shh* in zebrafish result in an inability of vagal neural crest to migrate to the anterior end of the gut in a similar fashion to su5402 treated embryos suggesting that *ihh, shh,* and *fgf* are required for enteric neural crest migration to the foregut.

3.5 DISCUSSION

Fibroblast growth factor signaling is essential in a variety of developmental processes. FGF factors have multiple functions and are most commonly known for their role as mitogens (Dorey and Amaya, 2010). They have also been shown to have morphological and regulatory effects, as well as many other biological functions (Silverio et al. 2007, Delatte et al. 2005). In this study we show that FGF signaling is required for normal ENS development. Loss of FGF signaling is sufficient to perturb the normal vagal neural crest migration to the foregut. As a result of the loss of vagal neural crest migration, there is a significant reduction in the number of enteric neurons present in the gut, directly implicating FGF signaling in ENS development.

In ENS development, a subset of vagal neural crest cells must migrate from the vagal region to the anterior gut tube (Le Douarin and Teillet 1973, Epstein et al. 1994). These enteric neural crest precursors are highly proliferative during this migratory stage. It is critical that the enteric neural crest cells arrive in the foregut within a small temporal window to properly innervate the gut (Burns, 2005). Our results demonstrate that su5402 treatment results in an inability of these vagal neural crest neural crest precursors to migrate to the gut tube. This lack of migration contributes directly to a decrease in enteric neurons and is sufficient to produce an aganonglionic phenotype. We showed that treating embryos with su5402 only during this period of vagal neural crest cell migration was sufficient to cause this reduction in enteric neurons in the intestine at 120hpf. This phenotype is also seen in embryos expressing dominant-negative

fgfr1 driven by a heat shock promoter. While the vagal neural crest region exhibits an increase in apoptotic cells during su5402 treatment, the enteric neuronal phenotype is not rescued by simultaneous treatment with the caspase3 inhibitor ZVAD. Therefore, the increase in apoptosis in su5402 embryos is a secondary effect of the perturbation of normal vagal neural crest development. As has been previously reported knocking-down FGF signaling during this period of vagal neural crest development leads to other vagal neural crest phenotypes, such as cranio-facial cartilage defects (Johnston and Bronsky 1995).

FGF signaling has been previously shown to affect cellular migration in other species. For example, the migratory roles of FGFR1 and FGFR2 have been well demonstrated in Drosophila (Dossenbach et al. 2001). FGFR1 is encoded by breathless in Drosophila, where it is required for directly cell migration during tracheal development, while FGFR2 is encoded by heartless and it necessary for directed mesodermal cell migration (Dossenbach et al. 2001). Thus in addition to FGF potentially acting as a mitogen effecting vagal neural crest development it may also affect cellular migration of vagal neural crest cells to the different tissues to which it is known to contribute.

Sonic hedgehog signaling has been previously shown to be required for normal ENS development in zebrafish (Reichenbach et al. 2008). *shh* is required in two phases of ENS development, an early migratory phase as well as during a proliferative phase. The role of *ihh* has been less well defined during zebrafish ENS development. While a reduction of enteric neurons has been described in

ihh mutants previously, the precise role of *ihh* has yet to be elucidated (Ramalho-Santos et al. 2000). *ihh* has been found to play a critical role in esophageal and swim bladder development and was shown to interact with *fgf10* (Korzh et al. 2011). The swim bladder arises as an outgrowth of foregut endoderm (Winata et al. 2009). Critically we show that knockdown of *ihh* results in an ENS defect due to a failure of migration of the enteric neural crest precursors from the vagal neural crest region to the anterior end of the gut tube, similar to loss seen when either *shh* function is perturbed (Reichenbach et al. 2008) or when FGF signaling is perturbed (this study). Thus both FGF and HH signaling are essential for this initial migration step and perturbation of either signaling pathway causes intestinal aganglionosis.

Previously, it was determined that a critical number of neural crest cells is required when migrating from the vagal neural crest to the anterior gut tube (Barlow et al. 2008). One way to possibly explain our results is that, like HH signaling, FGF signaling has a mitogenic effect on ENCCs and FGF knockdown reduces the neural crest number, causing an ENS phenotype. Another possibility is that FGF signaling is required to specify the ENCCs in the vagal neural crest, making them competent to respond to foregut signals. su5402 treatment therefore could cause a loss of this specification at this critical stage.

In summary, we demonstrate that FGF signaling is required for vagal neural crest development and that FGF signaling helps regulate enteric neural crest precursor migration to the anterior end of the gut in vivo in zebrafish. Additionally, we

show that FGF signaling influences Indian Hedgehog expression during this critical migratory phase, and that Hedgehog signaling is necessary for this normal migration. Further elucidating factors and signaling pathways interacting with FGF and Hedgehog signaling during ENS development could potentially lead to new candidate genes that might contribute to HSCR in human patients and provide potential new therapeutic approaches to treating the condition. Collectively, our results suggest a model in which FGF and Hedgehog are required for normal ENCC development in the vagal crest, and that perturbation of either of these signaling pathways during this critical periods leads to an inability of the vagal neural crest to migrate to the foregut and properly populate the gut with ENS precursors.

3.6 FIGURES AND FIGURE LEGENDS

Gut Expression					
Hours post fertilization	24	48	72	96	120
Receptors					
fgfr1a					
fgfr2	+	+	+	+	+
fgfr4	+	+	+	+	+
Ligands					
fgf3	+	+	+	+	
fgf8a	+	+	+	+	
fgf10a	+	+	+	+	+
fgf13a	+	+	+	+	+
fgf13b	+	+	+	+	+
Inhibitors					
spry2	+	+	+	+	+

Table 5: Expression of fgf factors during gut development in zebrafish

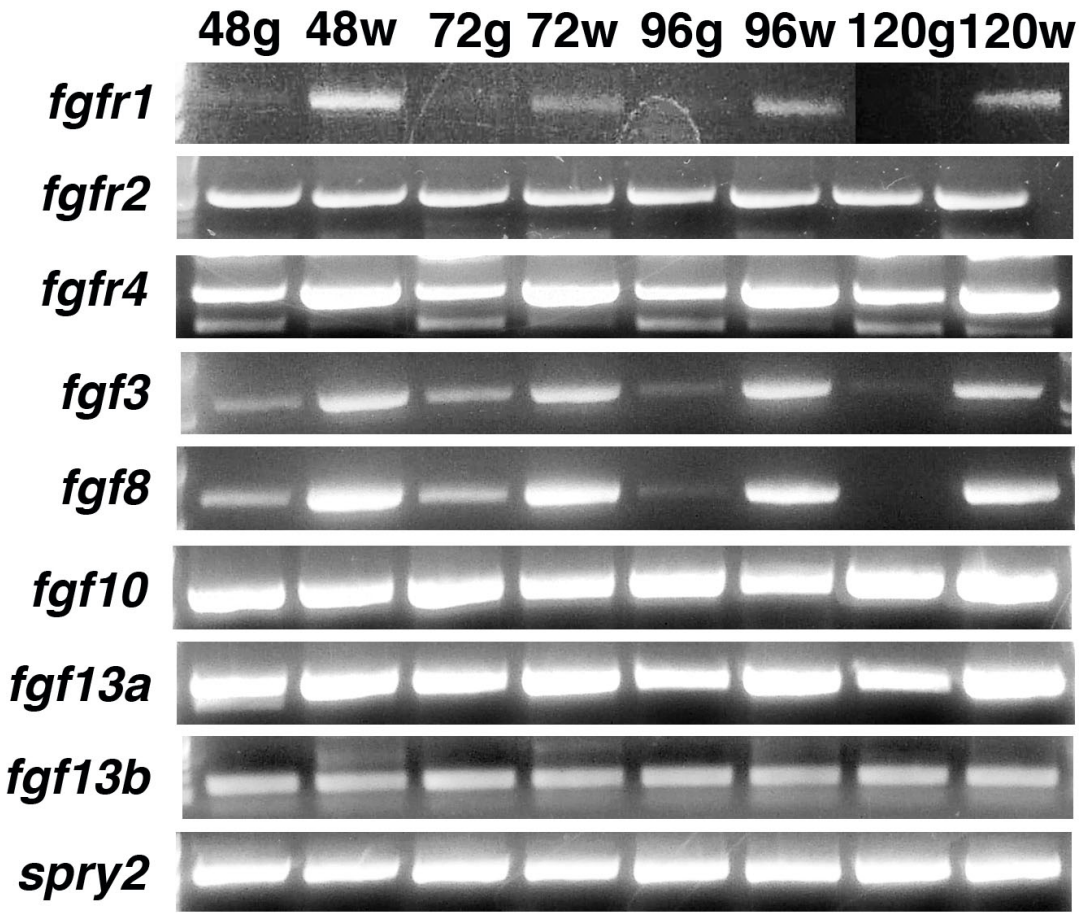

Figure 14: RT-PCR of FGF factors in dissected gut tissue

The guts of wild-type embryos were dissected at 48hpf, 72hpf, 96hpf, and 120hpf (48g, 72g, 96g, and 120g, respectively). Whole embryos from the same clutch were used as a control at the same time points (48w, 72w, 96w, and 120w, respectively). *fgfr1* is not expressed in the gut tissue. *fgfr2, fgfr4, fgf10, fgf13a, fgf13b,*and *spry2* are expressed at all time points in the gut tube. *fgf3* and *fgf8* are expressed at 48, 72, and 96hpf, but it are not expressed at 120hpf.

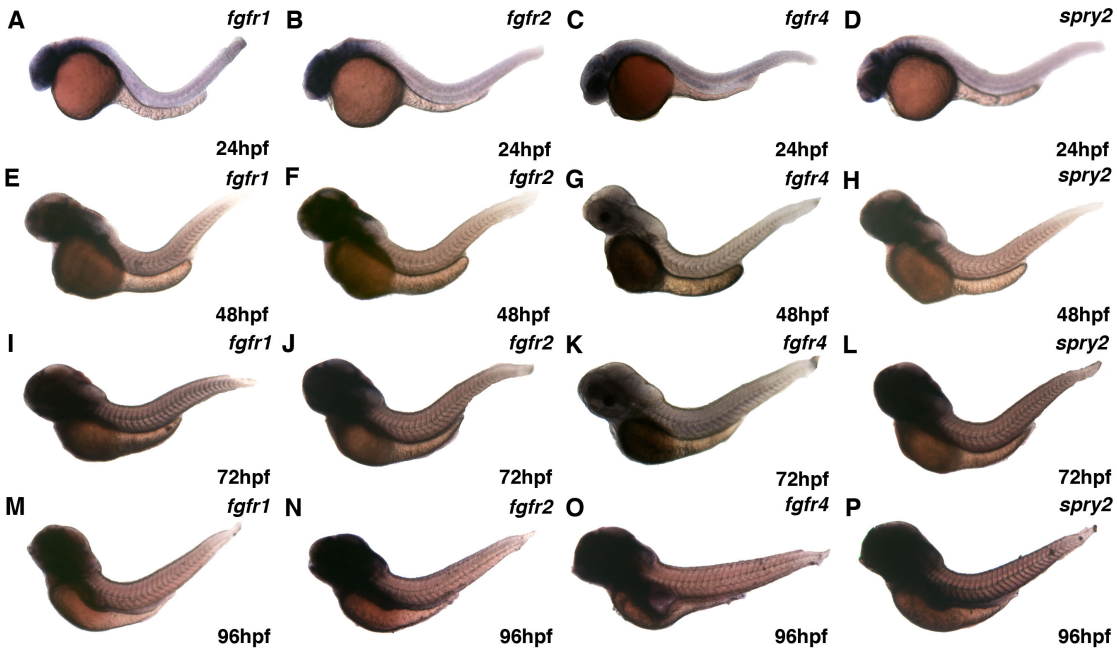

Figure 15: Expression of FGF receptors and an inhibitor

(A, E, I, M), *fgfr1 in situ* hybridization, (B, F, J, N), *fgfr2 in situ* hybridization, (C, G, K, O), *fgfr4 in situ* hybridization (D, H, L, P), *spry2 in situ* hybridization. (A, B, C, D), *in situ* hybridization on 24hpf embryos, *fgfr1, fgfr2, fgfr4* and *spry 2* are expressed in vagal region. (E, F, G, H), *in situ* hybridization on 48hpf embryos. *fgfr2, fgfr4*, and *spry2* are expressed in the gut at 48hpf. (I, J, K, L), *in situ* hybridization on 72hpf embryos. *fgfr2, fgfr4*, and *spry2* are expressed in the gut at 72hpf. (M, N, O, P), *in situ* hybridization on 96hpf embryos. *fgfr2, fgfr4*, and *spry2* are expressed in the gut at 96hpf. *fgfr1* is not expressed in the gut.

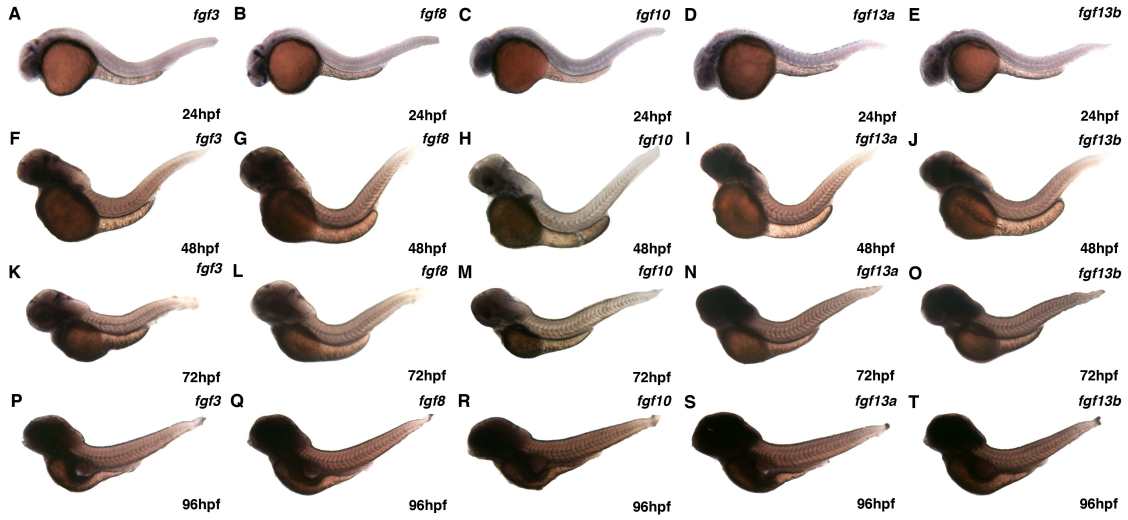

Figure 16: Expression of FGF ligands

(A, F, K, P), *fgf3 in situ* hybridization, (B, G, L, Q), *fgf8 in situ* hybridization, (C, H, M, R), *fgf10 in situ* hybridization (D, I, N, S), *fgf13a in situ* hybridization, (E, J, O, T), *fgf13b in situ* hybridization. (A, B, C, D, E), *in situ* hybridization on 24hpf embryos, all probes are expressed in vagal region. (F, G, H, I, J), *in situ* hybridization on 48hpf embryos, all probes are expressed in the gut at 48hpf. (K, L, M, N, O), *in situ* hybridization on 72hpf embryos, all probes are expressed in the gut at 72hpf. (P, Q, R, S, T), *in situ* hybridization on 96hpf embryos, *fgf10, fgf13a*, and *fgf13b* are expressed in the gut at 96hpf. *fgf3* and *fgf8* are not expressed in the gut at 96hpf.

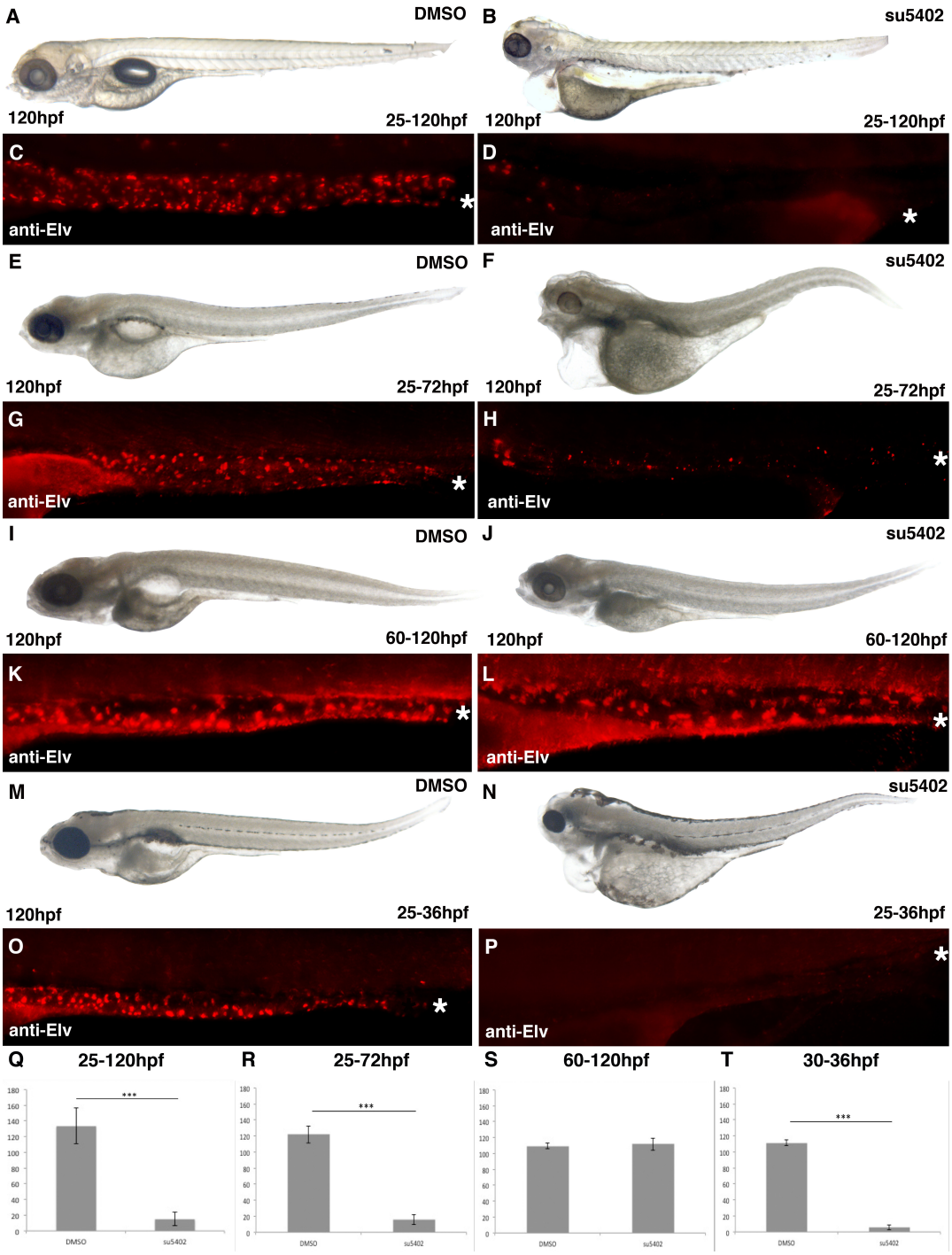

Figure 17: su5402 treatment results in a lack of enteric neurons in the distal colon.

(A, C, E, G, I, K, M, O) DMSO control embryos, (B, D, F, H, J, L, N, P) su5402 treated embryos. (A-D) 25-120hpf treated embryos. (A, B) Treatment with

su5402 results in swim bladder loss, decreased eye size, and adema. (C, D) Lateral views of 120hpf embryos stained with *anti-Elv* show an 88.6% decrease in enteric neurons (Q). (E-H) 25-72hpf treated embryos. (E, F) 120hpf embryos treated from 25-72hpf show a similar phenotype to embryos treated from 25-120hpf. (G, H) Lateral views of 120hpf embryos stained with *anti-Elv* show an 87.1% decrease in enteric neurons (R). (I-L) 55-120hpf treated embryos. (I, J) 120hpf embryos treated from 55-120hpf lack a swim bladder, but do not exhibit an additional phenotype. (K, L) Lateral views of 120hpf stained with *anti-Elv* show no significant decrease in enteric neurons (S). (M-P) 25-36hpf treated embryos. (M,N) 120hpf embryos treated from 25-36hpf show a similar phenotype to 25-120hpf and 25-72hpf treated embryos. (O, P) Lateral views of 120hpf stained with *anti-Elv* show a 94.9% decrease in enteric neurons (T). (Q-T) Bar graphs summarizing enteric neuron numbers for each su5402 treatment group (student's t-test). Error bars represent standard deviation. Black asterisks represent statistical significance. White asterisks indicate distal end of the gut. Anterior is to the left.

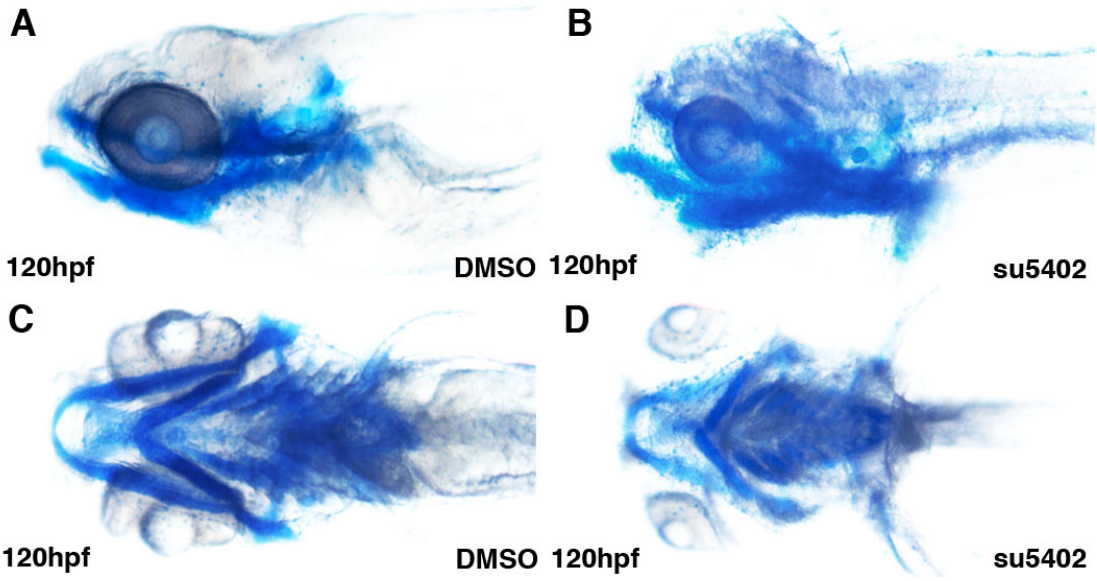

Figure 18: The cranio-facial cartilage is perturbed in su5402 treated embryos.

(A, C), DMSO treated control embryos, (B, D), su5402 treated embryos. (A,B), Lateral view of 120hpf embryos stained with alcian blue shows a shortening of the jaw in su5402 treated embryos, as compared to DMSO embryos. (C, D), Ventral view of 120hpf embryos stained with alcian blue demonstrates a malformation of the cranio-facial cartilage in su5402 treated embryos.

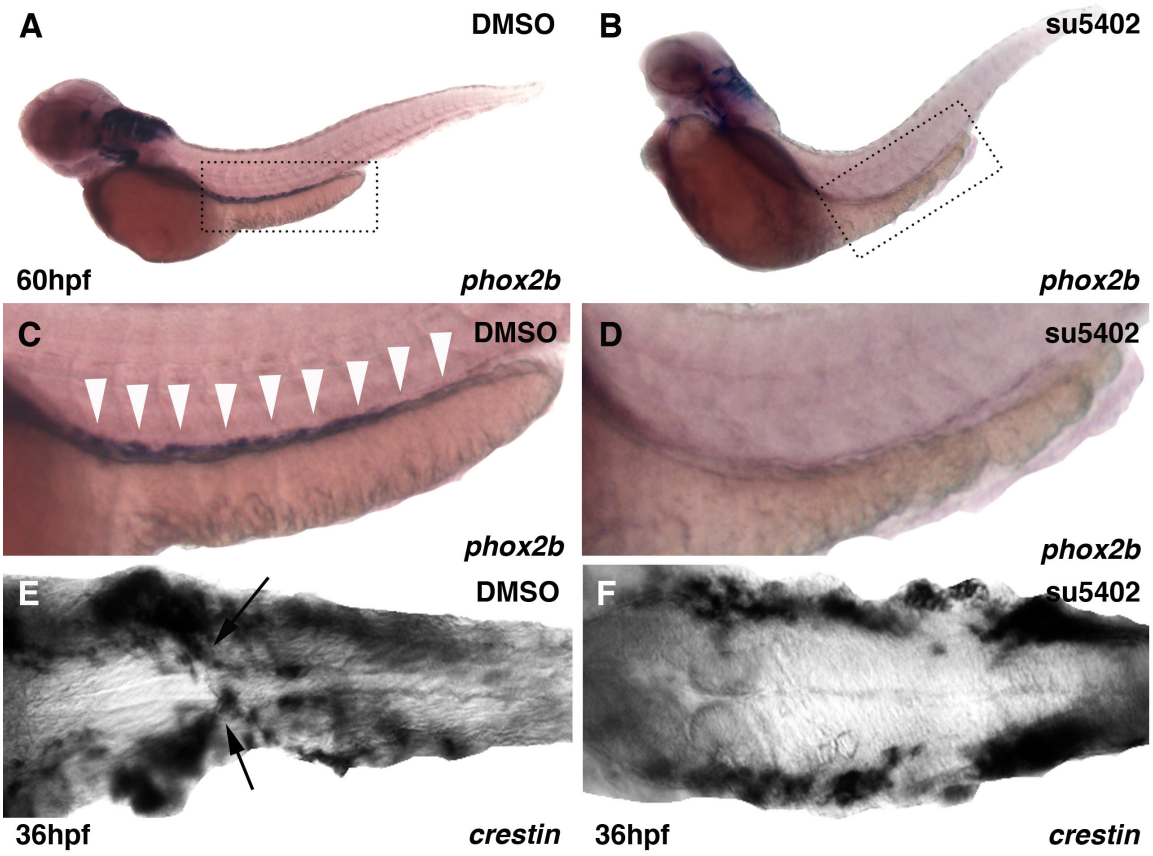

Figure 19: su5402 treatment results in an absence of enteric neural crest precursors in the gut and a failure of migration of vagal neural crest cells to the anterior gut tube.

(A, C, E) DMSO control embryos, (B, D, F) su5402 treated embryos. (A, B) Lateral view of embryos treated with DMSO and su5402 from 25-60hpf and hybridized with a *phox2b* riboprobe. (C, D) Up close lateral views of the gut that have been hybridized with a *phox2b* riboprobe show a lack of *phox2b* expressing cells populating the gut. (E, F) Ventral view of 36hpf embryos treated with DMSO and su5402 from 25-36hpf and hybridized with a *crestin* riboprobe demonstrate a failure of vagal neural crest cells to migrate to the anterior region

of the gut tube. White arrowheads (C) indicate phox2b expressing cells in the intestine. Anterior is to the left.

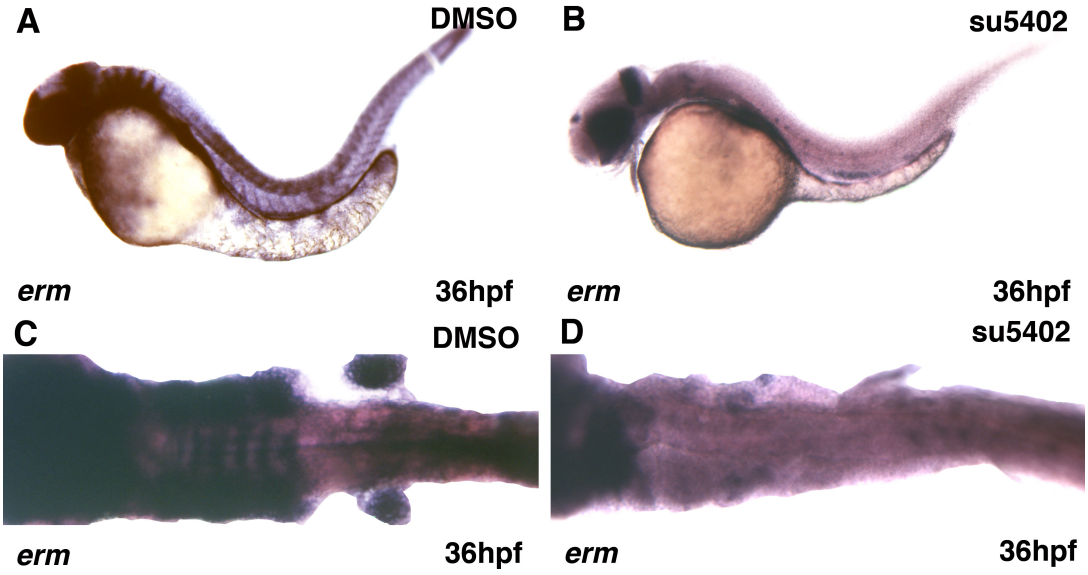

Figure 20: Expression of FGF downstream target *etv5b* is decreased in su5402 treated embryos.

(A,C) DMSO control embryos, (B, D) su5402 treated embryos. (A, B) Lateral view of 36hpf embryos treated with DMSO and su5402 from 25-36hpf and hybridized with an etv5b riboprobe. etv5b is strongly expressed in the hindbrain and rhombomeres in DMSO control embryos, but this expression is greatly decreased in su5402 treated embryos. (C, D) Ventral view of 36hpf embryos treated with DMSO and su5402 from 25-36hpf and hybridized with an erm riboprobe. Expression of etv5b in the rhombomeres and neural crest is lost in su5402 treated embryos. Anterior is to the left.

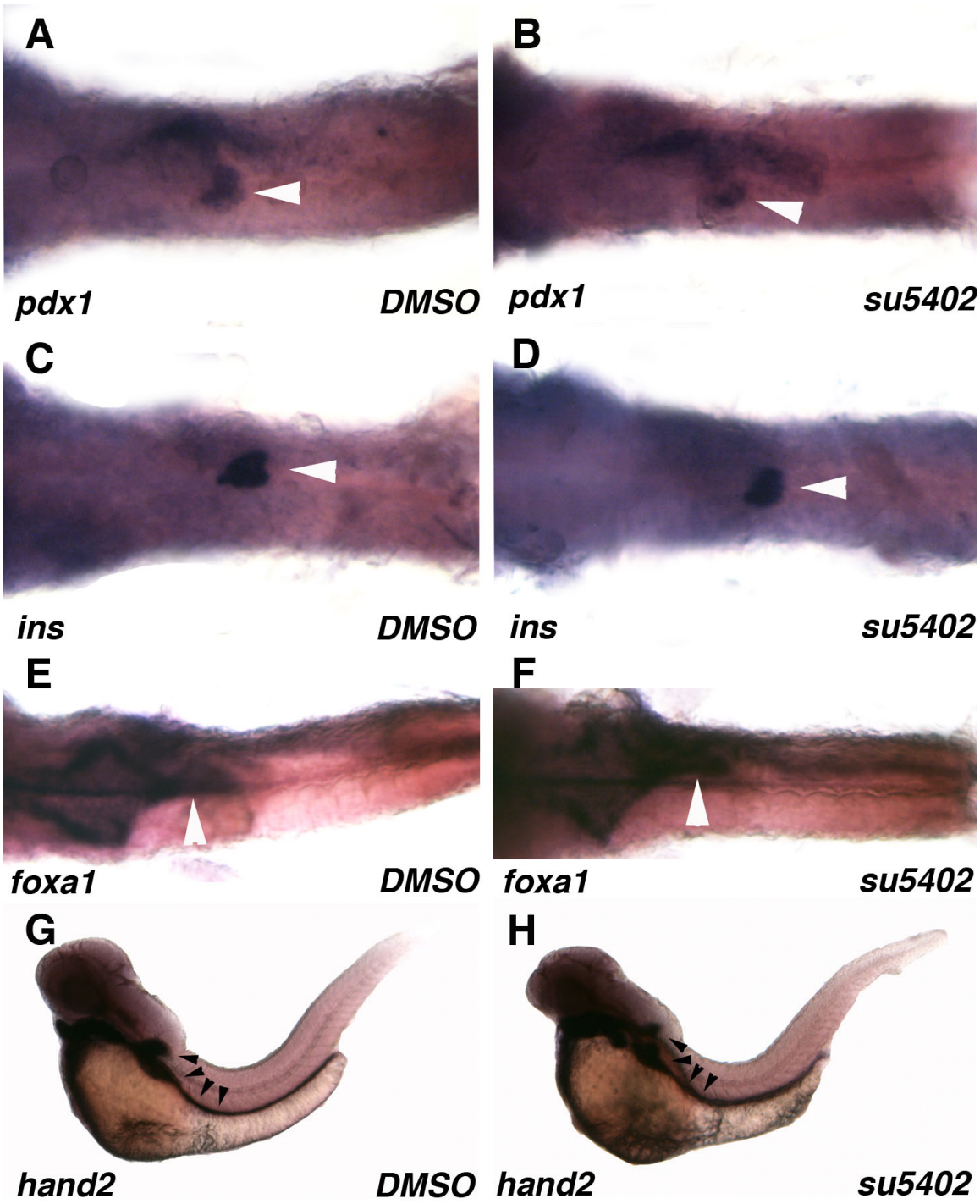

Figure 21: Pancreatic and intestinal factors are not perturbed in su5402 treated embryos.

(A, C, E, G) DMSO control embryos, (B, D, F, H) su5402 treated embryos. (A, B) Ventral view of 52hpf embryos treated with DMSO and su5402 from 25-36hpf

and hybridized with a *pdx1* riboprobe. Expression of *pdx1* is not perturbed in su5402 treated embryos. (C, D) Ventral view of 52hpf embryos treated with DMSO and su5402 from 25-36hpf and hybridized with an *ins* riboprobe. Expression of *ins* is not effected in su5402 treated embryos. (E, F) Ventral view of 52hpf embryos treated with DMSO and su5402 from 25-36hpf and hybridized with a *foxa1* riboprobe. Expression of *foxa1* is not disturbed in su5402 treated embryos. (G, H) Ventral view of 52hpf embryos treated with DMSO and su5402 from 25-36hpf and hybridized with a *hand2* riboprobe. Expression of *hand2* is not disrupted in su5402 treated embryos. White arrowheads (A, B, C, D, E, F) indicate expression. Black arrowheads (G, H) indicate expression. Anterior is to the left.

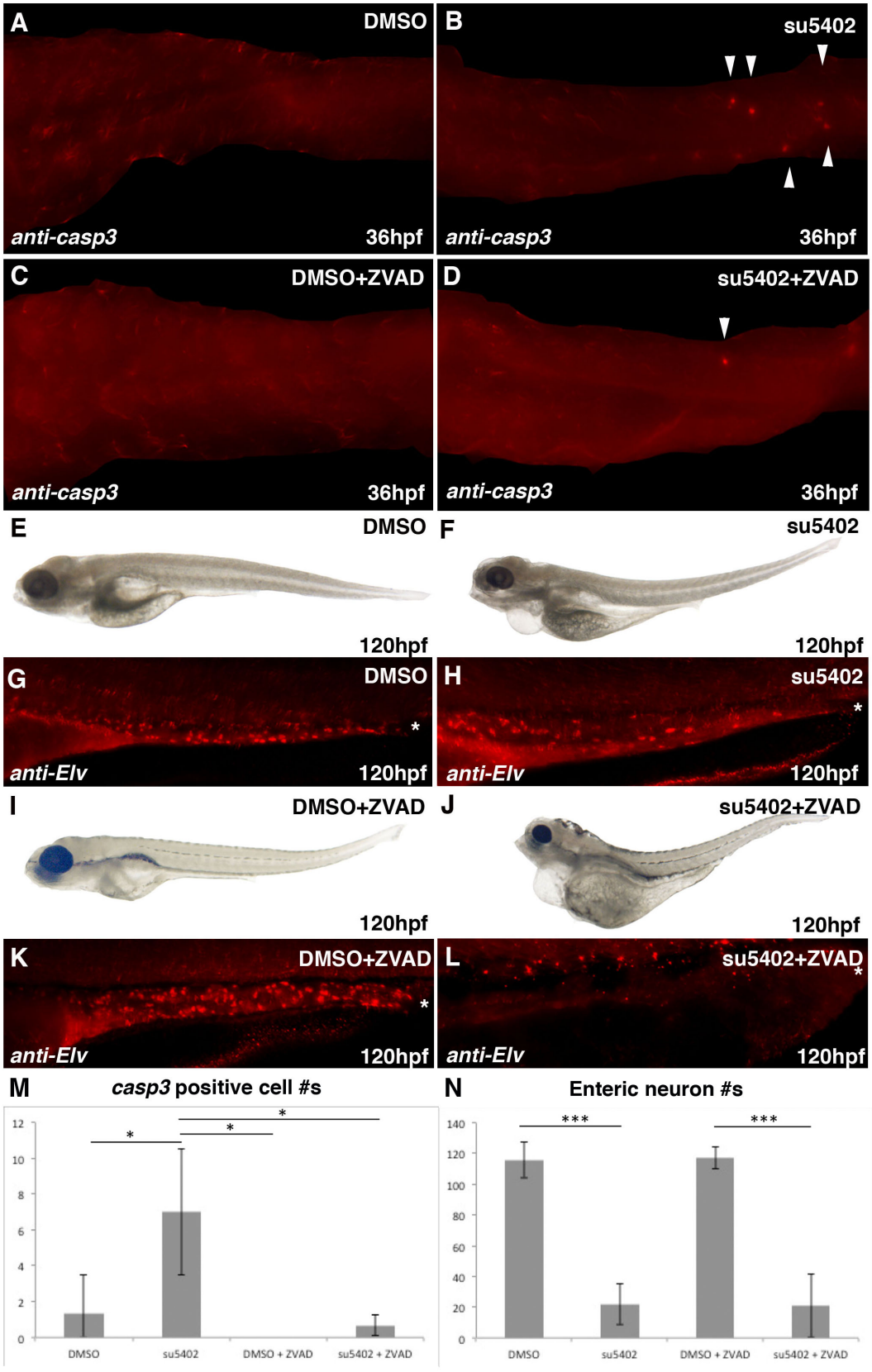
A
DMSO
anti-casp3
36hpf
B
su5402
anti-casp3
36hpf
C
DMSO+ZVAD
anti-casp3
36hpf
D
su5402+ZVAD
anti-casp3
36hpf
E
DMSO
120hpf
F
su5402
120hpf
G
DMSO
anti-Elv
120hpf
H
su5402
anti-Elv
120hpf
I
DMSO+ZVAD
120hpf
J
su5402+ZVAD
120hpf
K
DMSO+ZVAD
anti-Elv
120hpf
L
su5402+ZVAD
anti-Elv
120hpf
M
casp3 positive cell #s
12
10
8
6
4
2
0
DMSO
su5402
DMSO + ZVAD
su5402 + ZVAD
N
Enteric neuron #s
140
120
100
80
60
40
20
0
DMSO
su5402
DMSO + ZVAD
su5402 + ZVAD

Figure 22: Apoptosis is increased in su5402 treated embryos, but the decreased enteric neuron phenotype is not dependent on increased apoptosis.

(A, E, I) DMSO control embryos, (B, F, J) su5402 treated embryos, (C, G, K) DMSO and ZVAD treated embryos, (D, H, L) su5402 and ZVAD treated embryos. (A-D) Ventral view of 36hpf embryos stained with anti-caspase3. su5402 treated embryos show an 81.0% increase in caspase3 expressing cells. Treatment with caspase3 inhibitor ZVAD reduces the number of positive cells in su5402 treated embryos. (E-H) Lateral view of 120hpf embryos. su5402 embryos treated with ZVAD maintain a similar phenotype to embryos treated with su5402 alone. (I-L) Lateral view of 120hpf embryos stained with anti-Elv. su5402 treated embryos, with and without ZVAD, have decreased enteric neurons compared to DMSO controls, with and without ZVAD (81.1 and 82.2, respectively). (M,N), Bar graphs summarizing caspase3 positive cells (M) and enteric neuron number (N) in embryos treated with DMSO, su5402, DMSO+ZVAD, and su5402+ZVAD (student's t-test). Error bars represent standard deviation. Black asterisks represent statistical significance. White arrowheads indicate caspase3 positive cells. White asterisks indicate distal end of the gut. Anterior is to the left.

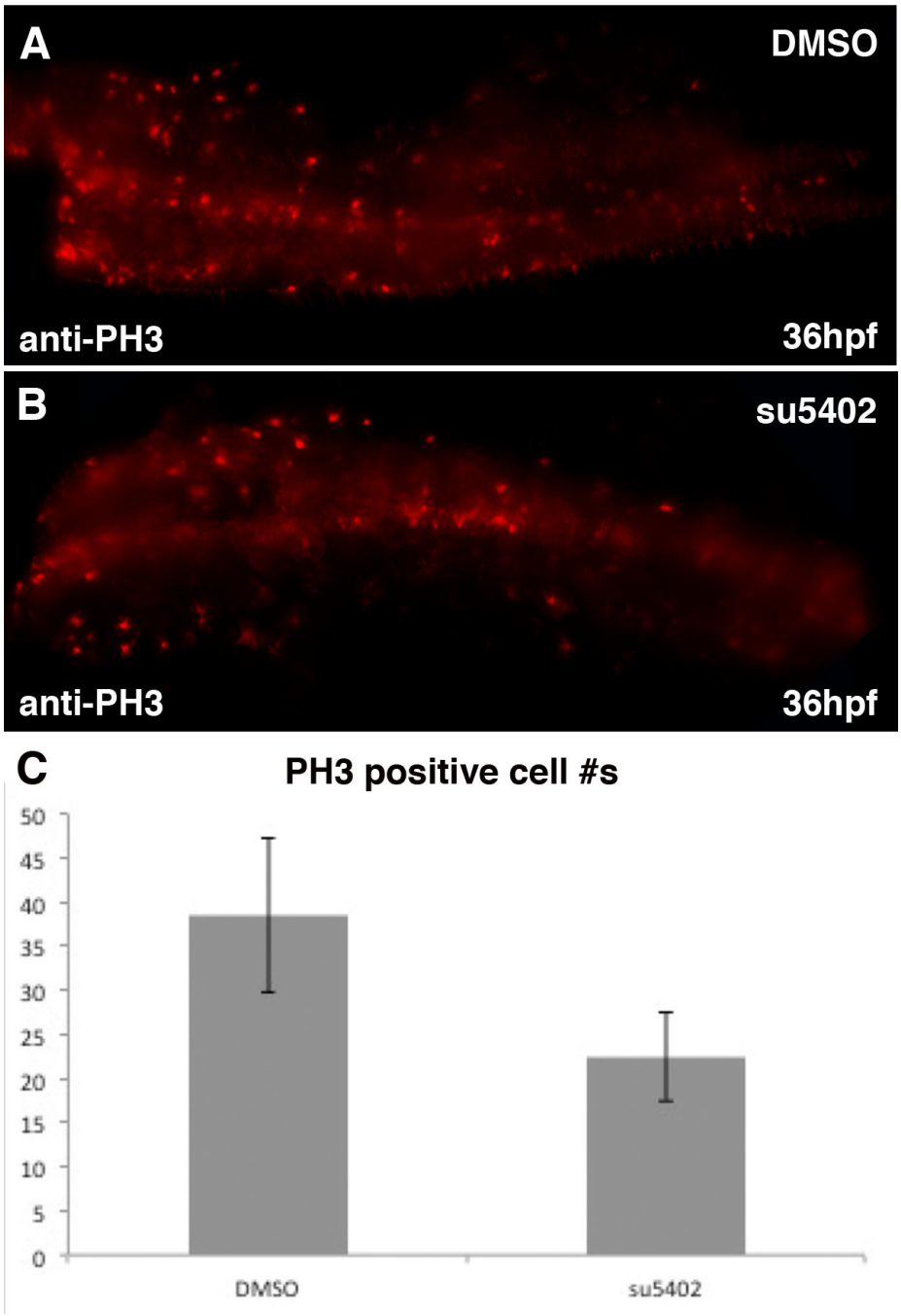

Figure 23: Proliferation is decreased in the vagal region in su5402 treated embryos.

(A)DMSO treated embryo, (B), su5402 treated embryo. (A,B) 36hpf su5402 treated embryos have a 41.6% decrease in PH3 positive cells, as compared to DMSO treated embryos (C). (C), Bar graph summarizing PH3 positive cell

numbers for each drug treatment group (student's t-test). Error bars represent standard deviation. Black asterisks represent statistical significance. Anterior is to the left.

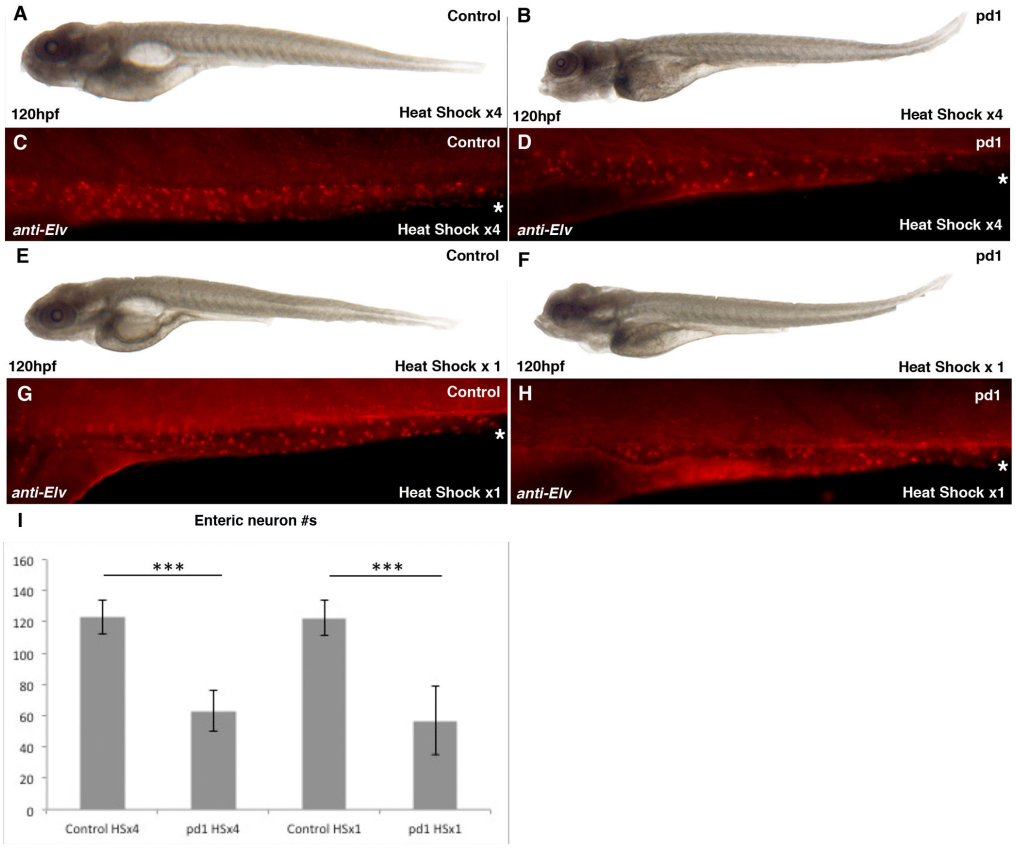

Figure 24: Enteric neurons are decreased in transgenic embryos expressing a dominant-negative *fgfr1*.

(A, C, E, G) EGFP-negative control Tg(hsp70l:dnfgfr1-EGFP) embryos (B, D, F, H) EGFP-positive Tg(hsp70l:dnfgfr1-EGFP) embryos. (A, B) Lateral view of 120hpf EGFP-negative and EGFP-positive embryos that were heat shocked at 37°C for one hour at 30hpf, 54hpf, 78hpf, and 102hpf. Embryos expressing dnfgfr1-EGFP lack a swim bladder. (C, D) Lateral view of 120hpf EGFP-negative and EGFP-positive embryos that were heat shocked at 37°C for one hour at 30hpf, 54hpf, 78hpf, and 102hpf and stained with anti-Elv. Embryos expressing dnfgfr1-EGFP have a 48.8% decrease in enteric neurons (I). (E, F) Lateral view of 120hpf EGFP-negative and EGFP-positive embryos that were heat shocked at

37°C for one hour at 30hpf. Embryos expressing dnfgfr1-EGFP lack a swim bladder. (G, H) Lateral view of 120hpf EGFP-negative and EGFP-positive embryos that were heat shocked at 37°C for one hour at 30hpf and stained with anti-Elv. Embryos expressing dnfgfr1-EGFP have a 53.5% decrease in enteric neurons (I). (I) Bar graph summarizing enteric neuron numbers for each heat shock group (student's t-test). Error bars represent standard deviation. Black asterisks represent statistical significance. Anterior is to the left.

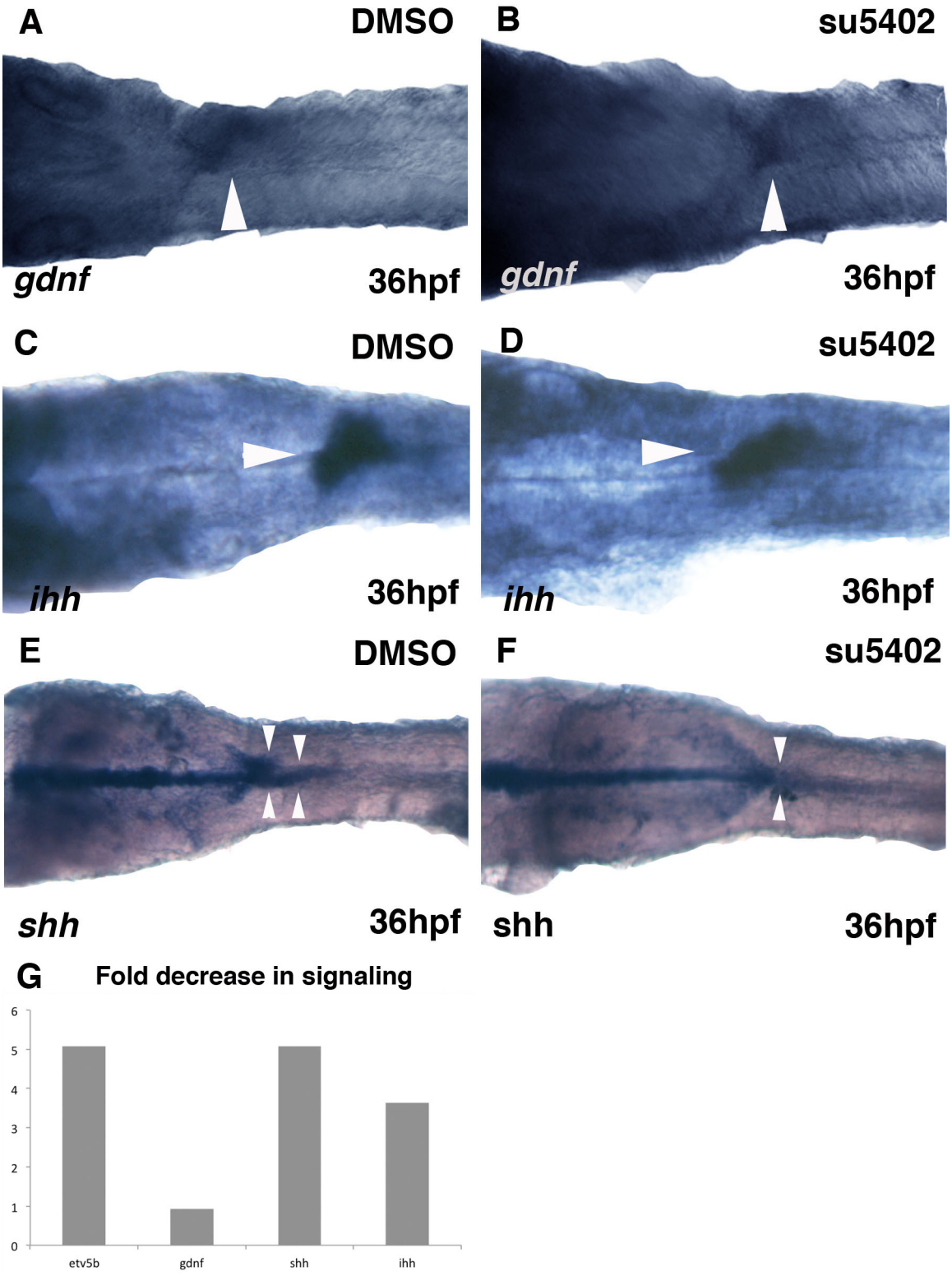
A
DMSO
gdnf
36hpf
B
su5402
gdnf
36hpf
C
DMSO
ihh
36hpf
D
su5402
ihh
36hpf
E
DMSO
shh
36hpf
F
su5402
shh
36hpf
G
Fold decrease in signaling
6
5
4
3
2
1
0
etv5b
gdnf
shh
ihh

Figure 25: su5402 treated embryos have a slight decrease in *gdnf*, *shh*, and *ihh* expression.

(A, C, E) DMSO control embryos, (B, D, F) su5402 treated embryos. (A, B) Ventral view of 36hpf embryos treated with DMSO and su5402 from 25-36hpf and hybridized with a gdnf riboprobe. gdnf expression is still present in su5402 treated embryos. (C, D) Ventral view of 36hpf embryos treated with DMSO and su5402 from 25-36hpf and hybridized with an ihh riboprobe. ihh expression is still present in su5402 treated embryos. (E, F) Ventral view of 36hpf embryos treated with DMSO and su5402 from 25-36hpf and hybridized with a shh riboprobe. shh expression is still present in su5402 treated embryos. (G) qRT-PCR analysis of gdnf, shh and ihh show a 0.93, 5.08, and 3.63 fold decrease in signaling, respectively. Bar graph summarizing normalized fold decrease against elf1a reference gene (ΔΔΔCt). Anterior is to the left.

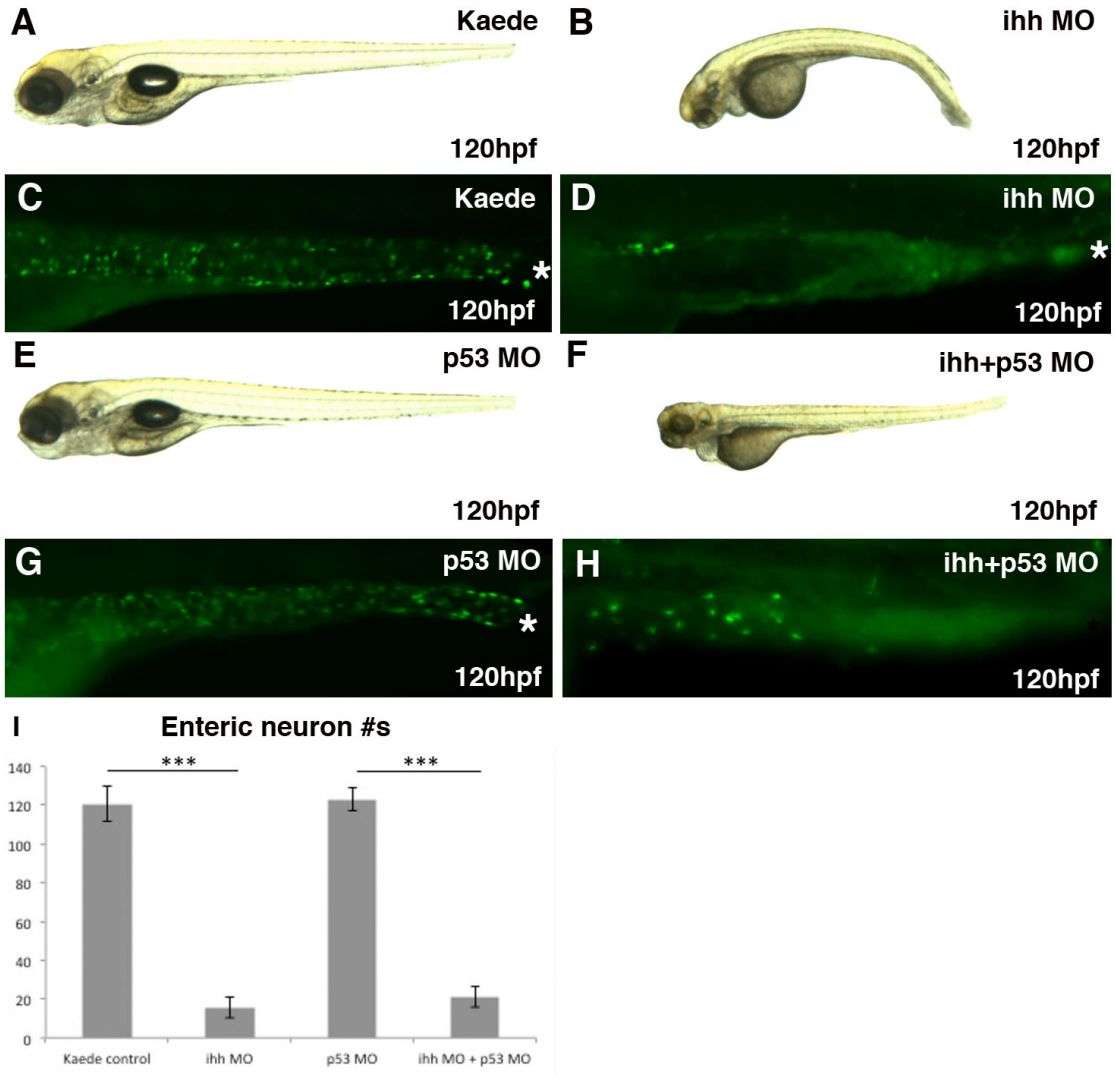

Figure 26: *ihh* morphant embryos exhibit a decrease in enteric neurons.

(A, C) Kaede uninjected control embryos, (B,D) ihh MO injected embryos, (E,G) p53 MO injected embryos, (F,H) ihh MO and p53 MO injected embryos. (A, B) 120hpf ihh MO injected embryos demonstrate a curvature of the body, a smaller eye, and a loss of swim bladder. (C, D) Lateral views of 120hpf embryos stained with *anti-Elv* show an 87.0% decrease in enteric neurons (I). (E, F) 120hpf embryos injected with p53 show a similar phenotype to uninjected Kaede control

embryos, while embryos injected with both ihh MO and p53 MO no longer have the curved body, but still exhibit a smaller eye and lack a swim bladder. (G, H) Lateral views of 120hpf embryos stained with *anti-Elv* show an 82.3% decrease in enteric neurons (I). (I) Bar graph summarizing enteric neuron numbers for each MO injection group (student's t-test). Error bars represent standard deviation. Black asterisks represent statistical significance. White asterisks indicate distal end of the gut. Anterior is to the left.

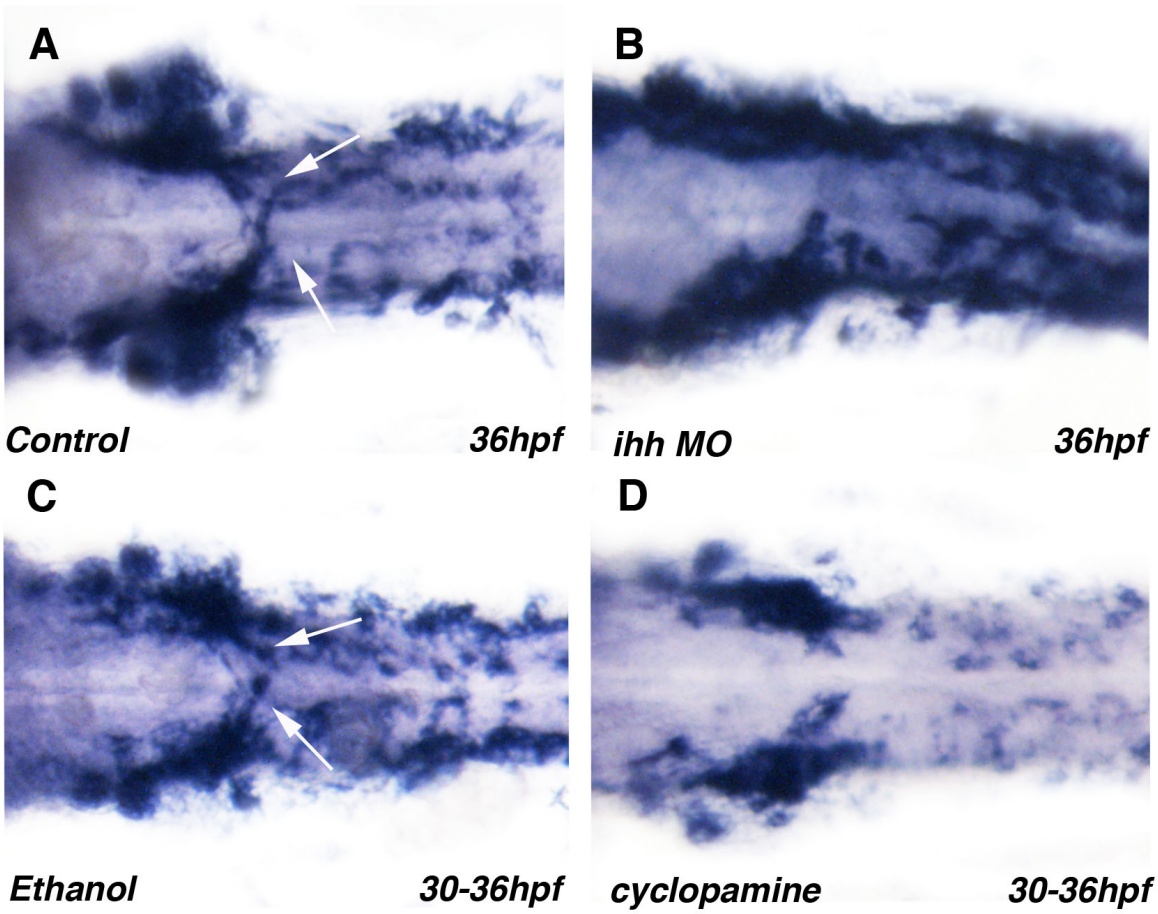

Figure 27: *ihh* morphant embryos and cyclopamine treated embryos lack of migration of vagal neural crest cells to the anterior gut tube. (A), Uninjected control embryo, (B) p53 morphant control embryo, (C) ihh morphant embryo, (D) ihh and p53 co-injected embryo, (E) ethanol treated control embryo, (F) cyclopamine treated embryo. (A-D) Ventral view of 36hpf embryos uninjected, injected with p53, ihh, and a combination and hybridized with a *crestin* riboprobe demonstrate a failure of vagal neural crest cells to migrate to the anterior region of the gut tube in ihh morphants. (E-F). Ventral view of 36hpf embryos treated with ethanol and cyclopmaine from 25-36hpf and hybridized with a *crestin* riboprobe demonstrate a decrease in vagal neural crest cells migrating to the anterior region of the gut tube. Anterior is to the left.

Chapter 4:

Summary and Conclusions

4.1 SUMMARY OF RESULTS

I have reported on the zebrafish models of two pediatric developmental intestinal diseases, congenital short bowel syndrome (CSBS) and Hirschsprung's diseases. Our collaborators identified CLMP as a candidate gene after scanning the genome of five CSBS patients. I helped confirm CLMP as a causative gene of CSBS. In zebrafish, two orthologs of CLMP were identified based on their predicted sequences. I showed expression of *clmpa* and *clmpb* in the developing gut in the zebrafish through wholemount *in situ* hybridization. *clmpa* demonstrated a pronounced expression in the developing zebrafish intestine. I then showed *clmpa* morphants exhibit a shorter intestine, and this phenotype is rescued with the addition of *clmpa* mRNA. These *clmpa* morphants were transversely sectioned and stained with H&E, which showed a loss of small intestinal goblet cells as well as the loss of epithelial contacts. By establishing a zebrafish model of CSBS, I helped confirm CLMP as the causative gene of CSBS, and well as allowing for the potential to eludicate the role of CLMP in intestinal development.

Additionally, I identified the role of fibroblast growth factor signaling in ENS development in zebrafish. After determining expression of FGF factors in the developing zebrafish gut, I showed that a loss of FGF signaling leads to a Hirschsprung's-like phenotype. Early treatment with an FGF inhibitor was sufficient to induce lack of neurons in the zebrafish gut. I demonstrated that enteric neural crest precursors are not migrating to the anterior gut tube during the first migratory phase in ENS development in zebrafish. This lack of migration results in a lack of enteric neural crest precursors along the gut,

resulting in the neuronal phenotype. While I demonstrated an increase in apoptosis in the vagal region in zebrafish treated with the FGF inhibitor, this increase was not the cause of the Hirschsprung's-like phenotype in the gut. The knockdown of FGF did not result in changes to the gut tube morphology. I showed that the ENS phenotype remains when using a transgenic line that allows for knockdown of FGF signaling. In the transgenic line with reduced FGF signaling, FGF was still an early requirement of ENS development. I showed, through quantitative real time PCR, that FGF is interacting with Hedgehog signaling. I also demonstrated that loss of *shh* and *ihh* results in a similar ENS phenotype with a similar lack of enteric neural crest cells to the foregut. Hedgehog and FGF are interacting, and this feedback loop is required for proper ENS development in zebrafish. I have identified a novel pathway in ENS development.

4.2 DISCUSSION OF RESULTS

The animal model of CSBS in zebrafish is significant because it provides a tool to allow for the identification of the role of CLMP in CSBS. Prior to our publication, the cause of CSBS was unknown. With its high mortality rate, it is imperative that we begin to understand more about the causes of CSBS and identify possible therapeutic treatments. We confirmed that CLMP is conserved in zebrafish, and *clmpa* is expressed during gut development. Using our CLMP knockdown zebrafish, we confirmed that CLMP is required for proper intestinal development. The full scope of intestinal development in humans, as well as animal models, is still being investigated, and identifying CLMP as a factor in intestinal development is important. Furthermore, the identification of the causative gene of CSBS will be critical in early diagnosis of patients, helping decrease patient mortality, as well as allow for the potential to identify therapeutic targets.

Because only approximately 20% of patients with Hirschsprung's disease have a known genetic mutation, it is critical to identify additional genetic factors in ENS development so that we can gain a complete picture of the process of ENS development and Hirschsprung's disease in humans. I have shown that both FGF and Hedgehog signaling are required for ENS development. Not only are these signaling pathways required for ENS development, but they are an early requirement for neural crest migration to the gut tube. Previously, FGF had not been identified as a potential genetic factor involved in ENS development or Hirschsprung's disease. While ihh had been previously implicated in ENS development, we confirmed its role, as well as determining its interaction with

FGF. Additionally, the factors driving neural crest migration, specification, and proliferation are still being identified, and this work could potentially lead to a greater understanding of the vagal neural crest, as well as the development of genetic tools in model systems. Identifying the role of FGF and Hedgehog in ENS development in zebrafish allows for the advancement in understand more about the neural crest, ENS development as a whole, and potential genetic abnormalities in human Hirschsprung's patients.

4.3 FUTURE DIRECTIONS

Now that we have identified CLMP as the causative gene of CSBS, it is important to elucidate the specific role of CLMP in intestinal development. Understanding changes in tight junction biology, proliferation, and apoptosis in CLMP knockout animals could further our knowledge into why CLMP is required for intestinal development. Using *in vitro* analyses, the changes in epithelial biology when CLMP is lost could lead to advancements in our basic understanding of the requirements of epithelial cells in the gut. We see a compensation for CLMP in humans that we do not see in the zebrafish, and determining the differences in genetics between the two could lead to learning more about critical genes in human embryonic development. Additionally, the role of CLMP in the lengthening of the human small intestine after birth needs to be identified. The identification of CLMP in CSBS could potentially lead to additional genetic abnormalities in CSBS, as well as possibly therapies.

Additionally we could determine if the loss of CLMP leads to defects in ENS development. Due to the importance of endoderm derived epithelial cells, the loss of CLMP could potentially affect the number of enteric neurons in the gut. Since cross-talk between the epithelial cells and mesenchyme has previously been shown to be critical in ENS development, we could potential look at the changes in known genes in ENS development in CLMP morphants. Conversely, we could look for changes in CLMP expression in FGF knockdown embryos or Hh morphants.

I have confirmed the roles of FGF and Hedgehog signaling in ENS development, but questions still remain. A critical inquiry is the cell autonomy of the enteric neural crest precursors in relation to these signaling pathways. Identifying whether FGF signaling is required in the enteric neural crest precursors themselves or their cellular environment will further our knowledge of both ENS development and neural crest cells. This can be accomplished through targeted knockdown of FGF and/or Hedgehog in specific tissues through the development of transgenic zebrafish lines. Additionally, the cellular expression of individual factors in the FGF pathway still needs to be identified. This information could determine which cells are secreting ligands and which cells express the receptors, leading to potential neural crest cell targets. In zebrafish and other models, additional genetic tools in the neural crest are still being pursued, and identification of specific promoters that drive FGF expression could provide advancement in neural crest biology. Mutations in FGF and Hedgehog signaling pathways have not yet been identified in humans, but this work allows for the potential to screen Hirschsprung's patients for mutations in these genes.

4.4 CONCLUSION

I have shown that zebrafish is an excellent model for pediatric intestinal disorders. Loss of CLMP in zebrafish exhibits a shortened gut phenotype with a loss of small intestinal goblet cells. This provides a critical tool for finding possible therapeutic targets of CSBS. I have also shown that FGF and Hedgehog signaling are required for early migration of enteric neural crest precursors in ENS development in zebrafish. Overall, I have identified genetic components of intestinal development in zebrafish and advanced the understanding of two pediatric developmental intestinal disorders in humans. I have contributed in confirming the causative gene of the highly fatal CSBS, as well as identified a novel signaling pathway in ENS development, and potentially Hirschsprung's disease.

Appendix A:

Figures in support of “CLMP Is Required for Intestinal Development, and Loss-of-Function Mutations Cause Congenital Short-Bowel Syndrome”

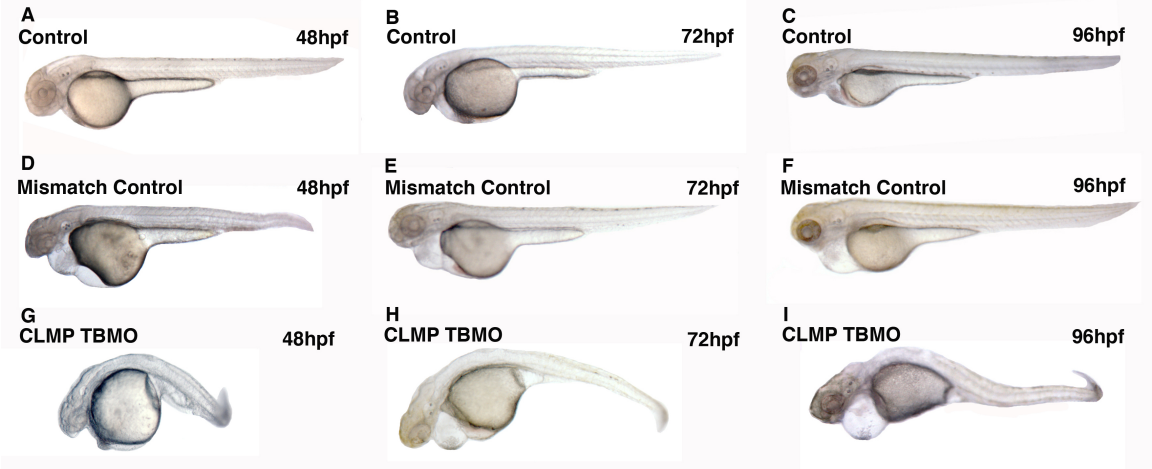

Figure 28: CLMP translation blocking morpholino and controls

(A, B, C) Uninjected control embryos, (D, E, F) mismatch morpholino control embryos, (G, H, I) CLMPa translation blocking morpholino. Embryos were imaged under DIC at 48hpf (A, D, G), 72hpf (B, E, H), and 96hpf (C, F, I). Mismatched controls (D, E, F) have some heart adema as compared to uninjected controls (A, B, C). CLMPa TBMO embryos exhibit a curved body phenotype, as well as heart adema as compared to controls.

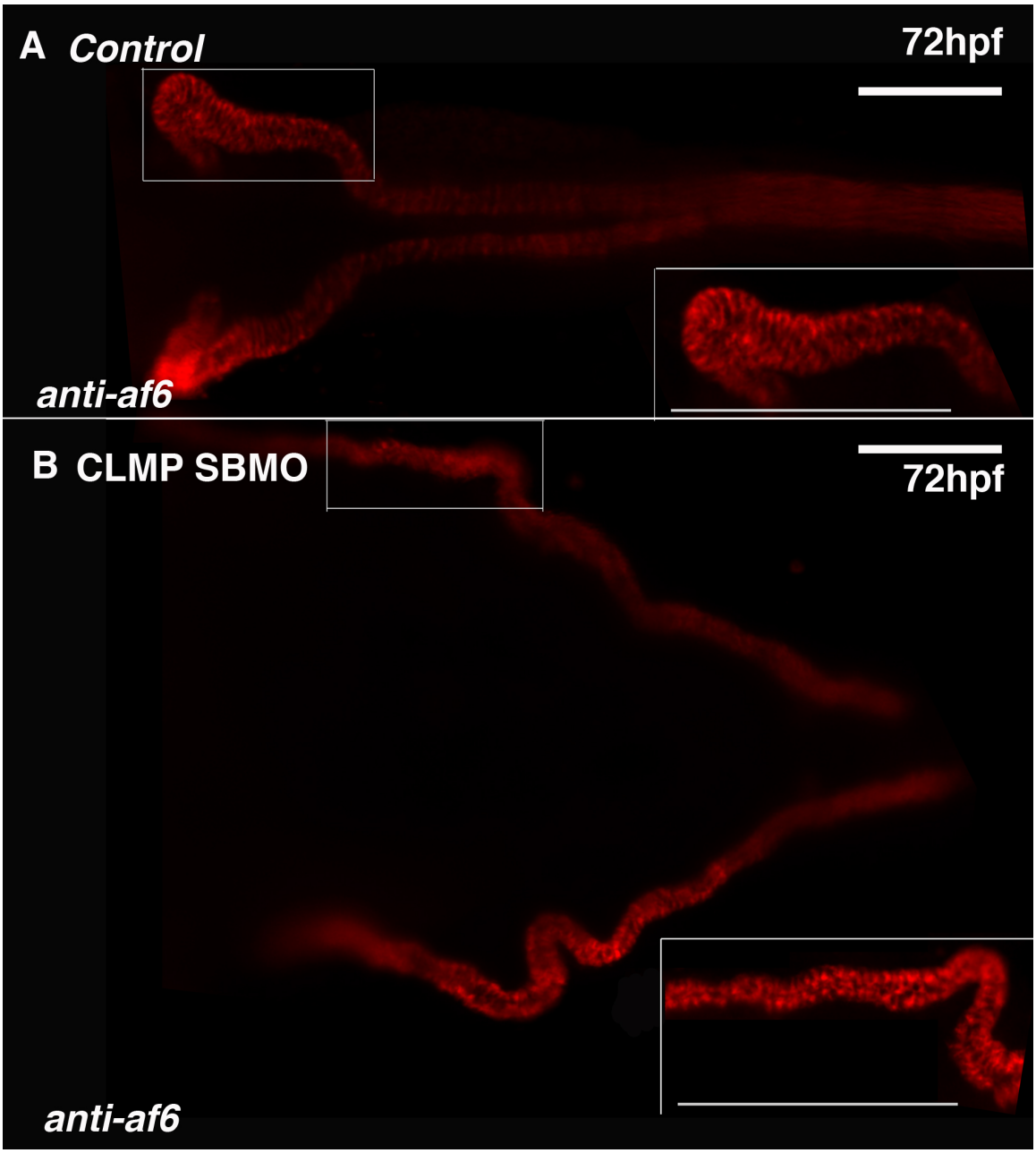

Figure 29: Kidney development is perturbed in CLMPa SBMO morphant embryos.

(A) Uninjected control embryo, (B) CLMPa morphant embryo. Ventral view of 72hpf embryos stained with an anti-af6 antibody labeling the zebrafish pronephros. The pronephric tubule is inset on both images. In the control

embryos, the pronephric tubule contains a fold, which is lacking in the CLMPa morphant embryos. CLMPa SBMO embryos also do not have the extension of the pronephric ducts that is seen in the control embryos. We hypothesize that the shortened body length phenotype in CLMPa morphants could be from an issue in convergent extension, which can be noted by the perturbation in kidney folding and extension.

Appendix B:

In Vivo Visualization of the Development of the Enteric Nervous System Using a Tg(28.3bphox2b:Kaede) Transgenic Zebrafish

Harrison, C.D. et al. *In vivo visualization of the development of the enteric nervous system using a Tg(-8.3bphox2b:Kaede) transgenic zebrafish*. Genesis, 2014

References provided at the end of the dissertation

My contributions to this work include making the Tol construct and performing proof of principle experiments to confirm the construct was functional. I subcloned the appropriate DNA fragments into the a vector to achieve a construct containing flanking Tol2 sites, -8.3Phox2b enhancer, c-fos minimal promoter, and Kaede. I microinjected this construct into 1-2 cell zebrafish embryos to confirm incorporation of the Kaede sequence, and exposed these embryos to ultraviolet light to confirm the photoconversion ability of the Kaede protein.

In Vivo Visualization of the Development of the Enteric Nervous System Using a Tg(28.3bphox2b:Kaede) Transgenic Zebrafish

Colin Harrison, Tara Wabbersen, Iain Shepherd.

Department of Biology, Emory University, Atlanta, Georgia

SUMMARY

The phox2b gene encodes a transcription factor that is expressed in the developing enteric nervous system (ENS). An enhancer element has been identified in the zebrafish phox2b locus that can drive tissue specific expression of reporter genes in enteric neuron precursor cells. We have generated a transgenic zebrafish line in which the Kaede fluorescent protein is under the control of this phox2b enhancer. This line has stable expression of the Kaede protein in enteric neuron precursor cells over three generations. To demonstrate the utility of this line we compared the migration and division rates of enteric neuron precursor cells in wild type and the zebrafish ENS mutant lessen.

Key words: enteric nervous system; phox2b; Kaede; in vivo; med24

Acknowledgements

The authors thank members of the shepherd lab for technical support. They also thank Dr. Andreas Fritz and Dr. Steve L'Hernault for comments on the manuscript.

INTRODUCTION AND RESULTS

The enteric nervous system (ENS) is the largest subdivision of the peripheral nervous system. Normal function of the ENS is essential to maintain proper function of the digestive system (Furness, 2012). The development of a fully functional ENS requires enteric neuronal precursor cells (ENPCs), which are largely derived from the cranial neural crest, to migrate to and along the gut while proliferating appropriately. Any errors in this developmental process can lead to aganglionosis of the gut, a condition commonly seen in the human clinical condition Hirschsprung's disease (Obermayr et al., 2013; Young, 2008).

While the general course of ENS development in many vertebrate species is known, better tools are needed to help understand all the intricacies of the process (Holmberg et al., 2004; Shepherd and Eisen, 2011; Young, 2008). Zebrafish are an ideal model system to develop these tools, given the ease with which one can image live embryos in vivo. Zebrafish embryos are externally fertilized, are transparent, and have a relatively fast generation time. Genetic tools are freely available that make it possible to generate transgenic animals in a time efficient and cost effective manner.

While green fluorescent protein is an excellent tool for visualizing developmental processes, alternative fluorescent proteins have shown great potential in unlocking new ways to observe biological phenomenon. One such protein, the Kaede protein, has the ability to shift its emission spectra when exposed to UV light (Ando et al., 2002; Mizuno et al., 2003). Normally this protein fluoresces

green, but when exposed to UV light the protein shifts to expressing red fluorescence (Ando et al., 2002; Mizuno et al., 2003). We have utilized this property of the Kaede protein, along with the live imaging benefits of the zebrafish, to develop a transgenic line to visualize development of the ENS in vivo.

To create this transgenic line we utilized the Tol2 transgenic system (Kawakami et al., 2000; Kawakami, 2004; Kwan et al., 2007). In this system, plasmids are generated with two Tol2 transposition sites flanking the target sequence of DNA to be integrated. When this Tol2 construct is injected into one-cell embryos along with the TOL2 transposase mRNA, the target sequence gets efficiently integrated into the host's genome. To express the Kaede protein in the ENPCs we utilized a zebrafish ENPC specific enhancer. The transcription factor Phox2b has previously been shown to be an excellent marker for ENPCs in zebrafish and other vertebrate species (Elworthy et al., 2005; Pattyn et al., 1999). Subsequent studies have shown that specific regions of the zebrafish phox2b enhancer are sufficient to drive GFP expression in ENPCs (McGaughey et al., 2008, 2009). Utilizing the 28.3bphox2b enhancer element we generated a plasmid containing the Kaede protein under control of this enhancer flanked by Tol2 sites (Fig. 30). Following injection into one-cell embryos, potential transgenics were isolated and raised to adulthood. These adults were then outcrossed with wild type adults and their progeny were re-screened for Kaede expression. One male was identified and was further outcrossed to establish the line. These transgenic embryos show stable expression of the Kaede protein in the neural crest and the

ENPCs with the ability to express the Kaede protein in the ENPCs we utilized a zebrafish ENPC specific enhancer. The transcription factor Phox2b has previously been shown to be an excellent marker for ENPCs in zebrafish and other vertebrate species (Elworthy et al., 2005; Pattyn et al., 1999). Subsequent studies have shown that specific regions of the zebrafish phox2b enhancer are sufficient to drive GFP expression in ENPCs (McGaughey et al., 2008, 2009). Utilizing the 28.3bphox2b enhancer element we generated a plasmid containing the Kaede protein under control of this enhancer flanked by Tol2 sites (Fig. 30). Following injection into one-cell embryos, potential transgenics were isolated and raised to adulthood. These adults were then outcrossed with wild type adults and their progeny were re-screened for Kaede expression. One male was identified and was further outcrossed to establish the line. These transgenic embryos show stable expression of the Kaede protein in the neural crest and the ENPCs with the ability to shift from red to green fluorescence after exposure to UV light (Fig. 31).

To demonstrate the utility of this line in studies of ENS development we carried out live imaging experiments with the transgenic embryos. We had previously identified a zebrafish ENS mutant in the lab, named lessen, that has a significantly reduced number of enteric neurons (Pietsch et al., 2006). This phenotype is caused by a null mutation in the med24 gene, a component of the mediator co-transcriptional activation complex (Pietsch et al., 2006). Subsequent experiments showed that med24 translation blocking morpholino produced a similar ENS phenotype to that seen in lessen mutants (Pietsch et al., 2006). The

ENS phenotype in the lessen mutant has been shown to be due to a decreased proliferation rate in the ENPCs (Pietsch et al., 2006). Utilizing the Tg(28.3bphox2b:Kaede) transgenic line we were able to look more closely at the med24 knockdown ENPC cellular phenotype in live imaged med24 morphant embryos.

We examined Tg(28.3bphox2b:Kaede) expression in uninjected control embryos and embryos that had been injected with the med24 morpholino. We compared both the migration and division rates between the two sets of embryos during the period ENPCs migrate along the gut (36–60 h post fertilization (hpf)) (Elworthy et al., 2005; Shepherd et al., 2004). We analyzed in detail a specific time period during this migration, comparing control and med24 morphant embryos from 50–56hpf (Fig. 32). From simple observation it is apparent that already at 50hpf ENPC migration in med24 morpholino injected embryos lags behind control embryo ENPC migration and the rate of this lag continues to increase over this time period. med24 morphant embryos show a 37.3% (66.7%) reduction in migration rate as compared to agematched controls (Fig. 33).

From observation of our control and med24 morphant embryos, we also see that there appears to be a decrease in division rate in the med24 morphants and that more division occurs at the leading edge than elsewhere in the migrating chain (Fig. 33). In photoconverted ENPCs, each cellular division decreases the amount of red photoconverted Kaede that is present in the cells. As these cells are dividing they are also continuing to make new green Kaede due to the continued

expression of the phox2b enhancer. Cells that are dividing rapidly will have higher levels of green fluorescence and lower levels of red fluorescence than cells that are dividing more slowly. To quantitate this data, we analyzed the levels of green and red fluorescence in the ENPCs over time. If the 28.3bphox2b enhancer is equally active in control and med24 morphants we would expect to see ENPCs in both gain green fluorescence back at the same rate after photoconversion. However, control embryos gain green fluorescence back faster than the med24 morphants (Fig. 34a). Some of this difference in the rate of change in color of the Kaede fluorescence could be due to higher 28.3bphox2b activity in our control embryos than compared to morphants. Alternatively, if the level of enhancer activity is the same in morphants and control embryos and the rate of ENPC cell division is less in med24 embryos we would expect to see the amount of red fluorescence in ENPCs to decrease at a slower rate than in control embryos. We do indeed see a significant decrease in the rate of loss of red fluorescence in our med24 morphants (Fig. 34b). This result is further validated when the number of divisions per cell is calculated, as we see a drop in this rate of ENPC cell division in our med24 morphants (Fig. 34c). This cell division count also confirms that division rates in the first two cells of the migrating chain are higher than the general rate for all ENPCs (Fig. 34c). This apparent proliferative migration driving the migration along the gut is consistent with our previous results and with experiments and observations in other species, as well as mathematical modeling of this developmental process (Barlow et al., 2008; Young et al., 2004).

In summary the Tg(28.3bphox2b:Kaede) transgenic line provides a powerful tool for studying ENS development. The ability to observe ENS development in vivo as well as selectively label specific cells will allow for a wide range of applications. In addition to what we have highlighted here, there are other potential uses for this transgenic line (Pan et al., 2012; Sato et al., 2006). One such use is the ability to label individual ENPCs and perform lineage analyses to determine if specific ENPCs give rise to specific ENS neuronal lineages at different time points during ENS development.

METHODS

Construct Generation

The 28.3bphox2b sequence was PCR amplified from genomic DNA and subcloned into the MCS of pBtol_cfosEGFP, a modified PBluescript vector containing the human cfos promoter and tol2 transposition sites, using EcoR1. The Kaede sequence was PCR amplified from a PCS2 Kaede containing plasmid and subcloned into pGW_cfosEGFP using BamH1 and Cla1 sites to attach SV40 poly A (Fisher et al., 2006b). Kaede SV40 was then subcloned into pBtol_cfosEGFP-8.3bphox2b by excising the EGFP in pBtol_cfosEGFP with BamH1 and Xba1.

Tg(28.3bphox2b:Kaede) Construct Injections

Wild type embryos were collected and injected at the one cell embryo stage. We established the line by injecting 400 embryos. The injection solution was prepared with 25 ng ll 21 of Tg(28.3bphox2b:Kaede) transposon construct, 35 ng ll 21 of transposase RNA, phenol red for visualization, and RNase-free water and kept on ice (Fisher et al., 2006a). About 1 nl of solution was injected into one cell embryos and embryos were raised at 28.5C.

Transgenic Screening and Raising

Injected Tg(28.3bphox2b:Kaede) embryos were screened for integration of the targeting construct by looking for Kaede fluorescence protein expression at 48 hpf. Twenty positive embryos were identified and raised to adulthood and outcrossed with wild type adults in the hope of generating germ line transmission

of the transgene. One adult male with germ line transgenic integration was identified and isolated. This male was then outcrossed to establish the line. Transgenic fish resulting from this line were phenotypically completely normal. The pattern of Kaede expression in ENPCs matches the phox2b mRNA expression pattern though the pattern of expression of Kaede in the CNS of the transgenic line does not appear to perfectly match the published pattern of phox2b in the CNS.

Med24 Morpholino Injections

Tg(28.3bphox2b:Kaede) transgenic adults were outcrossed with wild type adults and their embryos were injected at the one cell stage. One-cell embryos were injected with 1 ng of a med24 morpholino at a concentration of 5 ng ll 21 . The sequence for the translation blocking morpholino was 11/125, CCTGTTTCAGATTCACCACCTTCAT (Pietsch et al., 2006).

Stop Motion Filming

Embryos were raised to the desired age at 28.5C. med24 morphant and control embryos were then embedded in 0.6% agar (ringer's solution) in 35 3 10 mm2 filming dishes (Falcon) and covered with embryo media and mesab. Embryos were then exposed to UV light (358 nm) for 10 min to convert the Kaede protein from fluorescing green to red. Zstacked images were captured in SlidebookTM4.2 every fifteen minutes for 6–10 h (Olympus IX81). Subsequent images and movies were analyzed using NIH image J software (1.46r) (Rasband 199722012). To calculate the migration rate 24 control embryos and 20 med24 morphant

embryos were analyzed. Migration distances were obtained using the particle tracker plug-in for Image J to follow the path of the leading edge cell of the migrating ENPC chain (Sbalzarini and Koumoutsakos, 2005). To calculate florescence and division rates 64 starting ENPCs were analyzed. Flourescence was measured by calculating fluorescence intensity of the individual cell over the cell area. The particle tracker plug in was again used to follow the paths of ENPCs and new appearances of cells from previous cells to calculate division rate (Sbalzarini and Koumoutsakos, 2005). P values were calculated with a t test for division rate and within subjects ANOVA for all other cases.

FIGURE AND FIGURE LEGENDS

FIG. 30. Structure of the Tg(28.3bphox2b:Kaede) construct.

The 28.3bphox2b enhancer controls expression of the Kaede protein from a cFos minimal promoter. The flanking tol2 sites allow for integration of the construct into the genome when in the presence of the Tol2 transposase.

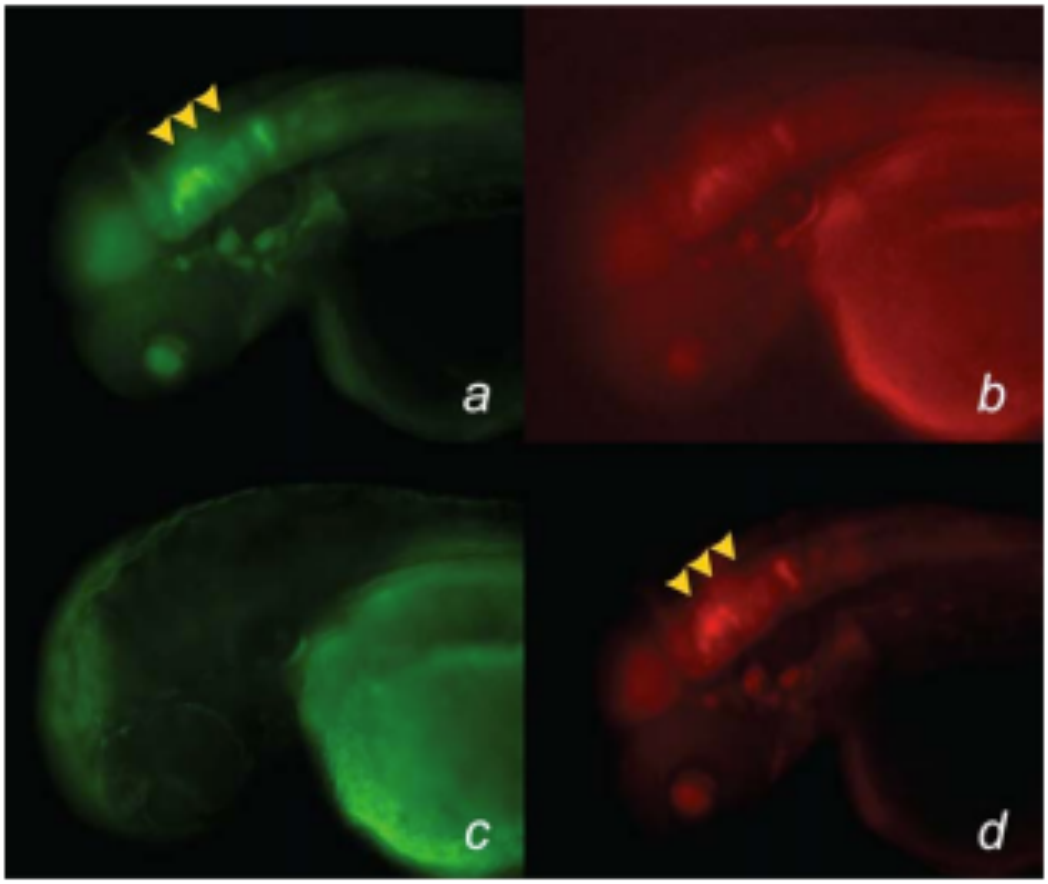

FIG. 31. Conversion of Kaede Protein from green fluorescence to red fluorescence after UV exposure.

(a) Tg(28.3bphox2b:Kaede) embryo expressing green fluorescence pre-conversion, arrowheads indicate expression in the hindbrain. (b) Tg(28.3bphox2b:Kaede) embryo expressing red fluorescence pre-conversion, there is a small amount of converted Kaede protein. (c) Tg(28.3bphox2b:Kaede) embryo expressing green fluorescence post-conversion, there is no green fluorescence in the neural crest after UV exposure D) Tg(28.3bphox2b:Kaede) embryo expressing red fluorescence post conversion, arrowheads indicate significant red fluorescence.

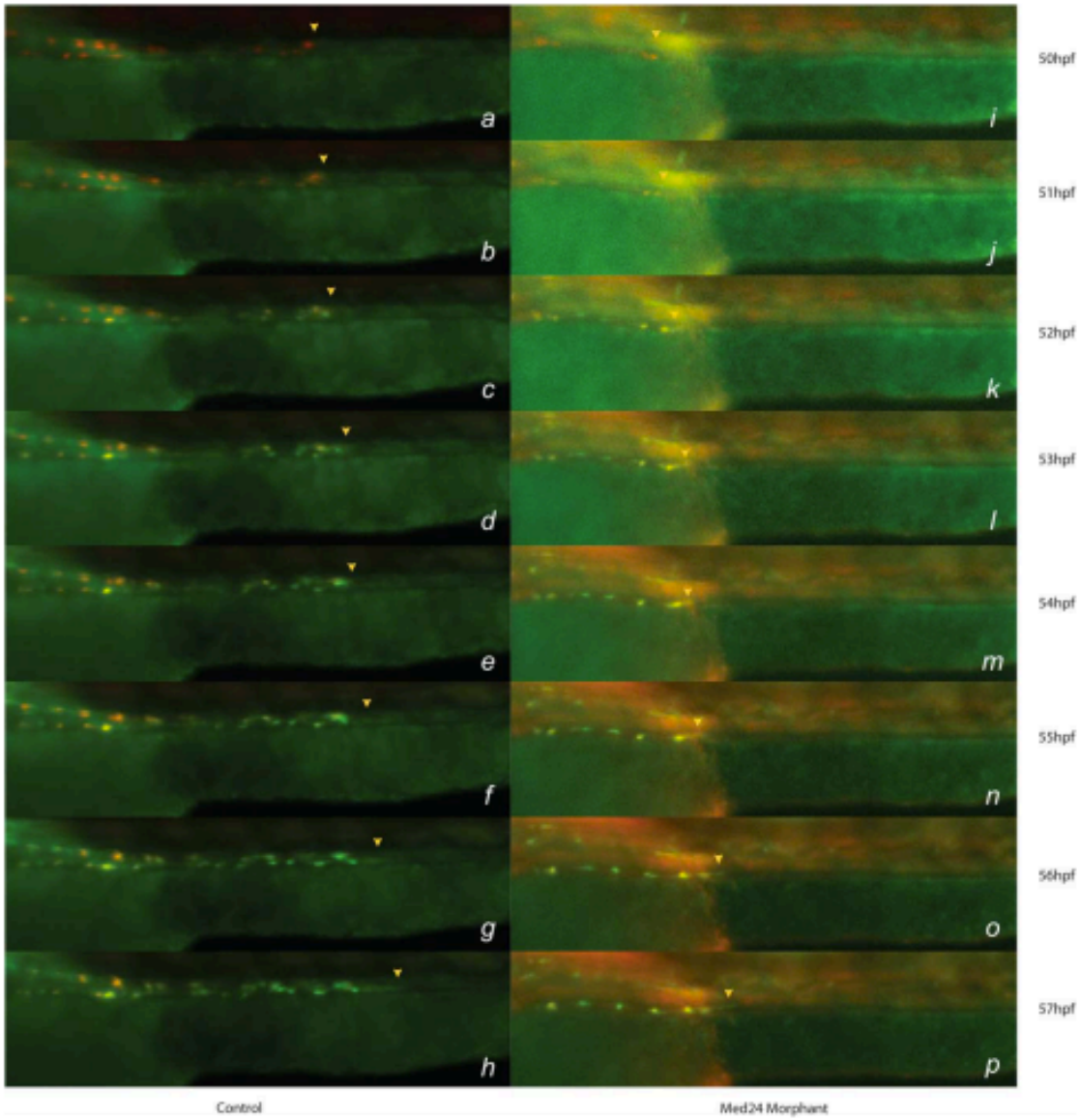

FIG. 32. Stills from a time-lapse movies of control and med24 injected Tg(28.3bphox2b:Kaede) transgenic embryos over the 50–57 hpf time period. Images (a–h) from control embryos while (j–p) are from med24 morpholino injected embryos. Each image is a stop motion image of the embryo on the hour. The left side of the each photo is the anterior portion of the gut and the yolk sac is at the bottom left of each image. The arrowheads indicate the leading cell in the migrating chain. The med24 embryos are initially lagging in

the migration of the ENPCs and continue to lag further over the course of the time period. ENPCs show green fluorescence more rapidly in control embryos.

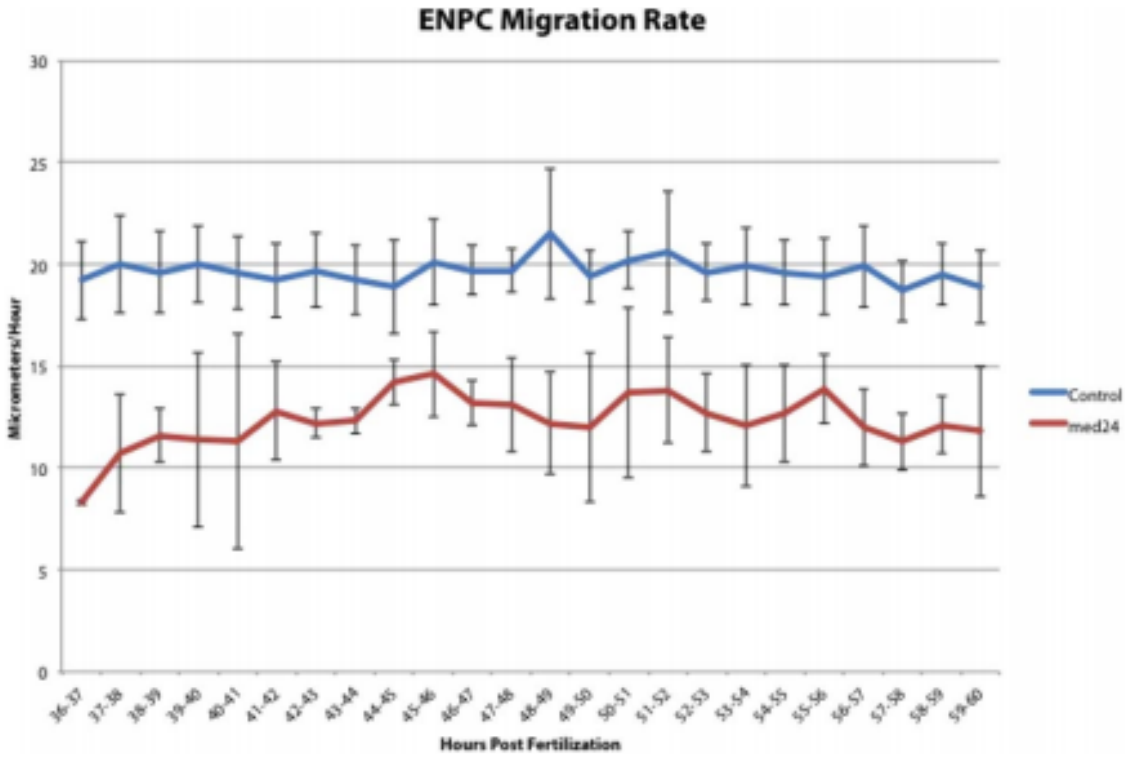

FIG. 33. Migration rate of the chain of enteric neuron precursors in control and med24 morpholino injected Tg(28.3bphox2b:Kaede) embryos.

The migration rate for med24 injected embryos is significantly less than that of the control embryos. Error bars are one standard deviation ($P < 0.0001$).

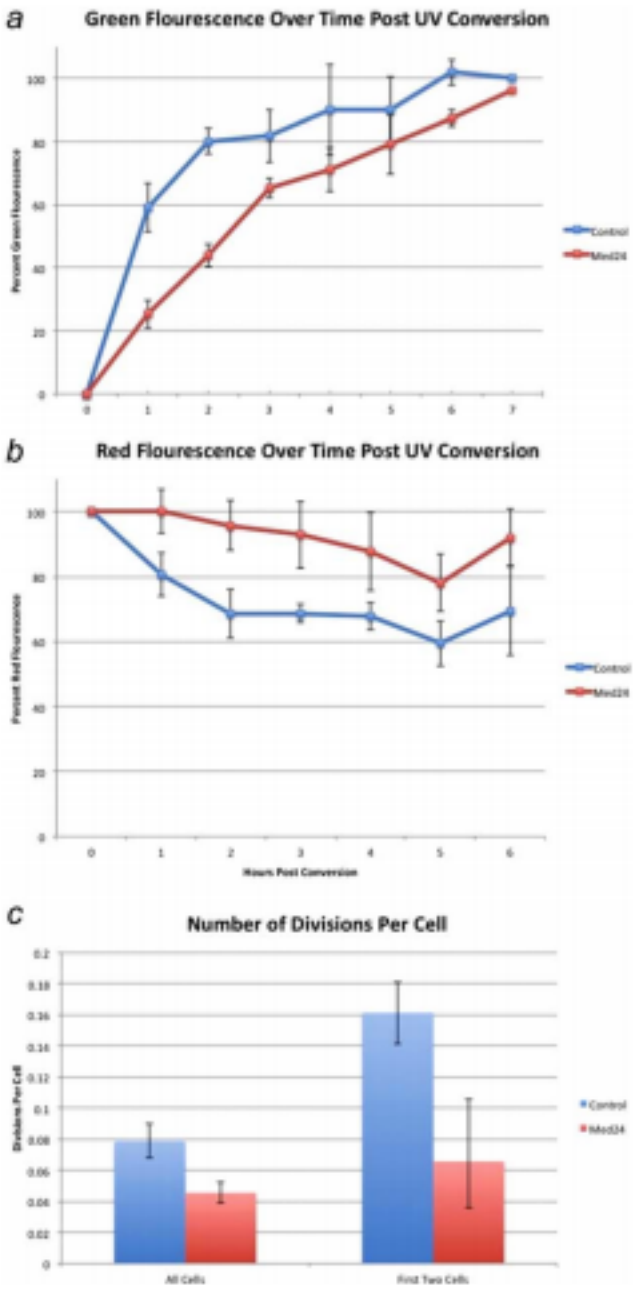

FIG. 34. Change in green and red fluorescence over time and cell division rate of ENPCs.

(a) Shows amount of green fluorescence relative to final levels of green fluorescence in control embryos. Control embryos see a faster increase in green fluorescence levels than in med24 embryos indicating a higher level of

28.3bphox2b enhancer activity (P 5 0.002). (b) Shows amount of red fluorescence relative to initial red fluorescence levels. Control embryos see a faster decrease in red fluorescence indicating a higher level of ENPC division (P 5 0.001). (c) Shows number of divisions per cell during ENPC migration. Division rate is significantly higher in control embryos as opposed to med24 embryos (P 5 0.03, P 5 0.04). The division rate is also higher in the first two cells of the migrating chain in control embryos but isn't significantly higher in med24 embryos (P 5 0.01, P 5 0.23).

References for Appendix B

Ando, R., Hama, H., Yamamoto-Hino, M., Mizuno, H., Miyawaki, A. (2002). "An optical marker based on the UV-induced green-to-red photoconversion of a fluorescent protein." Proc Natl Acad Sci USA. 99(20):12651-5.

Barlow, A.J., Wallace, A.S., Thapar, N., Burns, A.J. (2008). "Critical numbers of neural crest cells are required in the pathways from the neural tube to the foregut to ensure complete enteric nervous system formation." Development. 135(9):1681-91.

Elworthy, S., Pinto, J.P., Pettifier, A., Cancela, M.L., Kelsh, R.N. (2005). "Phox2b function in the enteric nervous system is conserved in zebrafish and is sox10-dependent." Mech Dev. 122(5):659-69.

Fisher, S., Grice, E.A., Vinton, R.M., Bessling, S.L., Urasaki, A., Kawakami, K., McCallion, A.S. (2006). "Evaluation the biological relevance of putative enhancers using Tol2 transposon-mediated transgenesis is zebrafish." Nat Protocols. 1(3):1297-305.

Furness, J.B. (2012). "The enteric nervous system and neurogastroenterology." Nat Rev Gastroenterol Hepatol. 9(5):286-94.

Holmberg, A., Schwerte, T., Pelster, B., Holmgren, S. (2004). "Ontogeny of the gut motility control system in zebrafish Danio rerio embryos and larvae." J Exp Biol. 207(Pt 23):4085-94.

Kawakami, K., Shima, A., Kawakami N. (2000). "Identification of a functional transposase of the Tol2 element, an Ac-like element from the Japanese medaka fish, and its transposition in the zebrafish germ lineage." Proc Natl Acad Sci USA. 97(21):11403-8.

Kwan, K.M., Fujuimoto, E., Grabher, C., Mangum, B.D., Hardy, M.E, Campbell, D.S.…Chien, C.B. (2007). "The Tol2kit: A multisite gateway-based construction kit for Tol2 transposon transgenesis constructs." Dev Dyn. 236(11):3088-99.

McGaughey, D.M., Stine, Z.E., Huynh, J.L., Vinton, R.M., McCallion, A.S. (2009). "Asymmetrical distribution of non-conserved regulatory sequences at PHOX2B is reflected at the ENCODE loci and illuminates a possible genome-wide trend." BMC Genom. 10(8).

McGaughey, D.M., Vinton, R.M., Huynh, J., Al-Saif, A., Beer, M.A., McCallion, A.S. (2008). "Metrics of sequence constraint overlook regulatory sequences in an exhaustive analysis at phox2b." Genome Res. 18(2):252-60.

Mizuno, H., Mal, T.K., Tong, K.I., Ando, R., Furuta, T., Ikura, M., Miyawaki, A. (2003). "Photo-induced peptide cleavage in the green-to-red conversion of a fluorescent protein." Mol Cell. 12(4):1051-8.

Obermayr, F., Hotta, R., Enomoto, H., Young, H.M. (2003). "Development and developmental disorders of the enteric nervous system." Nat Rev Gastroenterol Hepatol. 10(1):43-57.

Pan, Y.A., Caron, S.J., Schier, A.F. (2012). "BAPTI and BAPTISM birthdating of neurons in zebrafish." Cold Spring Harbor Protocols. 2012(1):87-92.

Pattyn, A., Morin, X., Cremer, H., Goridis, C., Brunet, J.F. (1999). "The homeobox gene Phox2b is essential for the development of autonomic neural crest derivatives." Nature. 399(6734):366-70.

Pietsch, J., Delalande, J.M., Jakaitis, B., Stensby, J.D, Dohle, S., Talbot, W.S....Shepherd, I.T. (2006). "Lessen encodes a zebrafish trap100 required for enteric nervous system development." Development. 133(3):395-406.

Rasband, W.S. (1997). "ImageJ." U.S. National Institutes of Health, Bethesda, Maryland, USA. Available at: http://imagej.nih.gov.proxy.library.emory.edu.ij/.

Sato, T., Takahoko, M., Okamoto, H. (2006). "HuC:Kaede, a useful tool to label neural morphologies in networks in vivo." Genesis. 44(3):136-42.

Sbalzarini, I.F., Koumoutsako, P. (2005). "Feature point tracking and trajectory analysis for video imaging in cell biology." J Struct Biol. 151(2):182-95.

Shepherd, I.T., Eisen, J. (2011). "Development of the zebrafish enteric nervous system." Methods Cell Biol. 101:143-60.

Shepherd, I.T., Pietsch, J., Elworthy, S., Kelsh, R.N., Raible, D.W. (2004). "Roles for GFRalpha1 receptors in zebafish enteric nervous system development." Development. 131(1):241-9.

Young, H.M. (2008). "Functional development of the enteric nervous system-From migration to motility." Neurogastroenterol Motil. 20(Suppl):20-31.

Young, H.M., Bergner, A.J., Anderson, R.B., Enomoto, H., Milbrandt, J., Newgreen, D.F., Whitington P.M. (2004). "Dynamics of neural crest-derived cell migration in the embryonic mouse gut." Dev Biol. 270(2):455-73.

REFERENCES

Amiel, J., Lyonnet, S. (2001). "Hirschsprung disease, associated syndromes and genetics: a review." J. Med. Genet. **38**(11): 729-39.

Amiel, J. Sproat-Emison, E., Garcia-Barcelo M., Lantieri, F., Burzynski, G., Borrego, S.,...Fernandez, R. (2008). "Hirschsprung disease, associated syndromes and genetics: a review." J. Med Genet. **45**(1):1-14.

Amiel, J., Laudier, B., Attie-Bitach, T., Trang, H., de Pontual, L, Gener, B.,... Lyonnet S. (2003). "Polyalanine expansion and frameshift mutations of the paired-like homeobox gene PHOX2B in congenitcal central hypoventilation syndrome." Nat Genet. **33**(4)459-61.

Anderson, J.M., Van Itallie, C.M. (2009). "Physiology and function of the tight junction." Cold Spring Harb Perspect Biol. **1**(2):a002584.

Anus. (n.d.). In *PubMed Health Glossary*. Retrieved from: http://www.ncbi.nlm.nih.gov/pubmedhealth/PMHT0022236/

Ascending colon. (n.d.). In *PubMed Health Glossary*. Retrieved from: http://www.ncbi.nlm.nih.gov/pubmedhealth/PMHT0022238/

Avaron, F., Smith, A., Akimenko, M.A., (2000). "Sonic Hedgehog Signaling in the Developing and Regenerating Fins of Zebrafish." Madame Curie Bioscience Database [Internet].

Avaron, F., Hoffman, L, Guay, D, Akimenko, M.A. (2006). "Characterization of two new zebrafish members of the hedgehog family: atypical expression of a zebrafish indian hedgehog gene in skeletal elements of both endochondral and dermal origins." Dev. Dyn. **235**(2):478-89.

Balda, M.S., Matter, K. (2000). "The tight junction protein ZO-1 and an interacting transcript factor regulate ErbB-2 expression." EMBO J. **19**(9):2024-33.

Betts, M.J., Russell, R.B. (2003). "Amino acid properties and consequences of substitutions." Wiley.

Baynash, A.G., Hosoda, K., Giaid, A., Richardson, J.A., Emoto, N., Hammer, R.E., Yanagisawa, M. (1994). "Interaction of endothelin-3 with endothelian-B receptor is essential for development of epidermal melanocytes and enteric neurons." Cell. **79**(7):1277-85

Briscoe, J., Therond, P.P. (2013). "The mechanisms of Hedgehog signalling and its role in development and disease." Nat Rev Mol Cell Biol. **14**(7):416-29.

Brookes, S.J. (2001). “Classes of enteric nerve cells in the guinea-pic small intestine.” Anat Rec. **262**(1):58-70.

Brooks, S.A., Oostra, B.A., Hofstra, R.M. (2005). “Studying the genetics of Hirschsprung’s disease: unraveling an oligogenic disorder.” Clin. Genet. **67**(1):6-14.

Barlow, A.J, Wallace, A.S., Thapar, N., Burn, A.J. (2008). “Critical numbers of neural crest cells are required in the pathway from the neural tube to the foregut to ensure complete enteric nervous system formation.” Development. **135**(9):1681-91.

Cacalano, G., Farinas, I., Wang, L.C., Hagler, K., Forgie, A., Moore, M.,…Rosenthal, A. (1998). “GFRalpha1 is an essential receptor component for GDNF in the developing nervous system and kidney.” Neuron. **21**(1):53-62.

Cacheux, V., Dastot-Le Moal, F., Kaariainen, H., Bondurand, N., Rintala, R., Boissier, B., …Goossens, M. (2001). “Loss-of-function mutations in SIP1 Smad interacting protein 1 result in a syndromic Hirschsprung disease.” Hum Mol Genet. **10**(14):1503-10.

Cecum (n.d.). In *PubMed Health Glossary*. Retrieved from: http://www.ncbi.nlm.nih.gov/pubmedhealth/PMHT0022237/

Chalazonitis, A., D’Autreaux, F., Guha, U., Pham, T.D., Faure, C., Chen, J.J.,…Gershon, M.D. (2004). “Bone morphogenetic protein-2 and -4 limit the number of enteric neurons but promote development of a TrkC-expressing neurotrophin-3-dependent subset.” J Neurosci. **24**(17):4266-82.

Cochran, W. (2013). “Overview of Congenital GI Anomalies.” Merck Manual. Retrieved from: https://www.merckmanuals.com/professional/pediatrics/congenital-gastrointestinal-anomalies/overview-of-congenital-gi-anomalies

Cohn, M.J., Tickle, C. (1996). “Limbs: a model for pattern formation within the vertebrate body plan.” Trends Genet. **12**(7):253-7.

Currie, P.D., Ingham, P.W. (1996). “Induction of a specific muscle cell type by a hedgehog-like protein in zebrafish.” Nature. **382**(6590):452-5.

De Moerlooze, L., Spencer-Dene, B., Revest, J.M., Hajihosseini, M. Rosewell, I., Dickson, C. (2000). “An important role for the IIIb isoform of fibroblast growth factor receptor (FGFR2) in mesenchymal-epithelial signaling during mouse organogenesis.” Development. **127**(3):483-92.

Delatte, M., Von den Hoff, J.W., Kuijpers-Jagtman, A.M. (2005). "Regulatory effects of FGF-2 on the growth of mandibular condyles and femoral heads from newborn rats." Arch Oral Biol. **50**(11):959-69.

Descending colon. (n.d). In *PubMed Health Glossary*. Retrieved from: http://www.ncbi.nlm.nih.gov/pubmedhealth/PMHT0022239/

Dooley, K., Zon, L.I. (2000). "Zebrafish: a model system for the study of human disease." Curr Opin Genet Dev. **10**(3):252-6.

Doray, B., Salomon, R., Amiel, J., Pelet, A., Touraine, R., Billaud, M., … Lyonnet, S. (1998). "Mutation of the RET ligand, neurturn, supports multigenic inheritance in Hirschsprung disease." Hum Mol Genet. **7**(9):1449-52.

Dorey, K., Amaya, E. (2010). "FGF signalling: diverse roles during early vertebrate embryogenesis." Development. **137**(22):3731-3742.

Dossenbach, C., Rock, S., Affolter, M. (2001). "Specificity of FGF signaling in cell migration in Drosophila." Development. **128**(22):4563-72.

Edery, P., Attie, T., Amiel, J., Pelet A., Eng, C., Hofstra, R.M., …Lyonnet S. (1996). "Mutation of the endothelin-3 gene in the Waardenburg-Hirschsprung disease (Shah-Waardenburg syndrome)." Nat Genet. **12**(4):442-4.

Ekker, S.C., Ungar, A.R., Greenstein, P., von Kessler, D.P., Porter, J.A., Moon, R.T., Beachy, P.A. (1995). "Patterning activities of vertebrate hedgehog protein in the developing eye and brain." Curr Biol. **5**(8):944-55.

Epstein, M.L., Mikawa, T., Brown, A.M., McFarlin, D.R. (1994). "Mapping the origin of the avian enteric nervous system with a retroviral marker." Dev. Dyn. **201**(3)236-244.

Fischer, S., Draper, B.W., Neumann, C.J. (2003). "The zebrafish fgf24 mutant identifies an additional level of Fgf signaling involved in vertebrate forelimb initiation." Development. **130**(15):3515-24.

FitzSimmons, J., Chinn, A., Shepard, T.H. (1988). "Normal length of the human fetal gastrointestinal tract." Pediatr Pathol. **8**(6):633-41.

Furness, J.B. (2006). "The Enteric Nervous System." Oxford: Blackwell Publishing.

Furness, J.B. (2012). "The enteric nervous system and neurogastroenterology." Nat Rev Gastroenterol Hepatol. **9**(5):286-94.

Furuse, M. (2010). "Molecular basis of the core structure of tight junctions." Cold Spring Harb Perspect Biol. **2**(1):a002907.

Garcia-Barcelo, M.M., Lee, W.S., Sham, M.H., Lui, V.C., Tam, P.K. (2003). "Is there a role for the IHH gene in Hirschsprung's disease?" Neurogastroenterol Motil. **15**(6):663-8.

Garcia-Barcelo, M.M., Ganster, R.W., Lui, V.C., Leon, T.Y., So, M.T., Lau, A.M., … Tam, P.K. (2005). "TTF-1 and RET promoter SNPs: regulation of RET transcription in Hirschsprung's disease." Hum Mol Genet. **14**(2):191-204.

Garcia-Barcelo, M.M. Tang, C.S. Ngan, E.S., Lui, V.C., Chen, Y., So, M.T., … Tam, P.K. (2009). "Genome-wide association study identifies NRG1 as a susceptibility locus for Hirschsprung's disease." Proc Natl Acad Sci USA. **106**(8):2694-9.

Gastrointestinal Tract (n.d.). In *PubMed Health Glossary*. Retrieved from: http://www.ncbi.nlm.nih.gov/pubmedhealth/PMHT0022855/

Gershon, M.D., Ratcliffe, E.M., (2004). "Developmental biology of the enteric nervous system: pathogenesis of Hirschspurng's disease and other congenital dysmotilities." Semin. Pediatr. Surg. **13**(4):224-35.

Gilbert, S.F. (2000). "Developmental Biology." Massachusetts: Sinauer Associates.

Goldstein, A.M., Brewer, K.C., Doyle, A.M., Nagy, N., Roberts D.J. (2005). "BMP signaling is necessary for neural crest cell migration and ganglion formation in the enteric nervous system." Mech. Dev. **122**(6):821-33.

Goldstein, A.M., Hofstra, R.M., Burns, A.J. (2013). "Building a brain in the gut: development of the enteric nervous system." Clin Genet. **83**(4):307-16.

Hagl, C.I., Wink, E., Heumuller-Klug, S., Weiss, C., Wessel, L., Gretz, N., Schafer, K.H. (2012). "Enteric neurons from postnatal Fgf2 knockout mice differ in neurite outgrowth responses." Auton. Neurosci. **170**(1-2):56-61.

Hamilton, J.R., Reilly, B.J., Morecki, R. (1969). "Short small intestine associated with malrotation: a newly described congenital cause of intestinal malabsorption." Gastroenterology. **56**(1):124-36.

Hasosah, M., Lemberg, D.A., Skarsgard, E., Schreiber, R., (2008). "Congenital short bowel syndrome: a case report and review of the literature." Can J Gastroenterol. **22**(1):7-14.

Heanue, T.A., Pachnis, V. (2006). "Expression profiling the developing mammalian enteric nervous system identifies markers and candidate Hirschsprung disease genes." Proc. Natl. Acad. Sci. **103**(18):6919-24.

Heanue, T.A., Pachnis, V. (2007). "Enteric nervous system development and Hirschsprung's disease advances in genetic and stem cell studies." Nat. Rev. Neurosci. **8**(6):466-79.

Heanue, T.A., Pachnis, V. (2008). "Ret isoform function and marker gene expression in the enteric nervous system is conserved across diverse vertebrate species." Mech Dev. **125**(8):687-99.

Heuckeroth, R.O., Lampe, P.A., Johnson, E.M., Milbrandt, J. (1998). "Neurturin and GDNF promote proliferation and survival of enteric neuron and glial progenitors in vivo." Dev. Biol. **200**(1):116-29.

Hofstra, R.M., Osinga, J., Tan-Sindhunata, G., Wu, Y., Kamsteeg, E.J., Stulp, R.P., … Buys, C.H. (1996). "A homozygous mutation in the endothelin-3 gene associated with a combined Waardenburge type 2 and Hirschsprung phenotype (Shah-Waardenburg syndrome)." Nat Genet. **12**(4):445-7.

Hofstra, R.M., Valdenaire, O., Arch, E., Osinga, J., Kroes, H., Loffler, B.M., … Buys, C.H. (1999). "A loss-of-function mutation in the endothelin-converting enzyme 1 (ECE-1) associated with Hirschsprung disease, cardiac defects, and autonomic dysfunction." Am J Hum Genet. **64**(1):304-8.

Hosoda, K., Hammer, R.E., Richardson, J.A., Baynash, A.G., Cheung, J.C., Giaid, A., Yanagisawa, M. (1994). "Targeted and natural (piebald-lethal) mutations of endothelin-B receptor gene produce megacolon associated with spotted coat color in mice." Cell. **79**(7):1267-76.

Hunziker, W., Kiener, T.K., Xu, J. (2009). "Vertebrate animal models unravel physiological roles for zona occludens tight junction adaptor proteins." Ann N Y Acad Sci. **1165**:28-33.

Huysman, W.A., Tibboel, D., Bergmeijer, J.H., Molenaar, J.C. (1991). "Long term survival of a patient with congenital short bowel syndrome and malrotation." J Pediatr Surg. **26**(1):103-5.

Ingham, P.W., McMahon, A.P. (2001). "Hedgehog signaling in animal development: paradigm and principles." Genes Dev. **15**(23):3059-87.

Itoh, N., Knoishi, M. (2007). "The zebrafish fgf family." Zebrafish. **4**(3):179-86.

Jessell, T.M. (2000). “Neuronal specification in the spinal cord:inductive signals and trasciptional codes.” Nat Rev Genet. **1**(1): 20-9.

Johnston, M.C., Bronsky, P.T. (1995). “Prenatal craniofacial development: new insights on normal and abnormal mechanisms.” Crit Rev Oral Biol Med. **6**(4):368:422.

Kato, Y., Yu, D., Schwartz, M.Z. (1998). “Enhancement of intestinal adaptation by hepatocyte growth factor.” J Pediatr Surg. **33**(2):235-9.

Kimmel, C.B., Ballard, W.W., Kimmel, S.R., Ullmann, B., Schilling, T.F. (1995). “Stages of embryonic development of the zebrafish.” Dev. Dyn. **203**(3):253-310.

Kimmelman, D, Kirschner, M., (1987). Syndergistic induction of mesoderm by FGF and TFG-beta and the identification of an mRNA coding for FGF in the early Xenopus embryo.” Cell. **51**(5):869-77.

Krause, G. Winkler, L, Mueller, S.L., Haseloff, R.F., Piontek, J., Blasic, I.E. (2007). “Structure and function of claudins.” Biochim Biophys Acta. **1778**(3):631-45.

Krauss, S., Concordet, J.P., Ingham, P.W. (1993). “A functionally conserved homolog of the Drosophila segment polarity gene hh is expressed in tissues with polarizing activitiy in zebrafish embryos.” Cell. **75**(7):1431-44.

Korzh, S., Winata, C.L., Zheng, W., Yang, S., Yin, A., Ingham, P.,…Gong, Z. (2011). “The interaction of epithelial Ihha and mesenchymal Fgf10 in zebrafish esophageal and swimbladder development.” Dev Biol. **359**(2):262-276.

Le Douarin, N.M., Teillet, M.A., (1973). “The migration of neural crest cells to the wall of the digestive tract in avaian embryo.” J Embryol Exp Morphol. **30**(1):31-48.

Le Douarin, N., Kalcheim, C. (1999). “The Neural Crest.” Cambridge: Cambridge University Press.

Lee, Y., Grill, S., Sanchez, A., Murphy-Ryan, M., Poss, K.D., (2005). “Fgf signaling instructs position-dependent growth rate during zebrafish fin regeneration.” Development. **132**(23):5173-83.

Manfroid, I., Delporte, F., Baudhuin, A., Motte, P., Neumann, C.J., Voz, M.L.,…Peers, B. (2007). “Reciprocal endoderm-mesdoderm interactions mediated by fgf24 and fgf10 govern pancreas development.” Development. **134**(22):4011-21.

Maroon, H., Walshe, J. Mahmood, R., Kiefer, P., Dickson, C., Mason, I. (2002). "Fgf3 and Fgf 8 are required together for formation of the otic placode and vesicle." Development. **129**(9):2099-108.

Martin, G.R., Beck, P.L., Sigalet, D.L. (2006). "Gut hormones, and short bowel syndrome: the enigmatic role of glucagon-like peptide-2 in the regulation of intestinal adaptation." World J Gastroenterol. **12**(26):4117-29.

Matter, K., Balda, M.S. (2003). "Signaling to and from tight junctions." Nat Rev Mol Cell Biol. **4**(3):225-36.

McKee, R., Gerlach, G.F., Jou, J. Cheng, C.N., Wingert, R.A. (2014). "Temporal and spatial expression of tight junction genes during zebrafish pronephros development." Gene Expr Patterns. **16**(2):104-13.

Moore, M.W., Klein, R.D., Farinas, I., Sauer, H., Armanini, M., Phillips, H.,...Rosenthal, A. (1996). "Renal and neuronal abnormalities in mice lacking GDNF." Nature. **382**(6586):76-9.

Moretti, S. Armougom, F., Wallace, I.M., Higgins, D.G., Jongeneel, C.V., Notredame, C. (2007). "The M-Coffee web server: a meta-method for computing multiple alignments by combining alternative alignment methods." Nucleic Acids Res. **35**(Web Server issue):W645-8.

Nasevicius, A., Ekker, S.C. (2000). "Effective targeted gene 'knockdown' in zebrafish." Nat Genet. **26**(2):216-20.

Nechiporuk, A., Linbo, T., Poss, K.D., Raible, D.W. (2007). "Specification of epibranchial placodes in zebrafish." Development. **134**(3):611-23.

Newgreen, D., Young, H.M., (2002a). "Enteric nervous system: development and developmental disturbances—part 1." Pediatr Dev Pathol. **5**(3):224-47.

Newgreen, D., Young, H.M., (2002b). "Enteric nervous system: development and developmental disturbances—part 2." Pediatr Dev Pathol. **5**(4):329-49.

Ng, A.N., de Jong-Curtain, T.A., Mawdlsey, D.J., White, S.J., Shin, J., Appel, B., ...Stainier, D.Y. (2005). "Formation of the digestive system in zebrafish: III. Intestinal epithelium morphogenesis." Dev. Biol. **286**(1):114-35.

Noah, T.K., Donahue, B., Shroyer, N.F. (2011). "Intestinal development and differentiation." Exp Cell Res. **317**(19):2702-10.

Norton, W.H., Ledin, J., Grandel, H., Neumann, C.J. (2005). "HSPG synthesis by zebrafish Ext2 and Extl3 is required for Fgf10 signalling during limb development." Development. **132**(22):4963-73.

Nomura, R., Kamei, E., Hotta, Y., Knoishi, M., Mikyake, A., Itoh, N. (2006). "Fgf16 is essential for pectoral fin bud formation in zebrafish." Biochem Biophys Res Commun. **347(**1):340-6.

Ordonez, P., Sondheimer, J.M., Fidanza, S., Wilkening, G., Hoffenberg, E.J. (2006). "Long-term outcome of a patient with congenital short bowel syndrome." J Pediatr Gastroenterol Nutr. **42**(5):576-80.

Pichel, J.G., Shen, L., Sheng, H.Z., Granholm, A.C., Drago, J., Gringberg, A., … Westphal, H. (1996). "Defects in enteric inneration and kidney development in mice lacking GDNF." Nature. **382**(6586):73-6.

Pingault, V., Bondurand, N., Kuhlbrodt, K., Goerich, D.E., Prehu, M.O., Puliti, A., …Goossens, M. (1998). "SOX10 mutations in patients with Waardenburg-Hirschsprung disease." Nat Genet. **18**(2):171-3.

Poss, K.D., Shen, J., Nechiporuk, A., McMahon, G., Thisse, B., Thisse, C., Keating, M.T. (2000). "Roles for Fgf signaling during zebrafish fin regeneration." Dev. Biol. **222**(2):347-58.

Postlethewait, J.H., Woods, I.G., Ngo-Hazelett, P., Yan, Y.L., Kelly, P.D., Chu, F.…Talbot, W.S. (2000). "Zebrafish comparative genomics and the origins of vertebrate chromosomes." Genome Res. **10**(12):1890-902

Prato, P., Rossi, V., Avanzini, S., Mattioli, G., Disma, N., Jasonni, V. (2011). "Hirschsprung's disease: what about mortality?" Pediatr Surg Int. **27**(5):473-8.

Puffenberger, E.G., Hosoda, K., Washington, S.S., Nakao, K., deWit, D., Yanagisawa, M., Chakravart, A. (1994). "A missense mutation of the endothelin-B receptor gene in multigenic Hirschsprung's disease." Cell. **79**(7):1257-66.

Puri, P., Ohshiro, K., Wester, T. (1998). "Hirschsprung's disease: a search for etiology." Semin Pediatr Surg. **7**(3):140-7.

Raible, D.W., Kruse, G.J., (2000). "Organization of the lateral line system in embryonic zebrafish." J Comp Neurol. **421**(2):189-98.

Ramalho-Santos, M., Melton, D.A., McMahon, A.P. (2000). "Hedgehog signals regulate multiple aspects of gastrointestinal development." Development. **127**(2):2763-72.

Rao, J.N., Wang, J.Y. (2010). "Regulation of Gastrointestinal Mucosal Growth." San Rafael CA: Morgan & Claypool Life Sciences.

Raschperger, E., Engstrom, U, Pettersson, R.F., Fuxe, J. (2004). "CLMP, a novel member of the CTX family and a new component of epithelial tight junctions." J Biol Chem. **279**(1):796-804.

Rectum. (n.d.). In *PubMed Health Glossary*. Retrieved from: http://www.ncbi.nlm.nih.gov/pubmedhealth/PMHT0022230/

Reichenbach, B., Delalande, J.M., Kolmogorova, E., Prier, A., Nguyen, T., Smith, C.M., ...Shepherd, I.T. (2008). "Endoderm-derived Sonic hedgehog and mesoderm Hand2 expression are required for enteric nervous system development in zebrafish." Dev. Biol. **318**(1):52-64.

Reiquam, C.W., Allen, R.P., Akers, D.R. (1965). "Normal and Abnormal Small Bowel Lengths: An Analysis of 389 Autopsy Cases in Infants and Children." Am. J. Dis. Child. **109**:447-51.

Robu, M.E., Larson, J.D., Nasevicius, A., Beiraghi, S., Brenner, C., ... Ekker, S.C. (2007). "p53 activation by knockdown technologies." PLoS Genet. **3**(5):e78.

Rossi, J., Luukko, K., Poteryaev, D., Laurikainen, A., Sun, Y.F., Laakso, T., ... Airaksinen, M.S. (1999). "Retarded growth and deficits in the enteric and parasympathetic nervous system in mice lacking GFR alpha2, a functiona neurturin receptor." Neuron. **22**(2):243-52.

Schalamon, J., Schober, P.H., Gallippi, P., Matthyssens, L., Hollwarth, M.E. (1999). "Congenital short-bowel; a case study and review of the literature." Eur J Pediatr Surg. **9**(4):248-50.

Schuchardt, A., D'Agati, V., Larsson-Blomberg, L., Costantini, F., Pachnis, V. (1994). "Defects in the kidney and enteric nervous system of mice lacking the tyrosine kinase receptor Ret." Nature. **367**(6461):380-3.

Short Bowel Syndrome. (n.d.). In *National Institute of Diabetes and Digestive and Kidney Diseases*. Retrieved from: http://www.niddk.nih.gov/health-information/health-topics/digestive-diseases/short-bowel-syndrome/Pages/facts.aspx

Siebert, J.R. (1980). "Small-intestine length in infants and children." Am J Dis Child. **134**(6):593-5.

Sigmoid colon. (n.d.). In *PubMed Health Glossary*. Retrieved from: http://www.ncbi.nlm.nih.gov/pubmedhealth/PMHT0022242/

Silverio, K.G., Martinez, A.E., Rossa, C. Jr. (2007). "Effects of basic fibroblast growth factor on density and morphology of fibroblasts grown on root

surfaces with or without condition with tetracycline or EDTA." J Oral Sci. **49**(3):213-20.

Shepherd, I.T., Pietsch, J. Elworthy, S., Kelsh, R.N., Raible, D.W. (2004). "Roles of GFRalpha1 receptors in zebrafish enteric nervous system development." Development. **131**(1):241-9.

Shepherd, I.T., Eisen, J. (2011). "Development of the zebrafish enteric nervous system." Methods Cell Biol. **101**:143-60.

Small Intestine. (n.d.). In *PubMed Health Glossary*. Retrieved from: http://www.ncbi.nlm.nih.gov/pubmedhealth/PMHT0022231/

Sukegawa, A., Narita, T., Kameda, T., Saitoh, K, Nohno, T, Iba, H., ...Fukuda, K. (2000). "The concentric structure of the developing gut is regulated by Sonic hedgehog derived from endodermal epithlium." Development. **127**(9):1971-80.

Sze, K.L., Lee, W.M., Lui, W.Y. (2008). "Expression of CLMP, a novel tight junction protein, is mediated via the interaction of GATA with the Kruppel family protein, KLF4 and Sp1, in mouse TM4 Sertoli cells." J Cell Physiol. **214**(2):334-44.

Taketomi, T, Yoshiga, D., Taniguchi, K. Kobayashi, T., Nonami, A., Kato, R., ... Yoshimura, A. (2005). "Loss of mammalian Sprouty2 leads ot enteric neuronal hyperplasia and esophageal achalasia." Nat Neurosci. **8**(7):855-7.

Thisse, C., Thisse, B., Schilling, T.F., Postlethwait, J.H. (1993). "Structure of the zebrafish snail1 gene and its expression in wild-type spadetail and no tail mutant embryos." Development. **119**(4):1203-15.

Transverse colon. (n.d.). In *PubMed Health Glossary*. Retrieved from: http://www.ncbi.nlm.nih.gov/pubmedhealth/PMHT0022243/

Turner, N., Grose, R. (2010). "Fibroblast growth factor signalling: from development to cancer." Nat Rev Cancer. **10**(2):116-29.

Van Der Werf, C.S., Wabbersen, T.W., Hsiao, N.H., Paredes, J., Etchevers, H.C, Kroisel, P.M., ... Hofstra, R.M. (2012). "CLMP is required for intestinal development, and loss-of function mutations cause congenital short-bowel syndrome." Gastroenterology. **142**(3):453-462.

Van Der Werf, C.S., Halim, D., Verheij, J.B., Alves, M.M., Hofstra, R.M. (2015). "Congenital Short Bowel Syndrome: from clinical and genetic diagnosis to the molecular mechanisms involved in intestinal elongation." *Biochim Biophys Acta*. **1852**(11):2352-61

Veldman, M.B., Lin, S. (2008). “Zebrafish as a developmental model organism for pediatric research.” Pediatr Res. **64**(5):470-6.

Wakamatsu, N., Yamada, Y., Yamada, K., Ono, T., Nomura, N., Taniguchi, H., …Nagaya, M. (2001). “Mutations in SIP1, encoding Smad interacting protein-1, cause a form of Hirschsprung disease.” Nat Genet. **27**(4):369-70.

Wales, P.W., Nasr, A., de Silva, N., Yamada, J. (2010). “Human growth hormone and glutamine for patients with short bowel syndrome.” Cochrane Database Syst Rev. **16**(6):CD006321.

Wallace, K.N., Akhter, S., Smith, E.M., Lorent, K., Pack, M. (2005). “Intestinal growth and differentiation in zebrafish.” Mech Dev. **122**(2):157-73.

Westerfield, M. (1993). “The Zebrafish Book.” Eugene, OR: University of Oregon Press.

Whitehead, G.G., Makino, S., Lien, C.L., Keating, M.T. (2005). “fgf20 is essential for initiating zebrafish fin regeneration.” Science. **310**(5756):1957-60.

Winata, C.L., Korzh, S., Kondrychyn, I, Zheng, W., Korzh, V., Gong, Z. (2009). “Development of zebrafish swimbladder: The requirement of Hedgehog signaling in specification and organization of the three tisuee layers.” Dev. Biol. **331**(2):222-36.

Wu, X., Howard, M.J. (2002). “Transcripts encoding HAND genes are differentially expressed and regulated by BMP4 and GDNF in developing avain gut.” Gene Expr. **10**(5-6):279-93.

Yang, H., Wildhaber, B.E., Teitelbaum, D.H. (2003). “Keratinocyte growth factor improves epithelial function after massive small bowel resection.” JPEN J Parenter Enteral Nutr. **27**(3):198-206.

Yamauchi, H., Hotta, Y., Konishi, M., Miyake, A., Kawahara, A., Itoh, N. (2006). “Fgf21 is essential for haematopoiesis in zebrafish.” EMBO Rep. **7**(6):649-54.

Yanagisawa, H., Yanagisawa, M. Kapur, R.P., Richardson, J.A., Williams, S.C. Couthier, D.E.,… Hammer, R.E. (1998). “Dual genetic pathways of endothelin-mediated intercullar signaling revealed by targeted disruption of endothelin converting enzyme-1 gene.” Development. **125**(5):825-36.

Yoneda, A., Wang, Y., O’Briain, D.S., Puri, P. (2001). “Cell-adhesion molecules and fibroblast growth factor signaling in Hirschsprung’s disease.” Pediatr Surg Int. **17**(4):299-303.

Your Digestive System and How It Works. (2013). In *National Institute of Diabetes and Digestive and Kidney Diseases*. Retrieved from: http://www.niddk.nih.gov/health-information/health-topics/Anatomy/your-digestive-system/Pages/anatomy.aspx

Zhang, J., Liss, M., Wolburg, H., Blasig, I.E., Abdelilah-Seyfried, S. (2012). "Involvement of claudins in zebrafish brain ventricle morphogenesis." Ann N Y Acad. Sci. **1257**:193-8.